Synthesis and modification of sequence-controlled styrene-maleic anhydride copolymer

Thesis presented in partial fulfilment of the requirements for the degree of MSc in Polymer Science at the University of Stellenbosch

By

Nelmari Harmzen

UNIVERSITEIT
iYUNIVESITHI
STELLENBOSCH
UNIVERSITY

Supervisor: Prof Bert Klumperman

Co-supervisor: Dr Rueben Pfukwa

University of Stellenbosch

Faculty of Science

Department of Chemistry and Polymer Science

March 2018

Declaration

By submitting this thesis electronically, I declare that the entirety of the work contained therein is my own, original work, that I am the sole author thereof (save to the extent explicitly otherwise stated), that reproduction and publication thereof by Stellenbosch University will not infringe any third party rights and that I have not previously in its entirety or in part submitted it for obtaining any qualification

Nelmari Harmzen

Stellenbosch, 2018

Abstract

Recently, there has been an immense fascination with replicating nature's ability to create polymers with perfectly controlled monomer sequences.

The work introduced in this thesis focuses on the synthesis of a sequence-controlled copolymer, along with its subsequent modification. Styrene (Sty) and maleic anhydride (MAnh) are the two monomers used in this study. The fact that this comonomer pair are added one at a time to the growing polymer chain during the addition-fragmentation cycle, along with the inability of MAnh to homopolymerize due to the steric hindrance served as a foundation to synthesize a sequence-controlled copolymer consisting of a repeating sequence that comprises one MAnh unit followed by two Sty units.

S-butyl-*S*'-(1-phenyl ethyl) trithiocarbonate (BPT) was selected as a reversible addition-fragmentation chain-transfer (RAFT) agent to synthesize the copolymer. The desired polymer was characterized mainly by ^{1}H NMR spectroscopy, and ^{13}C DEPT NMR spectroscopy, as well as by mass spectrometry (MS) and size exclusion chromatography (SEC). The DEPT results proved that the alternating sequence was suppressed, with 93 % of the Sty-centred sequences being MSS. The thermal studies of the synthesized polymer was compared to SMA2000, which is synthesized by conventional radical polymerization with a Sty:MAnh molar ratio of 2:1.

The synthesized sequence-controlled copolymer was modified, along with alternating styrene-maleic anhydride (SMA) derivatives of various molecular weights. The dissociation behaviour of these polymers were investigated and upon functionalization, a zwitterionic window was located for all the polymers. The isoelectric point (pI) was calculated using either the method of determining the maxima of first derivative or by a linear regression method reported by Johansson.

The latter method provided more precise pK_a values for the polymers, upon correlation with the obtained titration curves. The incorporation of a larger fraction of Sty in the sequence-controlled copolymer, resulted in a higher pI, which allows the pI to be manipulated in future studies. Cell viability tests of the functional groups revealed that the ionic groups present in these polymers, are not cytotoxic to cells.

Opsomming

Onlangs was daar 'n enorme fassinasie met die replisering van die natuur se vermoë om perfek beheerde volgorde te skep.

Die werk wat in hierdie verhandeling aangebied word, fokus op die sintese van 'n volgorde-beheerde kopolimeer, tesame met die behandeling daarvan met 'n nukleofiel. Stireen (Sty) en maleienanhidried (MAnh) is die twee monomere wat in hierdie studie gebruik word. Die feit dat hierdie monomeersisteem een vir een bygevoeg word aan die groeiende polimeerketting gedurende die addisie-fragmentasie siklus, tesame met die onvermoë van MAnh om te homopolymeriseer as gevolg van die steriese hindernis, dien as basis vir die sintese van 'n volgorde-beheerde kopolimeer wat bestaan uit een MAnh-eenheid gevolg deur twee Sty-eenhede.

S-butiel-S'-(1-fenieletiel) tritiokarbonaat (BPT) is gekies om die kopolimeer te sintetiseer. Die verlangde polimeer is hoofsaaklik gekenmerk deur ^{1}H NMR spektroskopie, en ^{13}C DEPT NMR spektroskopie, tesame met massaspektrometrie (MS) en grootteuitsluitingschromatografie (SEC). Die DEPT-resultate het bewys dat die wisselende volgorde onderdruk is, met 93% van die Sty-gesentreerde rye MSS. Die termiese studies van die gesintetiseerde polimeer is vergelyk met SMA2000, wat gesintetiseer word deur konvensionele radikale polimerisasie met 'n Sty: MAnh molêre verhouding van 2:1

Die gesintetiseerde volgorde-beheerde kopolimeer is aangepas, saam met afwisselende stireen-maleienanhidried (SMA) afgeleides van verskillende molekulêre gewigte. Die dissosiasiegedrag van hierdie genoemde polimere is ondersoek en op funktionalisasie was 'n zwitterioniese streekvenster vir al die polimere. Die isoelektriese punt (pI) is bereken deur óf die metode van maksima van eerste

afgeleide of 'n lineêre regressie metode wat deur Johansson gerapporteer is. Laasgenoemde het meer akkurate pKa-bepaling van die polimere voorsien, in ooreenstemming met die verkryde titrasiekurwes. Die inkorporasie van 'n groter fraksie van Sty in die volgorde-beheerde kopolimeer het gelei tot 'n hoër pI, wat die pI toelaat om in toekomstige studies gemanipuleer te word. Selbaarheidstudietoetse het getoon dat hierdie funksionele groepe nie sitotoksies vir selle is nie.

Acknowledgements

Foremost, I would like to express my gratitude to my supervisor Prof Bert Klumperman for the continuous support of my MSc study and research. I would also like to thank him for his enthusiasm, patience and immense knowledge. His guidance helped me in the research and the writing of this thesis. I would also like to thank my co-supervisor, Dr Rueben Pfukwa for always checking in.

Besides my supervisors, I would like to thank the free radical group, especially: soon to be Elrika Harmzen-Pretorius, Ingrid Heyns, Waled Hadasha, Lebohang Halale (Plascon), Rudolf Dreyer, Chandré Smit, Anna Kargaard and Lisa Fortuin for their encouragement, knowledge, drinks, questions during group meeting and for all the fun we have had in the last two years.

My sincere thanks also goes to Dr Robbie Luckay, Hezron Ogutu and Derik Wilbers at the Inorganic Chemistry Department for assisting me with titration reactions and always welcoming me at their facilities. I would also like to thank Prof Carine Smith and Johan Visser at Physiology for the conducting the cell studies and the processing of the data obtained.

I would also like to thank Stellenbosch University for this opportunity and the NRF for funding. Also CAF – especially Dr Jaco Brand and Elsa Malherbe who helped me tremendously with my work at the NMR facility.

A special thanks to all my friends – especially my three housemates whom supported me, and for making our house a much needed, relaxed space.

A very special thanks to Fred Mudge for his unconditional support and love, a thank you just isn't enough.

Last but not the least, I would like to thank my family: my parents Pieter and Elize Harmzen, for supporting me unconditionally, spiritually and financially, my brother-in-law Corné Pretorius and my sister (soon to be Dr) Elrika Harmzen-Pretorius, you were the best mentor in the lab.

Table of contents

List of figures

List of schemes

List of tables

Nomenclature

A	conjugate base in basic titration
C_B	concentration of titrant based on work done by Johansson[1]
$Đ$	dispersity index
d	fraction of chains terminated by disproportion
f	initiator efficiency
H^+	protons
HA	acid in basic titration
$[I]_0$	initial initiator concentration
K_a	acid dissociation constant
K_b	base dissociation constant
k_d	decomposition rate
$[M]_0$	initial monomer concentration
M_w	weight average molecular weight
M_n	number average molecular weight
$M_{n,th}$	theoretical number average molecular weight
MW_M	molecular weight of monomer
MW_{RAFT}	molecular weight of RAFT agent
pH	measure of the hydorgen ion concentration of a solution

$pH_{\text{half titration}}$	half of the volume where the equivalence point is reached, is known as the half-equivalence point. This is where pH=pK_a
pK_a	index to express the acidity of weak acids which is equal to the negative logarithm of the acid dissociation constant
pK_b	index to express the acidity of weak bases which is equal to the negative logarithm of the base dissociation constant
R	RAFT leaving group
r_1	reactivity ratio for monomer one
r_2	reactivity ratio for monomer two
$[RAFT]_0$	initial RAFT concentration
t	time
V	volume in basic titration
x	conversion of monomer
Z	RAFT stabilizing group

List of abbreviations

AIBN	2,2'-azobis(isobutyronitrile)
A-SMA	ring opened amino modified styrene-maleic anhydride copolymer based on analternating poly(styrene-co-maleic anhydride)
ATR	attenuated total reflection
ATRP	atom transfer radical polymerization
BA	butyric acid
BPT	butyl 1-phenylethyl trithiocarbonate
BPPT	butyl 2-phenylpropan-2-yl) trithiocarbonate
CDB	cumyl dithiobenzoate
CPDA	cumyl phenyl dithioacetate
CRP	controlled radical polymerization
CSIRO	Commonwealth Scientific and Industrial Research Organization
DEPT	Distortionless enhancement by polarization transfer
DMF	dimethylformamide
DNA	deoxyribonucleic acid
DMPAPA	dimethylaminopropylamine
DMPAPPA	*N*-(3-dimethylamino)propyl)propionamide

DMSO	dimethyl sulfoxide
FR	free radical
FTIR	fourier transform infrared
GPC	gel permeation chromatography
IUPAC	International Union of Pure and Applied Chemistry
IR	internal reference
KOH	potassium hydroxide
LRP	living radical polymerization
MAnh	maleic anhydride
MEK	methyl ethyl ketone
MPs	membrane proteins
MS	mass spectrometry
NMP	nitroxide mediated polymerization
NMR	nuclear magnetic resonance
PET	petroleum ether
pI	isoelectric point
PS	polystyrene
RAFT	reversible addition–fragmentation chain transfer
RDRP	reversible deactivation radical polymerization
RNA	ribonucleic acid

SDBM	Styrene-divinylbenze-maleic anhydride
SEC	size exclusion chromatography
SMA	styrene-maleic anhydride copolymer
SMA2000	styrene-maleic anhydride alternating copolymer with a Sty:MAnh ratio of 2:1 synthesized by conventional radical polymerization
SMA5000	styrene-maleic anhydride alternating copolymer with a molecular weight of 5000
SMA8000	styrene-maleic anhydride alternating copolymer with a molecular weight of 8000
SMA11000	styrene-maleic anhydride alternating copolymer with a molecular weight of 11000
SMUI	single monomer unit insertion
SSM	styrene-styrene-maleic anhydride copolymer synthesized via RAFT-mediated polymerization
SSM2100	styrene-maleic anhydride sequence-controlled copolymer with a molecular weight of 2100 ($(SSM)_6$ consisting of 6 SSM repeat units)
SSM4200	styrene-maleic anhydride sequence-controlled copolymer with a molecular weight of 4200 ($(SSM)_{13}$ consisting of 13 SSM repeat units)
Sty	styrene
TGA	thermogravimetric analysis

THF	tetrahydrofuran
TI	therapeutic index
TLC	thin layer chromatography
VAZO 88®	1,1′-azobis(cyanocyclohexane)
XTT	5,5'-(5-(phenylcarbamoyl)-2*H*-tetrazole-3-ium-2,3-diyl)bis(4-methoxy-2-nitrobenzenesulfonate).

Chapter 1

Prologue

Styrene-maleic anhydride (SMA) copolymers, and their copolymerization, have been extensively studied over numerous years. The monomer system is unique. Unlike several other monomer systems, the one monomer possesses the ability to homopolymerize effortlessly, while the other monomer only homopolymerizes under extreme and harsh conditions, due to the steric hindrance enforced by 1,2-distribution of the double bond.[1] The monomers do not exhibit a large difference in reactivity ratios,[2] but the inability of maleic anhydride (MAnh) to homopolymerize, results in the alternating nature of this copolymer. Some cases of a deviation from the alternating structure have been reported,[3–5] although the sequence has not been fully controlled.[6] The fact that the homopolymer of the one monomer is easily obtained, allows the sequence of the copolymer to be altered.

SMA copolymers are classified as a functional polymer, due to the reactive MAnh unit in the polymer backbone.[7] It is especially prone to reactions with nucleophiles.[7] Therefore, this copolymer is readily modified, and the ionic properties results in the use of the polymer for various applications, such as replicating cell membranes or the preparation of tailored surfaces.[8]

1.1 Objectives

The main objective of this study was to chemically synthesize a sequence defined copolymer of styrene (Sty) and MAnh consisting of a predetermined sequence of MAnh-Sty-Sty (SSM), followed by the utilization of chromatographic and spectroscopic techniques to fully characterize the desired polymer. The secondary objective was to successfully modify the sequence-controlled copolymer and determine if this polymer, along with alternating SMA copolymer derivatives, experiences a zwitterionic region.

1.2 Outline of thesis

The thesis comprises six chapters:

Chapter 1 gives a brief outline of the objectives that are presented in the study.

In Chapter 2, a literature review and background is given regarding SMA copolymers. The polymerization techniques employed, the type of modification and uses of this polymer system are also discussed.

In Chapter 3, a thorough investigation on the reversible addition-fragmentation chain transfer (RAFT) polymerization agents is presented. The importance of the leaving group (R) and stabilizing group (Z) are discussed and various classes of RAFT agents are employed.

In Chapter 4, the synthesis of a sequence-controlled copolymer of SSM is discussed. This is synthesized by the most efficient RAFT agent determined from the study in Chapter 3.

Chapter 5 presents a model study employed in order to investigate the effect of the modification on the zwitterionic abilities of the polymer. The modification of the

SSM and conventional, alternating SMA is also discussed in this chapter in order to impart the functional groups needed for the polymer to be ionizable. The effect of the Sty sequence was determined for the alternating system when using these polymers as zwitterionic agents. The zwitterionic region of the synthesized copolymers is also discussed in this chapter. In order to expand the applications to the biological field, the cytotoxicity of nanoparticles containing the same ionizable groups were investigated, in order to determine how the functional groups (present in the modified polymers and the modified nanoparticles) affect primary isolated human macrophages (type M1).

Finally, Chapter 6 concludes the thesis with a summary and discusses the challenges encountered during this study. Additional suggestions for future work are also discussed in this chapter.

References

1. Gaylord, N. G. *J. Macromol. Sci. Part C* 1975, *13*, 235–261
2. Musa, O. M. *Handbook of Maleic Anhydride Based Materials: Syntheses, Properties and Applications,* First edition, 2016, ISBN: 9783319294544
3. Lessard, B. & Marić, M. *Macromolecules* 2010, *43*, 879–885
4. Benoit, D., Hawker, C. J., Huang, E. E., Lin, Z. & Russell, T. P. *Macromolecules* 1999, *33*, 1505–1507
5. Barron, P. F., Hil1, D. J. T., O'Donnell, J. H. & O'Sullivan, P. W. *Macromolecules* 1984, *17*, 1967–1972
6. Moriceau, G., Gody, G., Hartlieb, M., Winn, J., Kim, H., Mastrangelo, A., Smith, T. & Perrier, S. *Polym. Chem.* 2017, *8*, 4152-4161
7. Mpitso, K. *Synthesis and characterization of styrene - maleic anhydride copolymer derivatives,* 2009, MSc, Stellenbosch University
8. Laschewsky, A. *Polymers* 2014, *6*, 1544–1601

Chapter 2

Introduction and theory

Poly and *meros* are two Greek words meaning "many" and "part", respectively, spurred the origin of the present-day term "polymer". This expression was initially introduced in 1833 by a Swedish chemist named Jöns Jakob Berzelius.[1,2] In 1861, the British chemist Thomas Graham shed some light on this interesting topic when he noted that the dissolution of certain organic compounds could not fully pass through even the finest of filter papers nor be purified into a crystalline form.[3] According to the International Union of Pure and Applied Chemistry (IUPAC), a polymer (also referred to as a macromolecule) is a relatively high molar mass substance, which consists of multiple linked, relatively low molar mass monomers. Polymer arises from intermolecular reactions between either chemical divergent monomers or monomer residues.[4] This is known as a polymerization. Monomers thus undergo polymerization reactions in order to form polymers.

The door to the Polymer Age (also known as the Age of Plastics) was opened in 1907 when the Belgian chemist Leo Hendrik Baekeland mixed phenol and formaldehyde in a sealed autoclave, subjected it to heat and pressure, and found that a sticky, amber-coloured resin was formed. This was the first ever polymer

created entirely from chemicals by the hands of man, and is now well known as Bakelite.[3] Since the invention of polymers, countless polymer-based applications have emerged worldwide and these are growing exponentially.

2.1 Styrene-maleic anhydride copolymers (SMA)

Copolymers consisting of styrene (Sty) and maleic anhydride (MAnh) monomer units have been synthesized on a commercial scale in a variety of high and low molar masses[5], compositions[6] and are used in a variety of applications (refer to Section 2.1.6).

The MAnh monomer is an electrophile and although acrylates polymerizes readily, the steric hindrance of the 1,2-distribution of the double bond results in the monomer only being able to homopolymerize under extreme and harsh conditions.[6] The small reactivity ratio of MAnh describes the nature of the monomer in terms of homopolymerization and therefore the tendency towards alternation. Contrary to MAnh, Sty consists of an electron-rich double bond and can therefore homopropagate effortlessly. The use of equimolar quantities of both monomers results in a strictly alternating polymer, (as shown in Figure 2.1), as the cross propagation rate is very high for this specific monomer system.[7] The high cross propagation rate ensures swift monomer addition to the polymer chain. A variation of copolymers are formed by reversible addition-fragmentation chain transfer (RAFT) polymerization – and conventional radical copolymerization. The latter produces copolymer blends, where RAFT copolymerization fabricates gradient copolymers.[8] When the Sty monomer fraction is increased in RAFT copolymerization, the alternating polymer microstructure perpetuates followed by a sheer polystyrene block, which results in a block copolymer.[9] Therefore, block

copolymers are readily formed with this monomer system[10–12], and the Sty monomer readily forms block copolymers with various other monomers.[13–20]

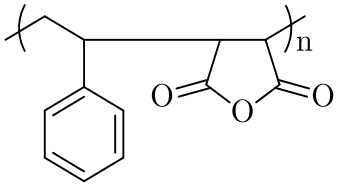

Figure 2.1: General representation of styrene-maleic anhydride alternating copolymer.

Monomer reactivity ratios describe the relative tendency of a monomer to homopropagate or crosspropagate. For a given monomer system, the monomer reactivity ratios, r_1 and r_2 are the ratios of the rate constants of the distinct propagation reactions.[21] The reactivity ratios for this monomer system are tabulated below:

Table 2.1: Monomer reactivity ratios of maleic anhydride and styrene.[22]

Copolymer	r_1	r_2	$r_1 \cdot r_2$
Maleic anhydride/styrene	0.005	0.05	2.5×10^{-4}

Reactivity ratios describe the ratio of the rate constants for a given radical to add to its own monomer (known as homopolymerization or homopropagation) compared to that of the other monomer (known as copolymerization or cross-propagation). If $r_1 > 1$, then the tendency of homopropagation will be larger. Where if $r_1 < 1$, copolymerization will be preferred. In other words, a MAnh radical preferentially reacts 200 times more rapidly, in an equimolar reaction mixture, with a Sty monomer than with itself. While a Sty radical preferentially reacts 20 times faster with MAnh than with itself. The alternating nature of this monomer system can be explained by the fact that MAnh contains a very low tendency to homopolymerize,

indicating that the MAnh-MAnh dyads are essentially absent in the polymer chain, and is, therefore, extremely favoured for cross propagation with Sty.[6,7] MAnh is known to be consumed extremely fast in the presence of Sty and the copolymerization rate is high compared to that of the homopolymerization of styrene.

2.1.1 Polymerization methods of SMA copolymers

The mechanism of polymerization categorizes polymers, while grouping the mechanisms into chain growth and step growth polymerizations. In the current study, only chain growth polymerization is relevant and will therefore be discussed in the following section. A brief summary of the available methods is shown in Figure 2.2.

Throughout the reaction, the reaction mixture only contains monomer, growing polymer chains, and the polymer chain formed. In step growth polymerization, all of the molecular species available in the reaction mixture can react, considering only propagating species and monomers can react in chain growth polymerization. Chain growth polymerization involves the polymerization of unsaturated monomers, as well as cyclic monomers which is known as ring-opening polymerization. All chain growth methods rely on the formation of reactive species (free radicals, cations or anions) for a polymer chain to grow and are usually faster than a step growth polymerization process.

The whole polymerization process unfolds via the reactions below.

i. Initiation of the polymer chain
ii. Propagation of the polymer chain
iii. Termination of the polymer chain

iv. Chain transfer can also occur, but is not necessarily present

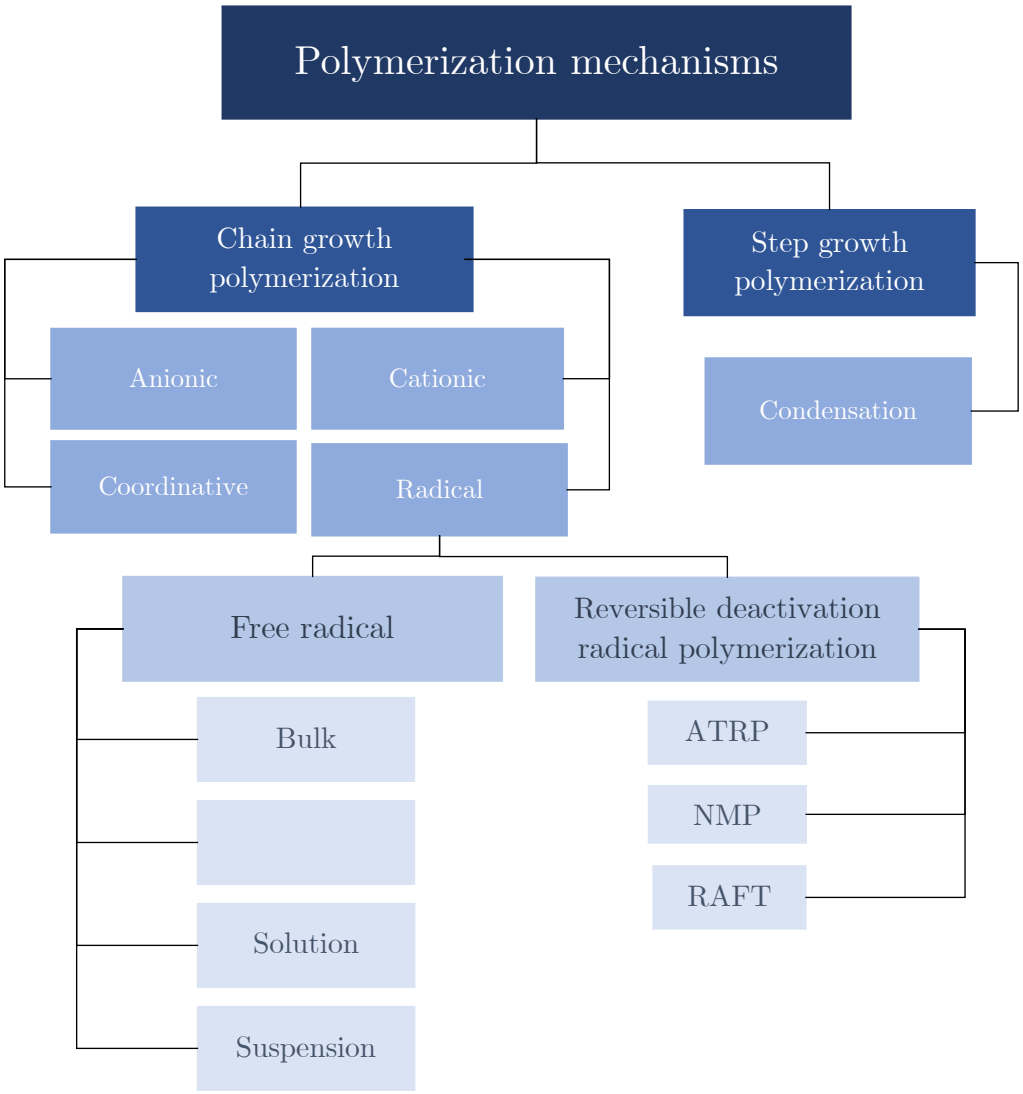

Figure 2.2: Summary of polymerization methods.

2.1.2 Conventional free radical polymerization

One of the most widely utilized polymerization techniques is free radical polymerization (FRP). This is due to the fact that the process does not require demanding conditions and it can be used for a wide range of vinyl monomers.[24] Poor

control over molecular weight, broad molecular weight distribution and dispersities around 2 are often obtained by this polymerization mechanism.[10] This led to the development of living radical polymerization (LRP). This term was discouraged by IUPAC as the process is not fully living due to inevitable chain termination by two radicals. This led to the development of the term controlled radical polymerization (CRP), but is nowadays more commonly known as reversible deactivation radical polymerization (RDRP).[25] Well-defined copolymers, with regard to composition, chain architecture and site-specific functionality are often obtained by this technique. From the mid-1990s, RDRP techniques were intensively explored and before this it was thought that FRP was a mature process with little discoveries to make.[23]

2.1.3 Reversible deactivation radical polymerization (RDRP)

RDRP is based on either a persistent (long-lived) radical effect or a degenerative transfer process. RDRP techniques such as reversible addition-fragmentation chain transfer polymerizations (RAFT), stable free radical polymerizations (SFRP) and atom transfer radical polymerizations (ATRP) are commonly used to obtain polymers with a narrow molecular weight distribution.[26,27] A typical progression of RDRP is displayed in Figure 2.3. It is evident that the molecular weight increases linearly with an increase in monomer conversion.

Copolymerization reactions consisting of an initiation and propagating step[9], such as ionic or radical copolymerization, are statistical processes which generally lead to microstructures where the placement of monomer follows a statistical rule (frequently described as "random" copolymers).[7,28–31] When copolymerizing monomers with different reactivity ratios, the monomer that possesses the highest reactivity ratio tends to be more prominent in the polymer. During RDRP, the

degree to which the monomer sequence can be controlled remains rather low as the sequence is dependent on the reactivity ratios of the monomer system.[7] It is, therefore, necessary for an in depth discussion of RAFT polymerization.

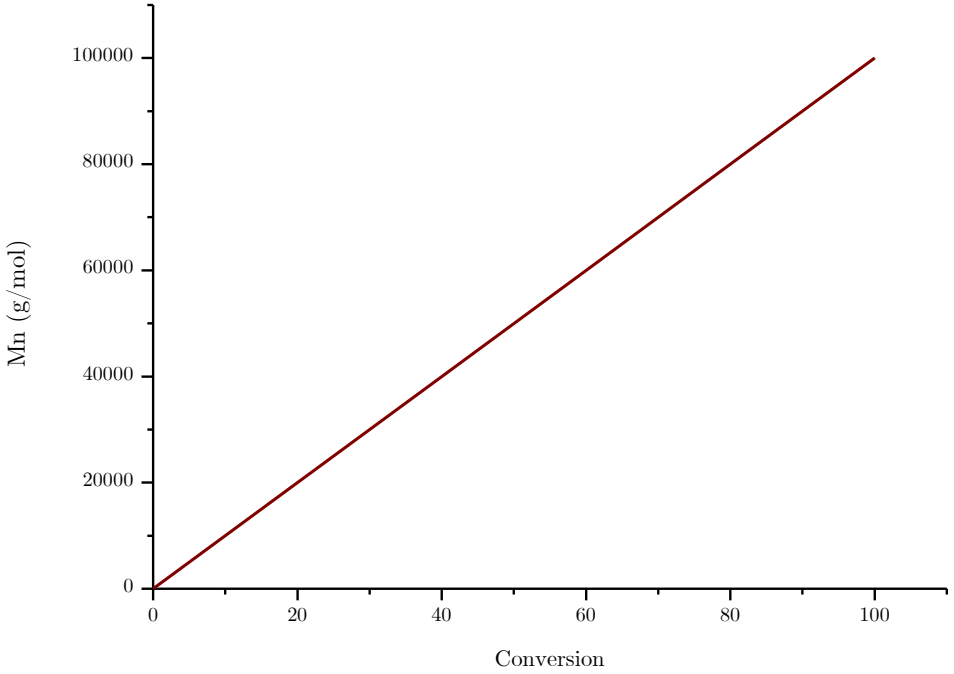

Figure 2.3: Representation of a typical living polymerization - molar mass as a function of monomer conversion.

2.1.3.1 RAFT polymerization

RAFT polymerization is based on a degenerative chain transfer mechanism. The reaction takes place between a propagating radical, which is provided by the thermal decomposition of an azo-initiator, in the presence of thiocarbonylthio compounds.[6] These compounds can act as reversible chain transfer agents (CTAs). The general structure of RAFT agents consist of R-S-C(=S)-Z, where the R group is the leaving group, which has the requirement that it should reinitiate the polymerization and

Z is known as the stabilizing group. The general structure of a RAFT agent is displayed in Figure 2.4

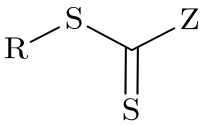

Figure 2.4: General structure of RAFT agent.

One of the main advantages of RAFT polymerization, is that tuning the molar ratio of monomer to RAFT agent allows for the creation of polymers with a predetermined molecular weight. This can be done by using Equation 2.1.

$$M_{n,th} = \frac{[M]_0 x}{[RAFT]_0 + (1+d) f [I]_0 (1\text{-}exp[-k_d t])} \cdot MW_M + MW_{RAFT} \qquad \text{Eq. (2.1)}$$

Where $M_{n,th}$ is the theoretical number-average molecular weight, $[M]_0$, $[RAFT]_0$ and $[I]_0$ are the initial concentrations of monomer, RAFT-agent and initiator respectively, x is the conversion of the monomer, d is the fraction of chains terminated by disproportionation, f is the initiator efficiency, k_d is the decomposition rate constant of the initiator, t is the elapsed time of the polymerization and MW_M and MW_{RAFT} are the respective molecular weights of both the monomer and RAFT-agent. Due to the control over the reaction in a RAFT-mediated polymerization, and the fact that most of the chains accommodate a RAFT-agent as end group, the fraction of chains formed via initiator-derived radicals remains extremely low, resulting in the second term in the denominator becoming negligible.[32]

Narrow molecular weight distributions and controlled architectures can be obtained by RAFT polymerization.[33] In comparison to the other RDRP techniques, RAFT

has proven to be the most versatile as it is applicable to most monomers polymerizable under free radical conditions.

The 'livingness' of a RAFT polymerization has been extensively studied[34–37] and is demonstrated by the following properties:

i. Low dispersity of polymer (<1.2)
ii. Linear increase of molecular weight with conversion
iii. Ability to produce block copolymers

The effectiveness of the RAFT agent depends on the reactivity of the monomers and the monomer system. Therefore, the major drawback of RAFT polymerization is that there exists no universal RAFT agent and different RAFT agents are required for different monomer systems. RAFT agents often also consist of a multistep synthetic procedure, frequently followed by purification steps.[38]

2.1.4 Multiblock copolymer synthesis

As mentioned in the previous section, block copolymers of Sty and various other monomers are readily formed. Multiblock copolymers differ from block copolymers as they typically consist of several alternating sequences, instead of long sequences of both monomers.[39]

Gody *et al.* prepared a multiblock copolymer by iterative RAFT polymerization (sequential addition of monomers).[40] They presented evidence that the RAFT polymerization is an excellent technique to synthesize multiblock copolymers with exceptionally low dispersities.[41] Moriceau *et al.* reported synthesizing a functional multisite copolymer consisting of Sty and MAnh by one-pot sequential RAFT polymerization.[42] They relied on single monomer unit insertion (SMUI) of the MAnh monomer unit followed by chain extension of the Sty monomer. They used 1.5

equivalents of MAnh for every 10 units of Sty, resulting in a deviation from strict SMUI, as more than one unit of MAnh is inserted during every addition. Therefore, various multiblock copolymers can be synthesized with this monomer system.

2.1.5 SMA copolymers as sequence-controlled multiblock copolymers

Sequence-controlled copolymers are described as macromolecules with chemically divergent monomer units that are ordered in a distinct yet precise fashion.[43] Controlled monomer sequences are readily found in biology – *i.e.*, nucleic acids, namely, DNA and RNA, and proteins. The ordered sequence has a phenomenal impact on the structure of the macromolecule and leads to remarkable properties.[43] The fascination with sequence-controlled polymers can be easily understood, especially over the past few years as scientists are striving to impart perfectly controlled sequences in synthetic polymers due to the promising physical and chemical properties that can exist as a result thereof.

Ouchi *et al.* reported that coded sequences are often obtained by attaching monomers one at a time.[44] Lutz stated that there are two core problems still to be solved by polymer scientists:[43]

(i) How to assemble comonomer units in a controlled, linear arrangement.

(ii) How ordered primary structures correlate with the structure and properties of matter.

The tools currently available for the characterization of precise sequencing are not sufficient to fully describe these sequence-controlled polymers.[43] However, ^{13}C NMR spectroscopy has been used to study the sequence distribution of SMA copolymers with varying the Sty content in the copolymer.[45,46] Barron *et al.* studied the appearance of the different Sty-centred triads in the methylene sub spectrum produced by ^{13}C DEPT NMR spectroscopy experiments.[45] They concluded that the

aliphatic region of the methylene spectrum obtained in a ^{13}C DEPT experiment of SMA copolymers contained three distinct regions, namely the SSS triad (42-47 ppm), MSS plus SSM triad (37-42 ppm,) and the MSM triad (33-37 ppm). Barron *et al.* also stated that the methylene (CH_2) subspectrum allows for an accurate estimation of the comonomer content due to no overlap from the CH and CH_3 subspectra.[45]

Although alternating copolymers of Sty and MAnh are readily formed,[6,10,46,47] their remarkable differences in electron densities and reactivity ratios make them suitable candidates for multiblock synthesis, while their sequences can be defined beforehand.

2.1.6 Applications of SMA copolymers

SMA copolymers are employed in various applications such as additives, microcapsules, blend compatibilizers and in various medical and pharmaceutical applications. Besides the commercial applications of SMA copolymers, these copolymers are also employed in the stabilization of phospholipid nano-discs.[48]

2.1.7 The use of SMA copolymers in phospholipid nano-discs

Membrane proteins (MPs), once displaced from their natural environment, rely on membrane-mimetic processes in order to maintain their indigenous structures and functions.[49] They are of great importance in the biological and medical fields.[50,51] MPs fold and operate readily while being highly stable in the lipid bilayer medium.[52,53] Styrene-maleic acid copolymers facilitate the arrangement of disc-like lipid bilayer mimetics that preserve the structural as well as the dynamic robustness of MPs.[49,54] Therefore, they have transpired as an essential tool for the isolation, solubilisation, purification and characterization of MPs.[55–57] Before the use of SMA

copolymers, detergent micelles and liposomes were used for *in vitro* membrane-protein research.[57,58] However, some conventional detergent solutions used to stabilize MPs, resulted in prompt inactivation of MPs.[53]

Nano-discs consist of a non-covalent assembly of phospholipids with the hydrophobic segment screened by amphipathic substances.[59] Nano-discs are therefore described as self-assembled discoidal fragments of lipid bilayers which are 8-16 nm in diameter and are stabilized in solution by amphipathic helical scaffold proteins.[56]

Copolymers consisting of SMA have also proved to be suitable candidates for the stabilization of phosholipid nano-discs.

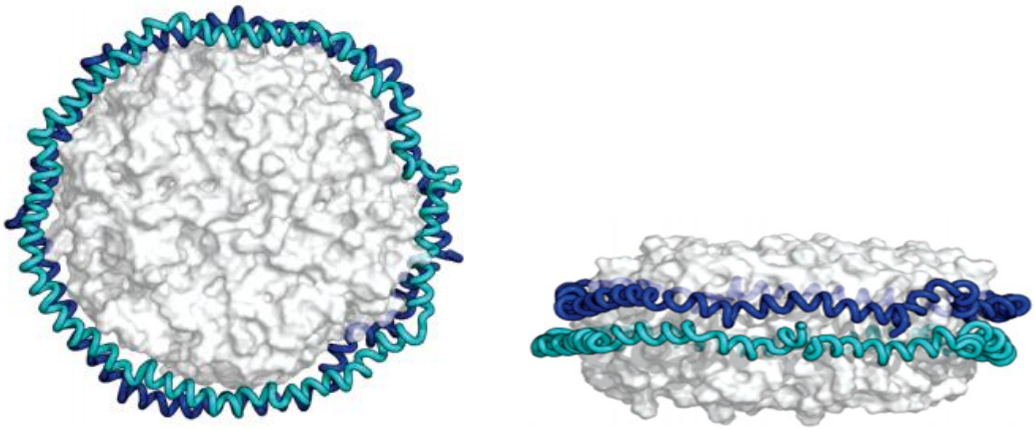

Figure 2.5: Nano-disc - perpendicular to the bilayer (left) and in the plane of the bilayer (right).[60]

Reprinted with permission (from "Applications of Phospholipid Bilayer Nanodiscs in the Study of Membranes and Membrane Proteins").

Dörr *et al.* reported that SMA can self-insert into membranes and is capable of extracting membrane patches in the form of nano-sized discoidal proteolipid particles or "native nanodiscs".[48] In

Figure 2.5, the blue and cyan spirals represent two members of the membrane scaffold protein that form an amphipathic helical belt around a segment of phospholipid bilayers (white).[60]

Dörr *et al.* reported that with the use of SMA copolymers for this application, the MPs exhibit superior structural and thermal stability. Earlier, the only SMA copolymers that were available for this application were conventional statistical copolymers with a molecular weight dispersity around 2. Below is a representation from Dörr *et al.* where they display non-bilayer systems versus bilayer systems (including SMA stabilized nano-discs).

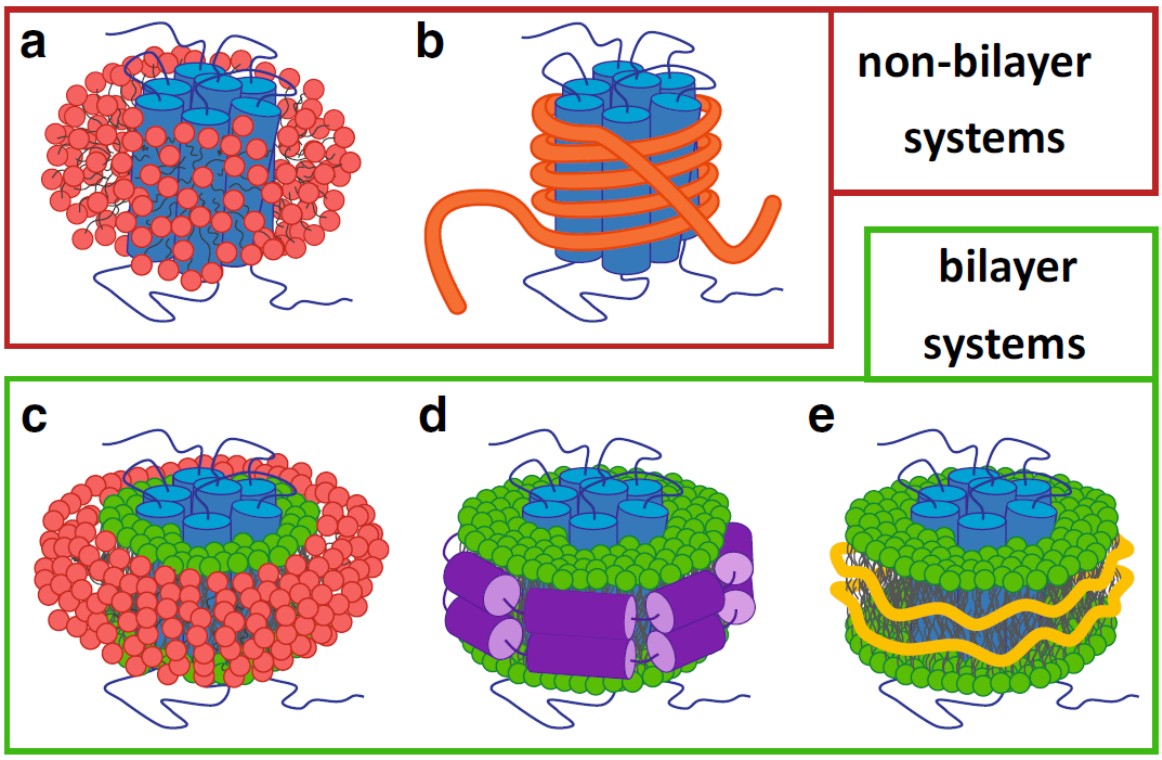

Figure 2.6: Representation of membrane-mimetic systems used for the stabilization of membrane proteins. The protein (blue) and lipids in bilayers (green) are indicated.[61] a – protein in detergent (red) micelle, b - protein stabilized by amphipol (orange), c - protein in bicelle (detergent in red), d - protein in nanodisc stabilized by MSP (purple) and e - protein in nanodisc stabilized by SMA (yellow).

Reprinted (from "The styrene–maleic acid copolymer: a versatile tool in membrane research").

SMA2000 is frequently used in the stabilization of phospholipid nano-discs. This is a commercial SMA copolymer with a molar Sty-MAnh ratio of 2:1, that is synthesized by conventional radical polymerization with a $Đ$ of 2.5 and number average molar mass (M_n) of ca. 3000 daltons (Da).[48]

2.2 Modification of SMA copolymers

The reactive MAnh moiety in the polymer backbone classifies the polymer as a reactive or functional polymer towards nucleophilic reagents.[62] Therefore, SMA is readily functionalized by reacting the MAnh moiety with an amine, as shown in Scheme 2.1. The nitrogen atom of the amine contains a lone pair of electrons resulting in the amine being basic and nucleophilic.

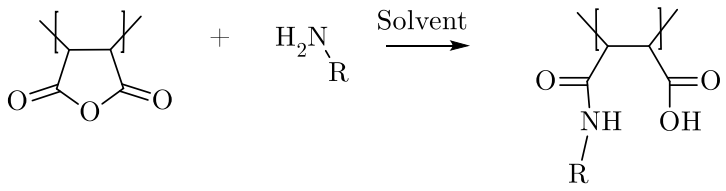

Scheme 2.1: Nucleophilic attack of MAnh by an amine.

The imidization of SMA yields SMI, when the removal of water results in an *N*-substituted maleimide as seen in Scheme 2.2.

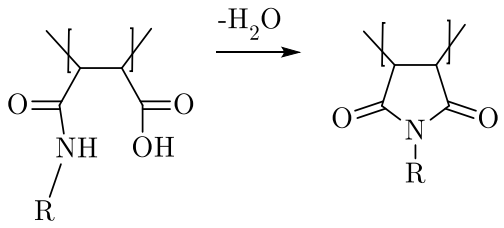

Scheme 2.2: Amine modified SMA (A-SMA) versus *N*-substituted SMI.

A zwitterion is a "hermaphrodite" ion meaning a hybrid ion carrying two different charges.[63] According to Hess *et al.*, a zwitterionic polymer, also known as an ampholytic polymer, is described as a polymer where the ionic groups of opposing charges are incorporated into the same pendant group.[64] Laschewsky explains that polyzwitterrions bear equal amounts of cationic and anionic groups and these groups are functional over a wide pHrange.[65] While zwitterionic species contain cationic and anionic groups, the overall net charge remains zero – resulting in a neutral molecule. Xuan *et al.* attributes the recent interest in zwitterionic polymers to their unique structures which contain ionic groups.[66–68]

A-SMA exhibits amphoteric properties due to its functional groups, namely the tertiary amine and carboxylic acid in the polymer chain. It should be noted that ring closure of the modified compound eliminates the ionizable carboxylic acid group. In other words, this will result in the elimination of a possible zwitterionic molecule.

Polymers containing positively and negatively charged groups in their polymer backbone are expected to have an isoelectric point (pI).[68] The pI is characteristic of a zwitterionic species being present. It is the point at which there is no net charge, i.e. equal numbers of positive and negative charges. The functional repeat unit of A-SMA is very similar to that of amino acids. The pI of amino acids has been extensively studied[63] and their pIs can, therefore, be related to compounds of similar

structure. Amino acids are amphiprotic compounds that consist of functional groups containing a weak acid and a weak base.[63] At the pI, all the original amino acid groups are present in their zwitterionic form:

$$[NH_2CR_2COOH] \leftrightarrow [NH_3^+CR_2COO^-] \qquad \text{Eq. (2.2)}$$

The amino group of the amino acid acts as a base, while the carboxylic acid group behaves as an acid. It is known that in aqueous solution, amino acids become internally ionized, where the carboxylic acid moiety loses a proton and becomes negatively charged while the amino group gains a proton and becomes positively charged. Although the pK values for amino acids cannot be quantitatively determined by direct titration (due to indistinct end points of complete protonation or deprotonation),[63] an estimation can be acquired (refer to Chapter 5).

The pK_a values of common compounds are readily available in literature. It is also possible to experimentally determine the pK_a value by conducting a titration experiment. The pK_a of a substance can be calculated by the use of a titration curve (constructed by plotting the measured pH versus the volume of titrant added). The method of pK_a calculation depends on the stage of the titration, as it is determined in various ways throughout a titration reaction. The relevant stages and methods of calculation are discussed in detail in Chapter 5.

2.2.1 Determination of the isoelectric point of zwitterionic polymers

The pI is described as the pH where there exists no surface charge or charge repulsion.[69] As mentioned in Section 2.2, amino acids are compounds readily known for their amphoteric properties, containing an amino and carboxyl acid group in

their general structure, which is similar to the polymer of interest in this study. The pI of amino acids is described in terms of their inability to migrate in an electric field.[63] Below the pI, the substance is positively charged and above the pI it is negatively charged.

According to literature, the pI can be estimated by Equation 2.3.[67] It should be noted that this is only an estimation, as the end points for complete deprotonation or protonation of a zwitterion are often indistinct.

$$pI = \frac{pK_a + pK_b}{2} \qquad \text{Eq. (2.3)}$$

The pI can be determined by performing a simple titration reaction (titrating from low to high pH or vice versa). From the titration, the plot of pH versus volume should yield two drops in the pH values over constant addition of acid– one corresponding to the base and one to the acid of the substance. Along with the Henderson-Hasselbalch equation, the pH values corresponding to the values right before the drop in pH occurs can be used to calculate the corresponding pK values (refer to Chapter 5). The average between these two pK values is equal to the pI, where the substance contains an overall neutral charge. Additional techniques such as electrophoresis can also be used to determine the pI of a substance.

2.2.2 Applications of zwitterionic polymers

Amphiphiles containing a cationic moiety are employed in cell membrane disruptions. Palmero *et al.* reported that whilst the mechanism regarding membrane disruption of cationic and amphiphilic polymers is not fully understood, they are nevertheless used as antimicrobial agents for this specific application.[70] Amphiphilic molecular interactions with lipid membranes are omnipresent and exist in numerous

biological processes.[71] The role of the cationic group in amphiphilic polymers has been thoroughly investigated by Palmero *et al.* who found that polymers containing primary amines surpass the tertiary and quaternary ammonium counterparts in membrane binding and disrupting abilities.[70]

2.2.3 Use of zwitterionic SMA for cell membrane disruption

Over the past 70 years, concrete evidence has confirmed that the pH of tumor tissue is generally lower than the pH of healthy tissue.[72–74] Hooley *et al.* stated that the pH of healthy tissue ranges from 7.00 to 8.06 compared to the pH of malignant tissue which ranges from 5.50 to 7.52.[73]

Based on the difference in tumor and healthy tissue acidity, it is believed that amine modified SMA (A-SMA) can be utilized in the polymer therapeutics field. This belief is based on the use of cationic substances for the utilization of cell membrane disruptions, along with the acidic nature of malignant cells. It is, therefore, expected that cell membrane disruption will not occur upon exposure of A-SMA to healthy tissue, but only upon exposure to tumor/acidic tissue.

The phrase "polymer therapeutics" was coined by Helmut Ringsdorf and Ruth Duncan.[75–77] It entails polymeric drugs, polymer conjugates with proteins, drugs and aptamers, along with block copolymer micelles and non-viral, multi-component vectors containing covalent linkages.[75] These intricate components are truly "drugs" and "molecular prodrugs" which differ from techniques that solely entrap the therapeutic agents in a non-covalent manner.[75] Often, polymer therapeutic agents would be referred to as nanomedicines.

In recent years, polymers have often been used in drug-delivery systems due to their promising properties such as controlled release, targeted delivery, enhancement of

solubility and increased biocompatibility.[78–80] Improvement of therapeutic efficiencies is also possible based on their physical properties.[77,81] Increasing the therapeutic index (TI) (which is known as the ratio of the dose causing a toxic effect compared to the dose that causes an efficacious effect), remains the sole motivation for much research conducted in therapeutic areas such as inflammation, cancer and infective diseases.[82] Alternative drug-delivery systems and improved methods for drug-delivery systems are the major incentive in polymer therapeutics.[76,82,83]

2.3 Our approach

This chapter focused on SMA copolymers, their applications and the polymerization methods often employed to synthesize these polymers. The importance of the reactivity ratios for this respective monomer system is also highlighted in this chapter. With SMA copolymers, the sequence of the growing polymer chain may be controlled to some extent, based on the fact that the Sty monomer possesses the ability to homopolymerize. Based on the specific reactivity ratios, and the fact that block copolymers of this monomer system are readily formed, we postulate that a sequence defined copolymer with a predetermined repeating sequence of MAnh-Sty-Sty can be synthesized via RAFT polymerization. This entails undergoing a polymerization where the system is optimized in terms of monomer consumption, in order to sequentially add monomers to the polymer chain while controlling the exact sequence.

As explained in this chapter, ^{13}C DEPT NMR spectroscopy will serve as a powerful tool due to the targeted absence of SSS and MSM triads. The average sequence composition of the polymer can be determined by integrating over the desired region and the separate triads in the methylene sub-spectrum.

The modification of SMA copolymers provides the foundation for the possible utilization of SMA copolymers in other applications, where the ionic characteristics play an important role. Exploitation of functionalized SMA exhibiting zwitterionic properties requires both ionic groups to be present in the copolymer. For the purpose of this study, the *N*-substituted maleimide modification will not be explored as it is essential that the anhydride unit remains ring opened after modification.

To the best of our knowledge, the synthesis of sequence-controlled SSM copolymers by RAFT polymerization has not yet been reported and will be the main focus of this study, along with the modification of the copolymers (by amine modification of the polymers) for the possible use in tumor targeted cell membrane disruption.

References

1. Jensen, W. B. *Chem. Educ. Today* 2006, *83*, 838–839
2. Jensen, W. B. *J. Chem. Educ.* 2008, *85*, 624
3. Powers, V. *American Chemical Society National Historic Chemical Landmarks* 1993, 1–2 Available at: http://www.acs.org/content/acs/en/education/whatischemistry/landmarks/bakelite.html. (Accessed: 14th June 2017)
4. Jenkins, A. D., Kratochvíl, P. & Stepto, R. F. T. *Pure Appl. Chem.* 1996, *68*, 2287–2311
5. Henry, S., El-Sayed, M. & Pirie, C. *Biomacromolecules* 2006, *7*, 2407–2414
6. Klumperman, B. *Polym. Chem.* 2010, *1*, 558–562
7. Pfeifer, S. & Lutz, J.-F. F. *J. Am. Chem. Soc.* 2007, *129*, 9542–9543
8. Moad, G., Rizzardo, E. & Thang, S. H. *Australian Journal of Chemistry* 2005, *58*, 379–410
9. Benoit, D., Hawker, C. J., Huang, E. E., Lin, Z. & Russell, T. P. *Macromolecules* 1999, *33*, 1505–1507
10. Lessard, B. & Marić, M. *Macromolecules* 2010, *43*, 879–885
11. Harrisson, S. & Wooley, K. L. *Chem. Commun.* 2005, *0*, 3259
12. De Brouwer, H., Schellekens, M. A. J., Klumperman, B., Monteiro, M. J. & German, A. L. *J. Polym. Sci. Part A Polym. Chem.* 2000, *38*, 3596–3603
13. Lessard, B. H., Mackay, S., Métafiot, A. & Marić, M. *Macromol. Res.* 2016, *24*, 710–715
14. Fukuda, T., Terauchi, T., Goto, A., Tsujii, Y. & Miyamoto, T. *Macromolecules* 1996, *29*, 3050–3052
15. Cornelissen, J. J. *Science* 1998, *280*, 1427–1430
16. Riegel, I. C., Eisenberg, A., Petzhold, C. L. & Samios, D. *Langmuir* 2002, *18*, 3358–3363
17. Gaur, U. & Wunderlich, B. *Macromolecules* 1980, *13*, 1618–1625
18. Tselikas, Y., Iatrou, H., Hadjichristidis, N., Liang, K. S., Mohanty, K. & Lohse, D. J. *J. Chem. Phys.* 1996, *105*, 2456

19. Okamura, H., Takatori, Y., Tsunooka, M. & Shirai, M. *Polymer* 2002, *43*, 3155–3162

20. Tommaso, G. *Polymer* 1995, *36*, 3987–3996

21. Brandrup, J., Immergut, E. & Grulke, E. A. *Polymer handbook*, Fourth edition, 1990 ISBN: 9780471481713

22. Musa, O. M.*Handbook of Maleic Anhydride Based Materials: Syntheses, Properties and Applications,* First edition, 2016 ISBN: 9783319294544

23. Odian, G. *Principles of Polymerization,* Fourth edition, 2004 ISBN: 0471274003

24. Matyjaszewski, K. & Spanswick, J. *Materials Today* 2005, *8*, 26–33

25. Jenkins, A. D., Jones, R. G. & Moad, G. *Pure Appl. Chem.* 2009, *82*, 483–491

26. Mishra, V. & Kumar, R. *J. Sci. Res.* 2012, *56*, 141–176

27. Chan-Seng, D., Zamfir, M. & Lutz, J. F. *Angew. Chemie - Int. Ed.* 2012, *51*, 12254–12257

28. Matyjaszewski, K. *Prog. Polym. Sci.* 2005, *30*, 858–875

29. Lutz, J.-F., Pakula, T. & Matyjaszewski, K. *ACS Symp. Ser.* 2003, *854*, 268-282

30. Coleman, M. M. & Painter, P. C. *Fundamentals of Polymer Science: An Introductory Text*, Second Edition, 1998 ISBN: 9781566765596

31. Chanda, M. *Introduction to Polymer Science and Chemistry,* Second edition, 2006 ISBN: 9781466553842

32. Van den Dungen, E. T. A *Self-healing coatings based on thiol-ene chemistry* 2009 PhD, Stellenbosch University

33. Feng, X. S. & Pan, C. Y. *Macromolecules* 2002, *35*, 4888–4893

34. Derboven, P., Van Steenberge, P. H. M., Vandenbergh, J., Reyniers, M. F., Junkers, T., D'Hooge, D. R. & Marin, G. B. *Macromol. Rapid Commun.* 2015, *36*, 2149–2155

35. Zetterlund, P. B., Gody, G. & Perrier, S. *Macromol. Theory Simulations* 2014, *23*, 331–339

36. Gody, G., Maschmeyer, T. & Zetterlund, P. B. *Macromolecules* 2014, *47*,

639–649

37. Zhang, H. *Eur. Polym. J.* 2013, *49*, 579–600

38. Moad, G., Rizzardo, E. & Thang, S. H. *Aust. J. Chem.* 2009, *62*, 1402–1472

39. Saldivar-Guerra, E. & Vivaldo-Lima, E. *Handbook of Polymer Synthesis, Characterization, and Processing*, First edition, 2013 ISBN: 9780470630327

40. Gody, G., Maschmeyer, T., Zetterlund, P. B. & Perrier, S. *Macromolecules* 2014, *47*, 3451–3460

41. Gody, G., Maschmeyer, T., Zetterlund, P. B. & Perrier, S. *Nat. Commun.* 2013, *4*, 1–9

42. Moriceau, G., Gody, G., Hartlieb, M., Winn, J., Kim, H., Mastrangelo, A., Smith, T. & Perrier, S. *Polym. Chem.* 2017, DOI: 10.1039/C7PY00787F (Manuscript accepted for publication)

43. Lutz, J.-F., Ouchi, M., R, L. D. & Sawamoto, M. *Science* 2013, *341*, 1238149-1-1238149–8

44. Ouahabi, A. Al, Kotera, M., Charles, L. & Lutz, J. F. *ACS Macro Lett.* 2015, *4*, 1077–1080

45. Barron, P. F., Hil1, D. J. T., O'donnell, J. H. & O'sullivan, P. W. *Macromolecules* 1984, *17*, 1967–1972

46. Lessard, B. & Mari, M. *Macromolecules* 2010, *43*, 879–885

47. Okudan, A. & Karasakal, A. *Int. J. Polym. Sci.* 2013, *2013*, 1–9

48. Dörr, J. M., Koorengevel, M. C., Schäfer, M., Prokofyev, A. V, Scheidelaar, S., van der Cruijsen, E. A. W., Dafforn, T. R., Baldus, M. & Killian, J. A. *Proc. Natl. Acad. Sci. U. S. A.* 2014, *111*, 18607–12

49. Oluwole, A. O., Danielczak, B., Meister, A., Babalola, J. O., Vargas, C. & Keller, S. *Angew. Chemie - Int. Ed.* 2017, *56*, 1919–1924

50. Von Heijne, G. *Journal of Internal Medicine* 2007, *261*, 543–557

51. Killian, J. A. & van Meer, G. *EMBO Rep.* 2001, *2*, 91–105

52. Haltia, T. & Freire, E. *Biochim. Biophys. Acta-Bioenergetics* 1995, *1228*, 1–27

53. Bowie, J. U. *Curr. Opin. Struct. Biol.* 2001, *11*, 397–402

54. Craig, A. F., Clark, E. E., Sahu, I. D., Zhang, R., Frantz, N. D., Al-Abdul-Wahid, M. S., Dabney-Smith, C., Konkolewicz, D. & Lorigan, G. A. *Biochim. Biophys. Acta - Biomembr.* 2016, *1858*, 2931–2939

55. Dominguez Pardo, J. J., Dörr, J. M., Iyer, A., Cox, R. C., Scheidelaar, S., Koorengevel, M. C., Subramaniam, V. & Killian, J. A. *Eur. Biophys. J.* 2017, *46*, 91–101

56. Schuler, M. A., Denisov, I. G. & Sligar, S. G. *Methods Mol Biol* 2013, *974*, 415–433

57. Malhotra, K. & Alder, N. N. *Biotechnol. Genet. Eng. Rev.* 2014, *30*, 79–93

58. Garavito, R. M. & Ferguson-Miller, S. *J. Biol. Chem.* 2001, *276*, 32403–32406

59. Bayburt, T. H. & Sligar, S. G. *FEBS Letters* 2010, *584*, 1721–1727

60. Nath, A., Atkins, W. M. & Sligar, S. G. *Biochem.* 2007, *46*, 2059–2069

61. Dörr, J. M., Scheidelaar, S., Koorengevel, M. C., Dominguez, J. J., Schäfer, M., van Walree, C. A. & Killian, J. A. *Eur. Biophys. J.* 2016, *45*, 3–21

62. Saad, G. R., Morsi, R. E., Mohammady, S. Z. & Elsabee, M. Z. *Polym. Res.* 2008, *15*, 115–123

63. Skoog, D. A., West, D. M., Holler, F. J. & Crouch, S. R. *Fundamentals of Analytical Chemistry,* Eight edition, 2004 ISBN: 100030355230

64. Hess, M., Jones, R. G., Kahovec, J., Kitayama, T., Kratochvíl, P., Kubisa, P., Mormann, W., Stepto, R. F. T., Tabak, D., Vohlídal, J. & Wilks, E. S. *Pure Appl. Chem.* 2006, *78*, 2067–2074

65. Laschewsky, A. *Polymers* 2014, *6*, 1544–1601

66. Cardoso, J., Manrique, R., Velasco, M. A. & Huanosta, A. *J. Polym. Sci. Part B Polym. Phys.* 1997, *35*, 479–488

67. Lowe, A. B. & McCormick, C. L. *Chem. Rev.* 2002, *102*, 4177–4189

68. Xuan, F. & Liu, J. *Polym. Int.* 2009, *58*, 1350–1361

69. Mark, H. F. *Encyclopedia of Polymer Science and Technology*, Second edition, 2001 ISBN: 9780471440260

70. Palermo, E. F., Lee, D., Ramamoorthy, A. & Kuroda, K. *J. Phys. Chem* 2011, *115*, 366–375

71. Fujiwara, T., Hirashima, N., Hasegawa, S., Nakanishi, M. & Ohwada, T.

Bioorg. Med. Chem. 2001, *9*, 1013–1024

72. Gerweck, L. E. & Seetharaman, K. *Cancer Res.* 1996, *56*, 1194–1198
73. Wike-Hooley, J. L., Haveman, J. & Reinhold, H. S. *Radiother. Oncol.* 1984, *2*, 343–366
74. Tannock, I. F. & Rotin, D. *Cancer Res.* 1989, *49*, 4373–4384
75. Duncan, R. & Vicent, M. J. *Advanced Drug Delivery Reviews* 2013, *65*, 60–70
76. Duncan, R. *Nat. Rev. Drug Discov.* 2003, *2*, 347–360
77. Duncan, R. *Nat. Rev. Cancer* 2006, *6*, 688–701
78. Langer, R. & Tirrell, D. A. *Nature* 2004, *428*, 487–492
79. Lutolf, M. P. & Hubbell, J. A. *Nat. Biotechnol.* 2005, *23*, 47–55
80. Fischbach, C. & Mooney, D. J. *Biomaterials* 2007, *28*, 2069–2076
81. Kiick, K. L. *Science* 2007, *317*, 1182–1183
82. Haag, R. & Kratz, F. *Angew. Chemie - Int. Ed.* 2006, *45*, 1198–1215
83. Gros, B. L., Ringsdorf, H., Schupp, H. & Kastner, E. *Angew. Chemie - Int. Ed.* 1981, *20*, 305–325

Chapter 3

RAFT agent investigation for sequence-controlled SMA copolymers

Various reversible addition-fragmentation chain transfer (RAFT) agents are employed in this study to determine the effect of the leaving group (R) and the stabilizing group (Z) primarily on monomer consumption. Previous studies have shown that *in-situ* ^{1}H NMR spectroscopy is an exceptionally useful tool for tracking the concentration profile of several species in a reaction mixture. Therefore, it is a functional method to resolve the mechanistic and kinetic characteristics of a reaction.[1–6] In this chapter, the RAFT process will be discussed in detail, considering the importance of the R and Z groups. The phenomenon often observed during RAFT polymerizations, known as the initialization period[3,4,6,7] is also touched on. Investigation into the RAFT group serves as a preliminary step for the synthesis of a sequence-controlled SMA copolymer.

It is proposed that a RAFT agent that provides high (if not full) conversion of all monomers in the system and adheres to feasible conversion times, can be used along with sequential addition of monomers to control the sequence of a copolymer consisting of one maleic anhydride (MAnh) unit followed by two styrene (Sty) units.

Different classes of RAFT agents were used in order to determine the most suitable RAFT agent to synthesize the copolymer.

3.1 Introduction on RAFT-mediated polymerization

The RAFT polymerization technique was invented by the Commonwealth Scientific and Industrial Research Organization (CSIRO) in 1998.[8,9] There exist four types of common RAFT-agents (refer to Figure 3.1) which are dependent on the activating group, namely:

- Dithioestsers (D), where the stabilizing group (Z) is either an aryl group or an alkyl group
- Trithiocarbonates (T), where the Z group is a thioalkoxy group
- Xanthates (X), where the Z group is an alkoxy group
- Carbamates (C), where the Z group is a tertiary amine

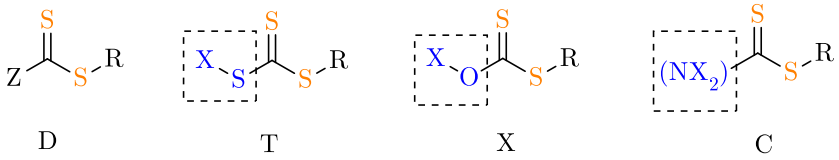

Figure 3.1: RAFT agent classes, where the different Z groups are indicated in the dashed box, displayed in blue.

It is essential that precise polymerization conditions be chosen for this process and that the RAFT agent/monomer combination is compatible under these conditions.[10–12] RAFT proves to be the most versatile amongst the reversible deactivation radical polymerization (RDRP) techniques with regards to the polymerizable monomers, including monomers containing various functional groups.[13–15] RAFT polymerization serves as a precursor to synthesize distinctly ordered and specific architectures which include functional polymers, block

copolymers, graft copolymers, gradient copolymers, star copolymers etc.[14–22]

Using a RAFT-agent provides precise control of the polymer chain growth. Although termination occurs via combination or disproportionation nonetheless, they are limited by the formation of the intermediate radical[15], in turn, controlling the molecular weight and dispersity of the polymer.

The leaving group in RAFT-mediated polymerizations plays a very important role. The leaving group is much more versatile than the stabilizing group and should display the following properties:

- Excellent homolytic leaving group
- Proficiency in reinitiating polymerization
- Compatibility with the conditions of polymerization

RAFT is usually used in conjunction with a thermal initiator, which yields the initiating radical. The RAFT mechanism is familiar amongst polymer chemists. The reaction scheme for RAFT polymerization is displayed in

Scheme 3.1 and based on the schemes from Moad *et al.*[23]

$$M_{n,th} = \frac{[M]_0 x}{[RAFT]_0 + (1+d) f [I]_0 (1-exp[-k_d t])} \cdot MW_M + MW_{RAFT} \qquad \text{Eq. (3.1)}$$

Theoretically, every polymer chain should carry a RAFT-moiety at its end, although some carry the primary (initiator derived) radical. Therefore, the targeted molecular weight of polymer is calculated by using Equation 3.1.

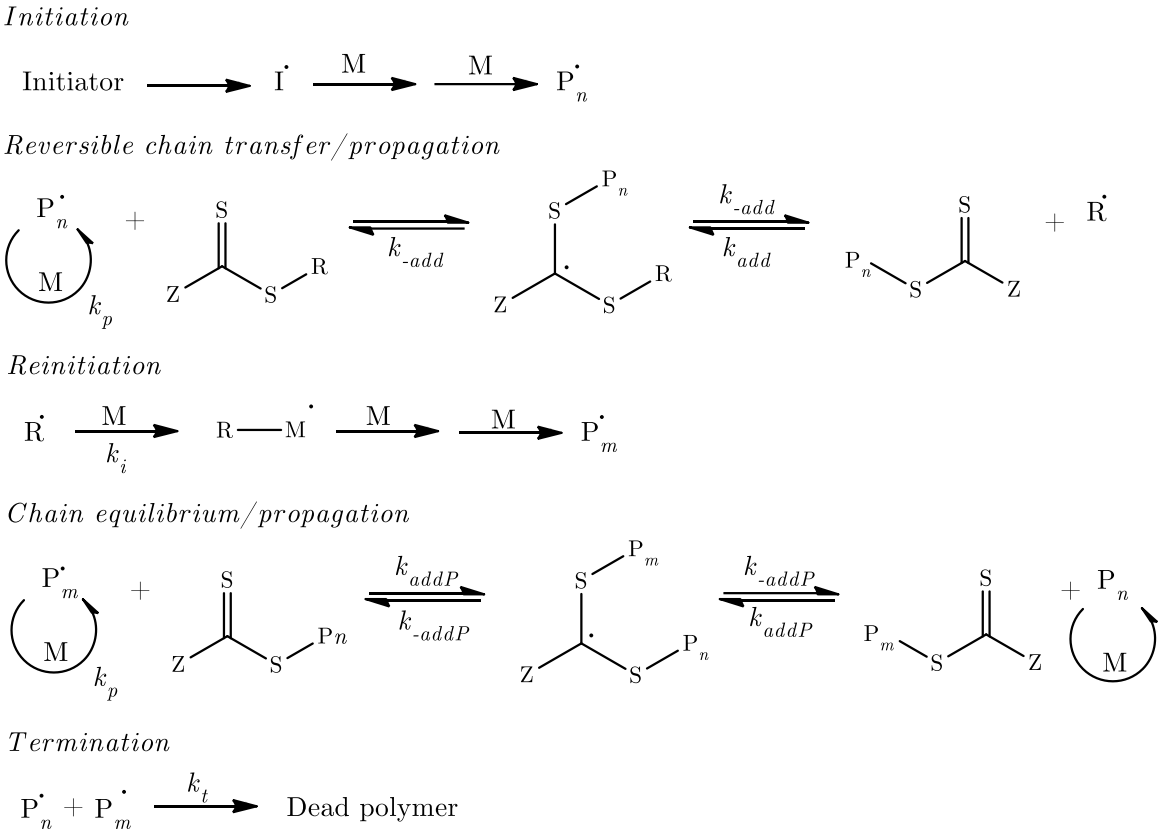

Scheme 3.1: Overall reaction for RAFT polymerization.

3.1.1 Trithiocarbonate RAFT groups

Trithiocarbonate RAFT groups generally exhibit the common RAFT mechanism displayed above. It should be noted that the R group must consist of a significant reactivity towards the growing polymer chain, above the reactivity of the Z group. The polymer growth using a RAFT agent is displayed by the blue dots in Figure 3.2.

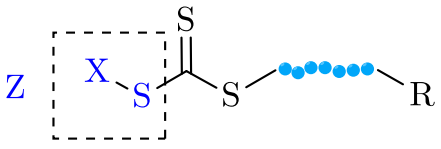

Figure 3.2: Trithiocarbonate RAFT group polymer growth.

The alkyl group of the thioalkyl is not sufficiently stabilized to undergo homolytic fragmentation. Hence, fragmentation will only take place on the R group and result in chain growth on either side of the sulphur double bond.

3.1.2 Initialization in RAFT-mediated polymerizations

An induction period describes the phase at the start of a polymerization where inhibition is observed – where no conversion can be observed. Rate retardation of polymerization refers to the reduction of the polymerization rate, *e.g.* in the presence of a RAFT agent, when compared to a conventional free radical polymerization. Over the last couple of years, the reason for retardation in RAFT polymerization has been discussed.[7,24–26] Perrier *et al.* reported that the origin for inhibition often experienced in RAFT polymerizations are either related to the leaving group of the RAFT group or to slow fragmentation of the intermediate macro-RAFT radical.[27] They concluded that slow fragmentation is the most probable reason for inhibition. In 2004, McLeary *et al.*[3,28] concluded that an initialization period exists, where the RAFT agent is converted to a single monomer adduct before the polymerization proceeds. Recently, Gao *et al.* reported that a reason for rate retardation in RAFT polymerizations can be ascribed to the cross-termination reaction between intermediate radicals and additional active radicals.[25] Van den Dungen proposed mechanisms regarding inhibition and rate retardation, observed in RAFT-mediated polymerizations.[29] These phenomena are known as initialization, intermediate radical termination and slow fragmentation and are displayed in Scheme 3.2.

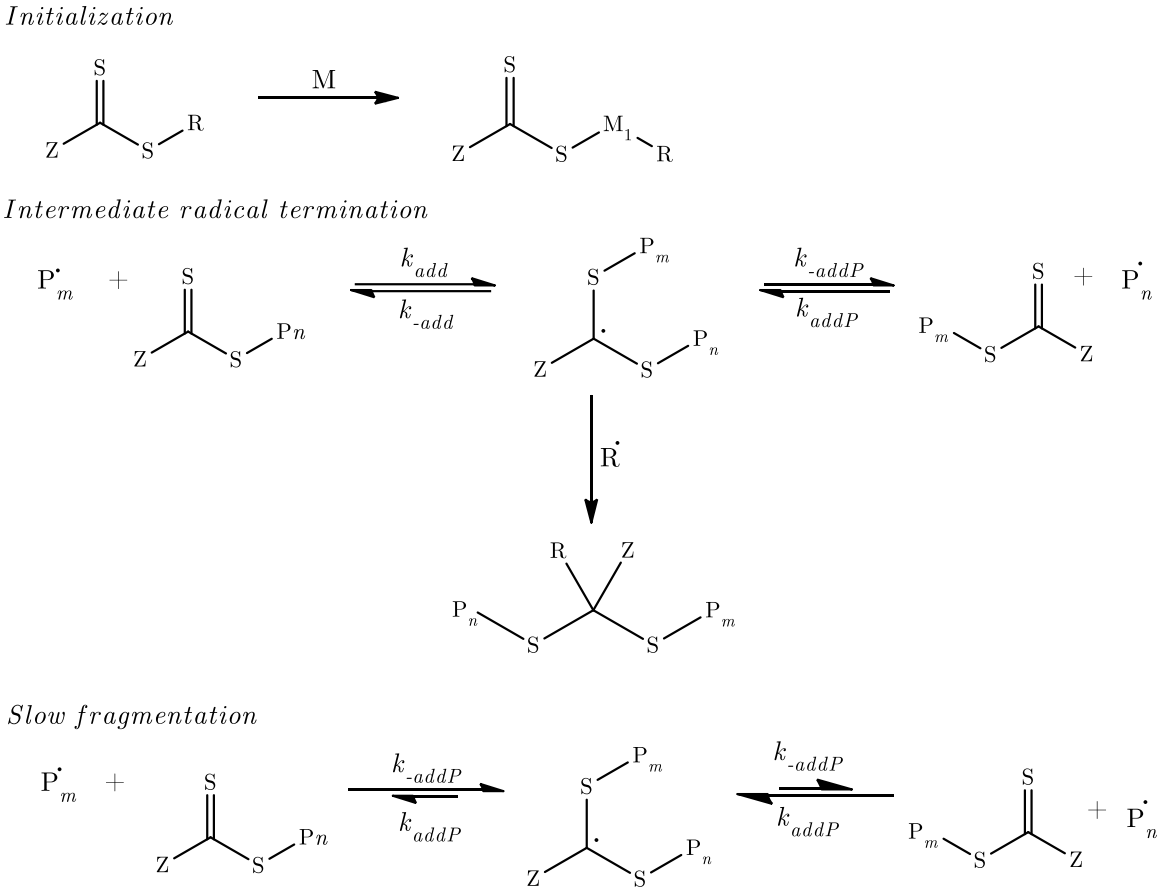

Scheme 3.2: Proposed inhibition and rate retardation mechanisms in RAFT polymerization.[29]

The initialization phenomenon was first published by McLeary *et al.* in 2004.[1,28] They concluded that initialization, *i.e.* the selective first monomer insertion in a RAFT agent, is the mechanistic cause of previously reported inhibition at the start of a RAFT-mediated polymerization. This conclusion was drawn after monitoring the reaction using *in-situ* ^{1}HNMR spectroscopy. The initialization period is characteristic to the early stages of polymerization. It refers to a single monomer adduct (also known as a macro-RAFT agent) that is formed before the polymerization proceeds. This means that the RAFT agent (selectively) inserts one

monomer unit into itself. This selectivity is determined by strong chain length dependence of the relevant rate constants. McLeary *et al.* differentiated amongst the rate constants of the addition of the R group radical to the monomer and the propagation of the monomer to support their findings.[28]

The initialization periods of various RAFT agents depend on the combination of monomer and RAFT agent used, and has been extensively studied by van den Dungen *et al.*[4] It has been found that in a Sty/MAnh copolymerization, the cumyl leaving group of cumyl dithiobenzoate (CDB) preferentially adds to the MAnh monomer. After the initialization period (when the first monomer adduct has formed), the polymerization of the polymer chain begins when the second monomer adduct is formed – *i.e.* when the first Sty monomer is consumed. Van den Dungen *et al.* also found sufficient results to dismiss the so-called induction period, as a rate retardation phenomena, observed with RAFT polymerization, by replacing it with the initialization period.[2,4]

3.2 Experimental details

3.2.1 Chemicals

MAnh was purified via sublimation (estimated purity of 99 % by ^{1}H NMR) (Merck). Styrene was purified via fractional distillation (estimated purity of 100 % by ^{1}H NMR) or the inhibitors were removed by washing the styrene with a KOH solution and passing it through a basic alumina column (Sigma-Aldrich). 1,1′-Azobis(cyclohexanecarbonitrile) (VAZO 88®) and 2,2′-azobis(2-methylpropionitrile) (AIBN) were recrystallized from ethanol, filtered and dried under vacuum at room temperature for 24 hours (estimated purity of 95 % and 98

% by ^{1}H NMR, respectively) (Merck). DMF and $CDCl_3$-d1 were used as received (Sigma-Aldrich), and DMSO-d6 was bought from MagniSolv.

3.2.2 Characterization

^{1}H - and ^{13}C NMR spectroscopy spectra were obtained with Varian VXR-Unity (400 MHz and 300 MHz) spectrometers at various temperatures.

^{1}H NMR *in-situ* spectroscopy was performed on a 400 MHz Varian Unity Inova spectrometer. The ^{1}H NMR spectra were acquired with a 3 µs (40°) pulse width and a 4 seconds acquisition time.

3.2.3 Synthesis of RAFT agents

For this study, four RAFT agents were used, namely CDB, *S*-cumyl phenyldithioacetate (CPDA), *S*-butyl-*S*'-(1-phenyl ethyl) trithiocarbonate (BPT) and *S*-*n*-butyl *S*'-(2-phenylpropan-2-yl) trithiocarbonate (BPPT). Three of the methods used to synthesize the RAFT agents (CDB, CDPA and BPT) are found in literature.[30–32] No evidence of the synthesis of BPPT could be found in literature. Therefore, it is described in this section. The synthesis of BPPT is similar to that of BPT, but requires 2-bromo-2-phenyl propane as a starting material.

3.2.3.1 Synthesis of 2-bromo-2-phenyl propane

Equimolar amounts of hydrobromic acid (HBr) and alpha methyl styrene were used. HBr (6.846 g, 84.611 mmol) was added dropwise to alpha methyl styrene (8.801 g, 74.535 mmol) in dry diethyl ether (35 mL) and left to stir overnight at room temperature. The formation of the product was confirmed by ^{1}H NMR spectroscopy by comparing the starting reagents with the products. The consumption of the reagents was also monitored by thin layer chromatography (TLC). Excess solvent

was removed under reduced pressure and purification via column chromatography was performed to yield a brownish liquid (13.135 g, 89 %). ^{1}H NMR (300 MHz, $CDCl_3$) δ 7.37-7.27 (m, 5H, aromatic), 2.12 (s, 6H, CH_3). ^{13}C NMR (300 MHz, $CDCl_3$) δ: 146.6, 124.1 (2), 128.4 (2), 125.9, 46.1. The scheme is displayed in Scheme 3.3.

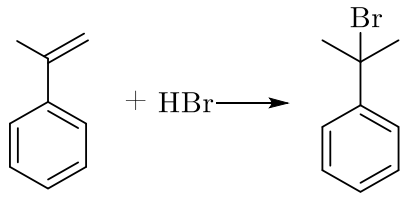

Scheme 3.3: Synthesis of 2-bromo-2-phenyl propane.

3.2.3.2 Synthesis of *S*-*n*-butyl *S'*-(2-phenylpropan-2-yl) trithiocarbonate

A mixture containing 1-butanethiol (5.010 g, 0.056 mol) and carbon disulfide (8.450 g, 0.111 mol) in THF (33.34 mL) was added to a round bottom flask while triethyl amine (TEA) (11.217 g, 0.111 mol) was added drop wise and stirring commenced at room temperature. The solution became orange as addition proceeded. Upon complete addition, the mixture was stirred at room temperature for a further 3 hours. 2-Bromo-2-phenyl propane (10.067 g, 0.051 mol) was added to the solution in a drop wise manner and the mixture was stirred overnight at room temperature. The product was purified by flushing it through a flash column using petroleum ether (PET) as solvent. The filtrate was concentrated by applying vacuum at 40 °C. Workup for S-n-butyl S'-(2-phenylpropan-2-yl) trithiocarbonate (BPPT) yielded a yellow-orange oil. ^{1}H NMR (300 MHz, $CDCl_3$) δ 7.37-7.27 (m, 5H, aromatic), 3.17 (t, 2H, S-CH 2), 2.11 (q, 2H,-CH2-CH 2-), 1.92 (s, 6H, CH_3), 1.48 (m, 2H, -CH2CH2-CH 2-), 0.82 (t, 3H, -CH2CH2-CH2-CH 3). ^{13}C NMR (300 MHz, $CDCl_3$) δ: 221.86, 144.44, 127.99 (2), 126.48 (2), 125.33, 57.97, 36.02, 29.70, 29.17 (2), 21.93, 13.49.

The formation and purity of the product were estimated using ^{1}H NMR spectroscopy with a purity of 98 %.

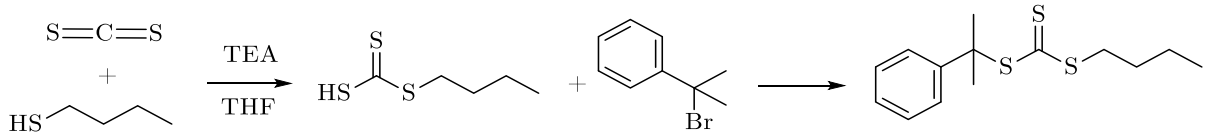

Scheme 3.4: Synthesis of BPPT.

3.2.4 RAFT-mediated copolymerization reactions

The kinetics and consumption of monomers of the reactions were investigated using *in-situ* ^{1}H NMR spectroscopy. Where ^{1}H NMR spectroscopy was not used, the consumption of monomers was monitored by taking samples throughout the reaction and performing ^{1}H NMR spectroscopy individually on the samples.

3.2.4.1 *In-situ* RAFT-mediated copolymerization

For a typical *in-situ* ^{1}H NMR spectroscopy experiment, styrene (0.141 g, 1.354 mmol), maleic anhydride (0.065 g, 0.663 mmol), CDB (0.182 g, 0.669 mmol), VAZO 88® (0.0329 g, 0.0135 mmol), 1,3,5-trioxane (0.0197 g, 0.219 mmol), DMF (0.150 g, 2.052 mmol) and d_6-DMSO (0.201 g, 2.573 mmol) were accurately weighed, homogenized and transferred to an NMR tube. The oxygen present in the reaction mixture was removed by performing four freeze-pump-thaw cycles (the first cycle consisted of 30 minutes, followed by a cycle of 20 minutes, followed by a cycle of 10 minutes and lastly followed by a cycle of 5 minutes) on the sample. After the last cycle, the tube was backfilled with N_2 gas. The reaction was carried out at 80 °C in order to obtain information about the early stages of monomer addition.

The sample was inserted into the magnet at 25 °C where sufficient shimming was conducted on the sample. A reference spectrum was collected at 25 °C. After removal

of the sample, the cavity of the magnet was heated to the desired temperature. Upon stabilization, the sample was re-introduced into the cavity of the magnet at elevated temperature, where additional shimming was performed in order to establish optimum conditions. The first spectrum was collected approximately 2 minutes after re-insertion of the sample. Phase – and baseline correction, as well as integration of the spectra acquired were carried out manually using either MestReNova 11.0.1 or ACD Labs 10.0 ^{1}H processor. The data was transferred and plotted in OriginPro 8.5.

The same experiment was conducted at 120 °C.

3.2.4.2 *In-situ* RAFT mediated homopolymerization of Sty

Styrene (0.210 g, 2.016 mmol), CDB (0.182 g, 0.669 mol), VAZO 88® (0.0329 g, 0.0135 mmol), (0.0197 g, 0.219 mmol), DMF (0.150 g, 2.052 mmol) and d_6-DMSO (0.163 g, 2.087 mmol) were accurately weighed off, homogenised and transferred to an NMR tube. The oxygen was removed by performing four freeze pump thaw cycles (the first cycle consisted of 30 minutes, followed by a cycle of 20 minutes, followed by a cycle of 10 minutes and lastly followed by a cycle of 5 minutes). The same procedure was followed as discussed in Section 3.2.4.1. The reaction was carried out at 120 °C and a spectrum was taken every 2 minutes. The reaction was left to run for 13 hours in order to determine the amount of Sty that is consumed.

3.3 Results and discussion

The effect of the RAFT agent on the polymerization kinetics is determined using ^{1}H NMR *in-situ* spectroscopy. This allows for full monitoring of the concentration profiles of all the species present in the reaction mixture at various stages of the polymerization.

Van den Dungen *et al.* have extensively studied the early stages of SMA copolymerization using CDB as RAFT agent. They found that during the initial stages of the polymerization, a macro-RAFT agent is formed as the cumyl leaving group preferentially adds to the MAnh monomer.[4] This macro-RAFT contains only one monomer unit and is capable of re-initiating the polymerization process. After the initialization period, the polymer chain starts to grow as the Sty monomer is inserted into the macro-RAFT.

Considering this, along with the rapid cross propagation between Sty and MAnh due to their small reactivity ratios, it is proposed that a system can be developed where a sequence-controlled polymer is synthesized with a target sequence of MAnh-Sty-Sty via the sequential addition of monomers. This belief relies on high conversions of the monomers used within a feasible time. Therefore, the focus of the chapter is on the determination of conditions that lead to high monomer conversion within two-three hours, with the focus on the RAFT agent that provided to yield the highest conversion of the Sty monomer.

3.3.1 Assignment of peaks for concentration profiles

In order to track the concentration profile of species in the reaction mixture, certain peaks need to be assigned. Figure 3.3 displays the ^{1}H NMR spectrum of the reaction mixture in the NMR tube before the reaction commenced. The peak at 4.5 ppm is assigned to 1,3,5-trioxane, which serves as an internal reference throughout the *in-situ* reactions of the various RAFT agents. The DMF solvent peaks are located around 2 ppm. The MAnh monomer peak could not be tracked, as it overlaps with the aromatic region. This peak can be seen in the aromatic region, as the highest peak. The consumption of MAnh occurs so swiftly, that even before the first spectrum was recorded at the polymerization temperature, the monomer peak disappears. The Sty monomer peak at 5.25 ppm was used to track the amount of

Sty monomer left in solution for all the RAFT agents, as this specific monomer peak was the only one that did not experience any peak overlapping towards the end of the reaction. Figure 3.3 displays the various RAFT agents before the reaction commenced.

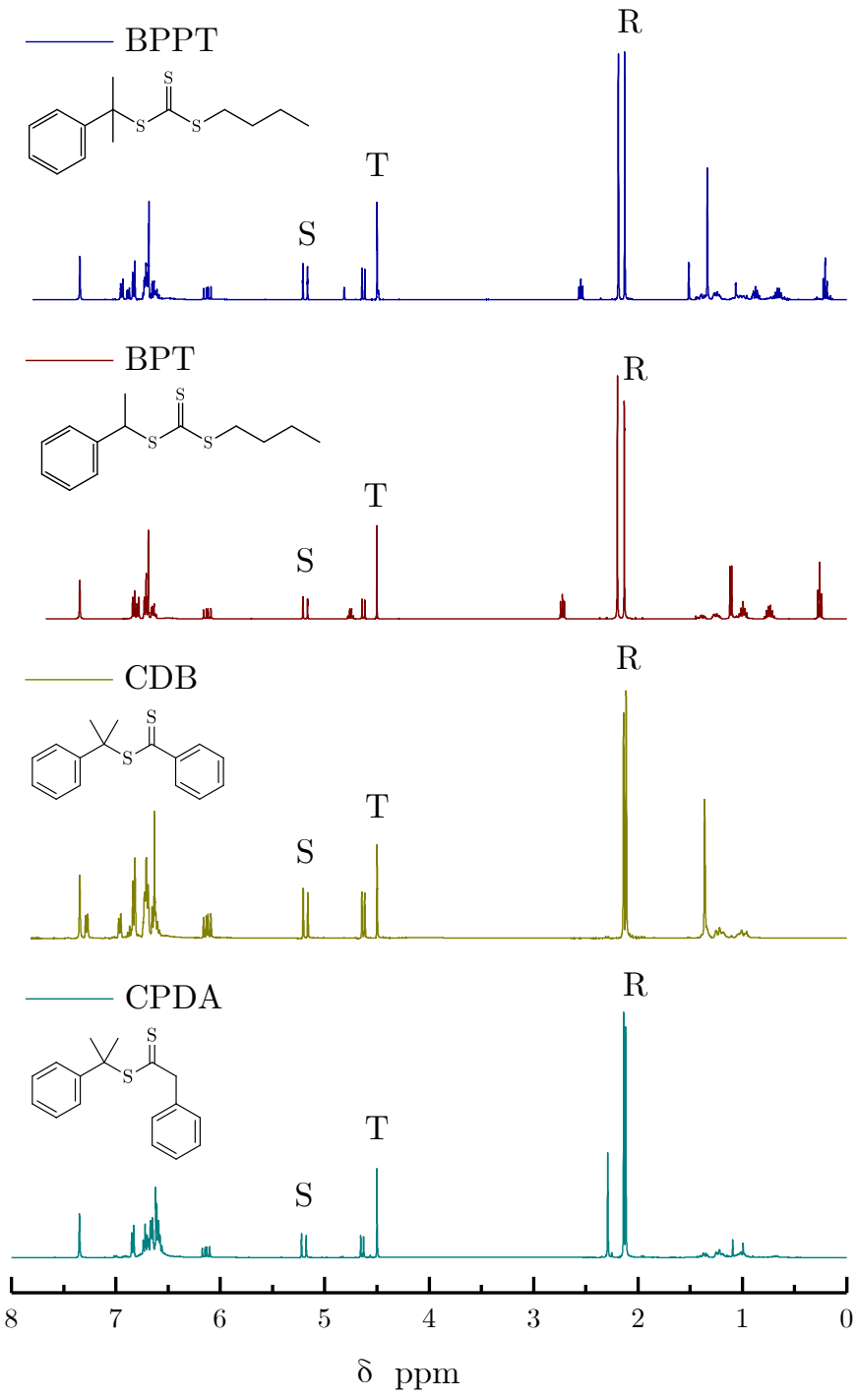

Figure 3.3: Peaks used for the assignment for the tracking of the various RAFT species in solution during the reactions done at 80 °C and 120 °C. The aromatic region also contains a signal corresponding to 5 protons of the Sty monomer. These peaks do not show the first adduct that forms, only the peak used for the total RAFT percentage (labelled R). The peaks labelled T are the internal reference and the peaks labelled S are the Sty monomer peaks used.

3.3.2 RAFT mediated polymerization using various RAFT agents

Four RAFT agents were used to investigate the Sty consumption throughout a polymerization reaction.

Figure 3.4 displays the conversion of Sty versus time plots for the respective RAFT agents at 80 °C. In order to investigate the effect of temperature on the consumption of the Sty monomer, the same reactions were employed at 120 °C. These results are displayed in Figure 3.6.

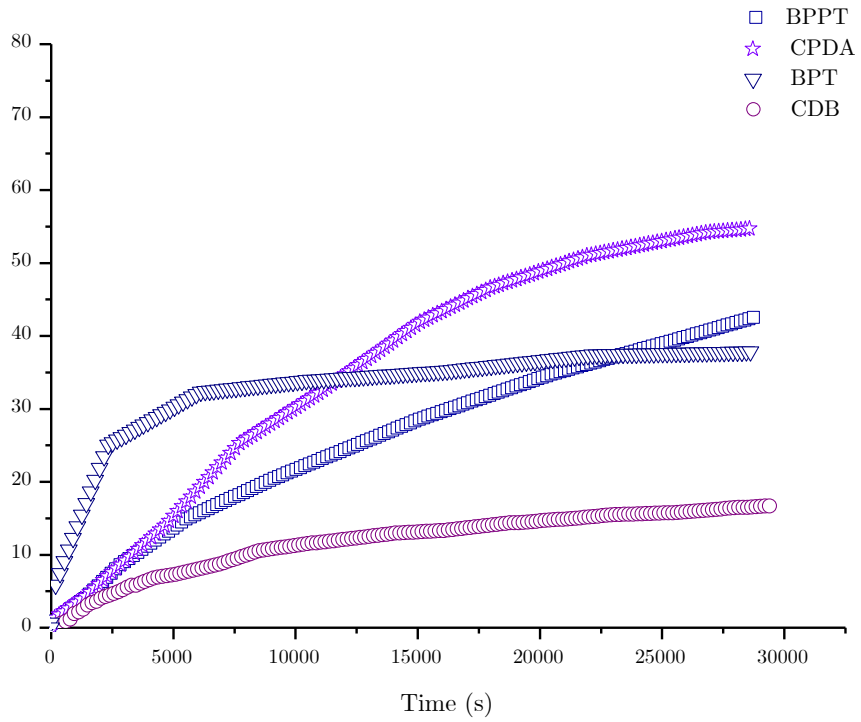

Figure 3.4: Conversion vs. time plot of Sty for CDB, BPT, BPPT and CPDA at 80 °C with a targeted monomer consumption of three units (one MAnh followed by two Sty units). A spectrum was taken every 3 minutes for 9 hours.

For the reaction carried out at 80 °C with CDB, the consumption of even one Sty monomer appeared to be extremely slow. Van den Dungen showed that the cumyl leaving group of CDB, preferentially adds to the MAnh monomer.[29] This results in the formation of a macro-RAFT as displayed in Figure 3.5. He showed that after approximately 35 minutes at 60 °C, the RAFT agent has been fully converted to the macro-RAFT.

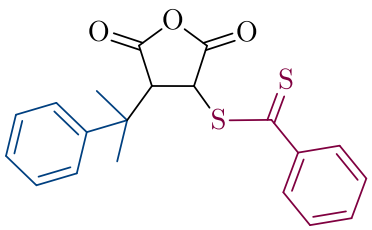

Figure 3.5: Macro-RAFT formed with MAnh monomer.

In Figure 3.4, sharp inflection points can be seen for the reaction with BPT as RAFT agent. The total percentage of RAFT species in the polymerization mixture were tracked in order to determine adduct formation (discussed in more detail in the section following). The total RAFT agent percentage plotted as a function of time can be seen in Appendix A. There exist no such inflection points on the figure shown, however after about 30 % of the RAFT agent is used, the rate of consumption decreases. The inflection points can, therefore, be ascribed to a processing error (as the chemical shifts of the peaks change slightly as the reaction proceeds). A further investigation is however needed to determine exactly what is happening as the conversion rate decreases.

Due to the low Sty monomer conversions obtained at 80 °C, the same reaction was carried out at 120 °C. For the reaction employed at 120 °C, the conversion of the macro-RAFT to the first Sty adduct, has already occurred before the first spectrum was acquired.

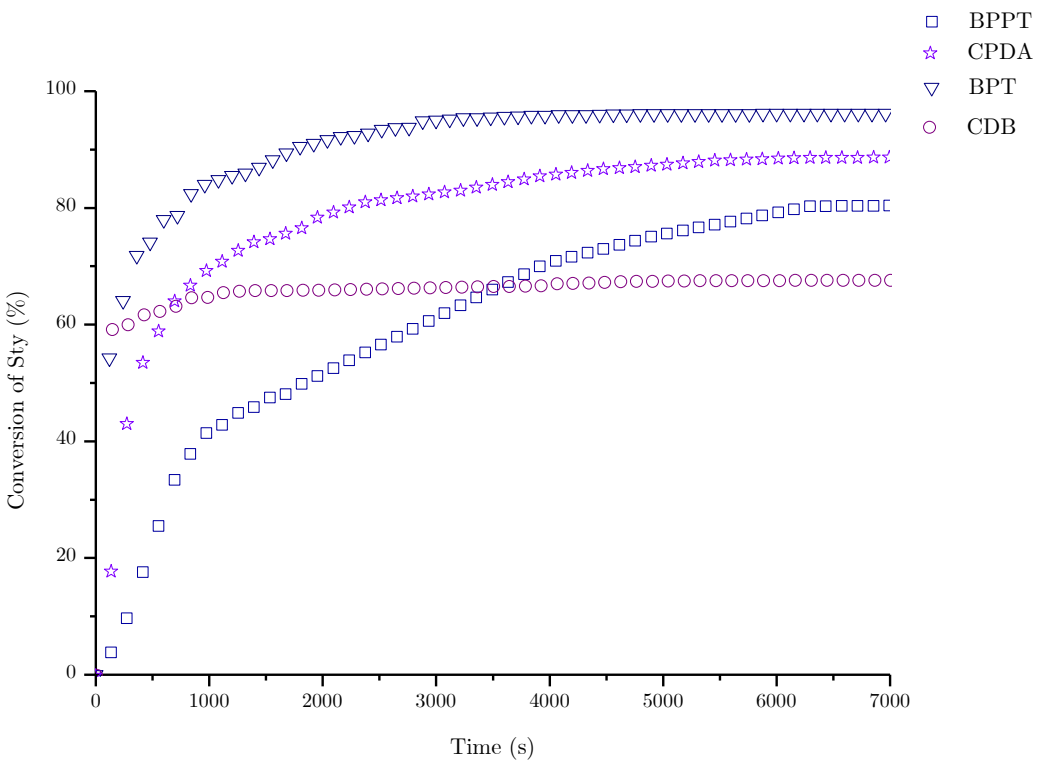

Figure 3.6: Conversion vs. time plot of STY for CDB, BPT, BPPT and CPDA at 120 °C with a targeted monomer consumption of three units (one MAnh followed by two Sty units). A spectrum was taken every minute for 2 hours. The outliers were removed.

The reactions employed at 80 °C provide detailed information of the consumption of monomers, during the early stage of the polymerization, and adducts that form as the time evolves. The half-life of VAZO 88® at 80 °C is approximately 33 hours, while at 120 °C it is equal to 24 minutes.[33] The most significant difference between the two reactions is that an increase in the temperature of the reaction, did not lead to an increase in the amount of Sty consumed while using CDB as RAFT agent.

For the reaction at 120 °C, the first Sty monomer addition happens rapidly, as is expected due to the reactivity ratios of the two monomers and the high rate of cross propagation. The kinetics of the reaction change drastically after the first Sty

addition, resulting in either an inhibition or retardation of the consumption of the second Sty monomer. This is unexpected at such high temperatures and an investigation of varying the R and Z group of the RAFT agent was done.

The same reaction was done with CPDA as RAFT agent. The same plot is not obtained for CPDA as for CDB. From Figure 3.4 it can be seen that CPDA is in fact the RAFT agent that results in the highest conversion of the Sty monomer at 80 °C. It is, therefore, clear that the inhibition observed with CDB is not present in the reaction done with CPDA. A slight change in the slope of Sty conversion is observed when using CPDA as RAFT agent after the consumption of circa. 25 % of Sty monomer.

This indicates that the rate of Sty consumption, after approximately half of the original RAFT agent has been converted to the single monomer adduct, decreases.

For the employment of BPT, it is evident that the Sty monomer is essentially completely consumed when using BPT as transfer agent at 120 °C (see Figure 3.7).

The high conversion of Sty with BPT as RAFT agent at 120 °C, along with other preliminary studies (see Chapter 4) provides evidence that BPT can be used to synthesize a sequence-controlled copolymer of Sty and MAnh. The basis of synthesizing sequence-controlled in this study relies on sequential addition of monomers, after successful consumption of the previous addition of monomers. Therefore, it is important to choose a RAFT agent that provides high (if not complete) conversion of both monomers. Overall, BPT proved to be the most promising RAFT agent to synthesize the desired sequence-controlled copolymer. For the polymerization with BPT as RAFT at 120 °C, the formation of the macro-RAFT (P-MAnh-BT) happens so swiftly that even before the first spectrum is acquired after re-insertion, the formation of the macro-RAFT agent had occurred

(see Figure 3.7). The second adduct, P-MAnh-Sty-BT, has also already reached its maximum concentration before the first spectrum is acquired. RAFT mediated polymerization using BPPT as transfer agent was also employed. The reason for experimenting with yet another RAFT agent, was due to the fact that the second adduct forms so swiftly with CDB. Again, this is due to the swift addition of the cumyl leaving group to the MAnh, followed by the addition to the Sty which appears to happen almost instantly. The promising results obtained with BPT, resulted in the hypothesis that the use of a cumyl leaving group, combined with a trithio RAFT group should result in swift consumption of both monomers. The use of BPPT provided similar results to BPT, but with lower Sty conversion. It appears that it takes longer for a Sty unit to be inserted into the RAFT agent, compared to BPT. These results assist in the dismissal of the previously stated hypothesis. Therefore, although BPPT proved to be a suitable option, the effortless synthesis and purification of BPT resulted in the continuation of the study with this RAFT agent.

During the reaction, the total percentage of RAFT species was monitored along with adducts that form. To track the total percentage of RAFT species, a well-defined peak was used, that didn't exhibit any overlap with other peaks. This was only done for BPT, as it yielded the highest Sty conversions. The inability of the other RAFT agents (along with the possibility of side reactions) are discussed as future recommendations in Chapter 6. The focus was, therefore, now on using BPT as RAFT agent. The peak used for the initial total RAFT percentage for BPT is present at the start of the reaction at a chemical shift of 1.7 ppm and 4 ppm and corresponds to 3 and 1 protons respectively.

Monitoring the total percentage of RAFT species allows for the assumption that no side reactions occur and that the only reaction the Sty undergoes, is insertion into the RAFT agents. Figure 3.7 shows the RAFT species versus reaction time for the

reaction employed with BPT at 120 °C. The first adduct formation (P-MAnh-BT) occurred so rapidly that it was not detected by the time the first spectrum was acquired. The second adduct (P-MAnh-Sty-BT) had already reached its maximum by the time the first spectrum was acquired. After 6000 seconds, the conversion of the second Sty monomer unit into the third adduct, slows down. Therefore, after 3 hours, a small amount of Sty monomer remains in solution.

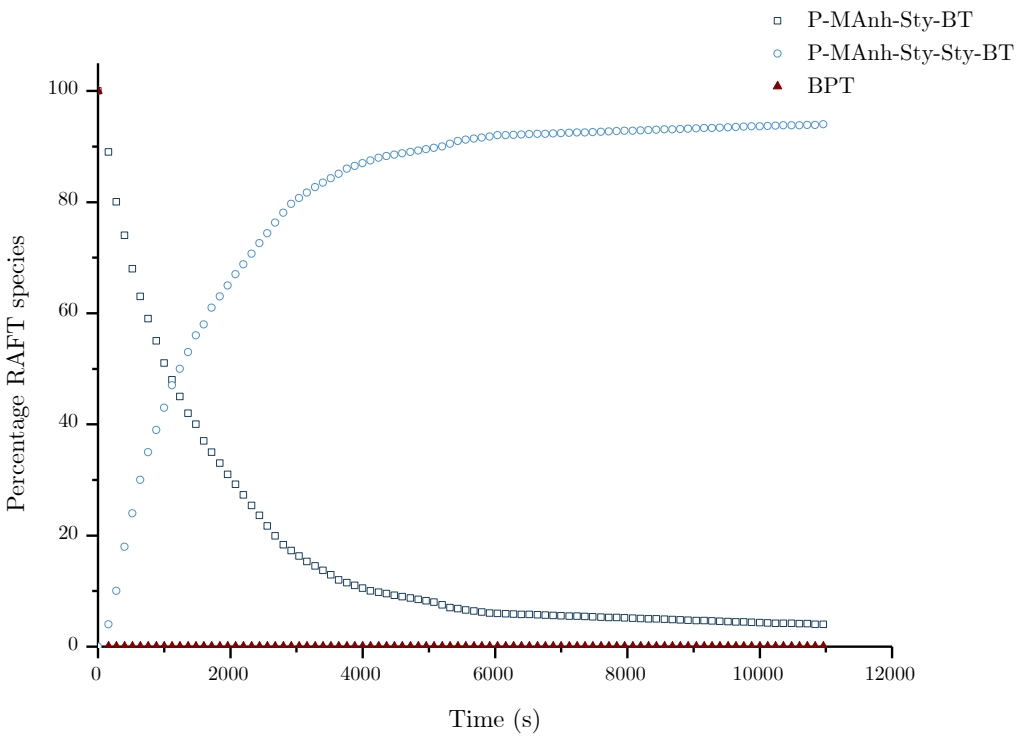

Figure 3.7: Total percentage of RAFT species as a function of time while monitoring adduct formation at 120 °C using BPT as RAFT agent. The figure displays the total amount of BPT, the second adduct (P-MAnh-Sty-BT) and the third adduct (P-MAnh-Sty-Sty-BT) that forms. The reaction was employed for 3 hours.

3.3.3 Effect of Sty polymerization on the kinetics of CDB and BPT

As discussed in Section 3.3.2, even a tremendous increase in the temperature during the polymerization mediated with CDB (with a 2:1 ratio of Sty to MAnh) did not lead to a higher Sty monomer conversion. For this reason, polymerizations

containing only Sty (with similar molar ratio to the RAFT agent than those reactions employed in the *in-situ* copolymerizations) were employed in order to determine the effect of both the absence of MAnh and the increase in Sty monomer concentration on the polymerization kinetics.

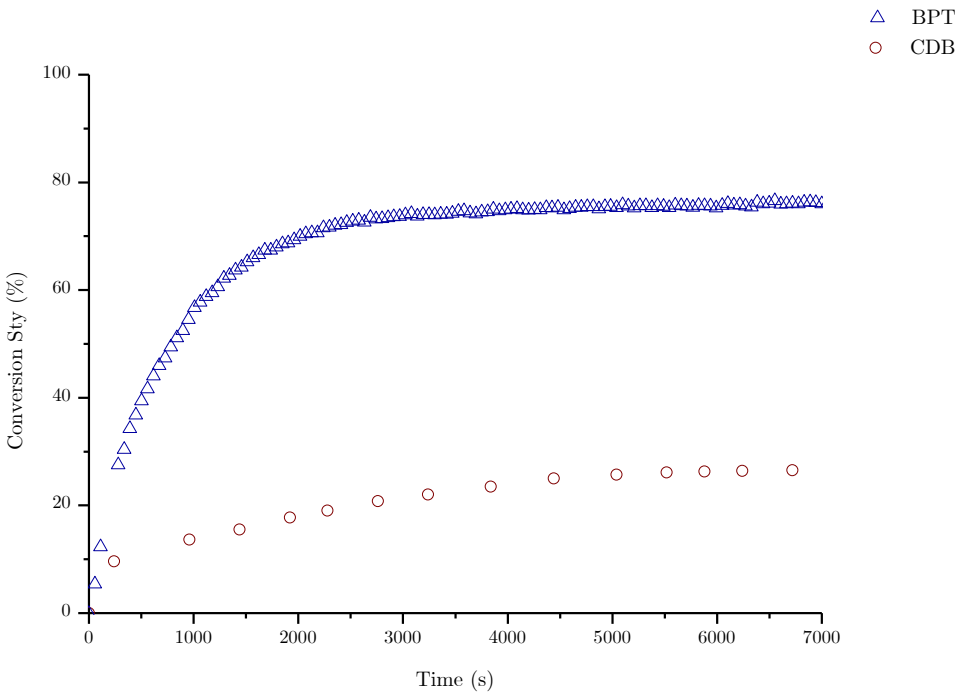

Figure 3.8: *In-situ* homopolymerization of Sty with CDB and BPT as RAFT agents at 120 °C with a 3: 1 Sty: RAFT ratio (in the absence of MAnh).

As can be seen in Figure 3.8, approximately 2/3 of the Sty monomer remains in the reaction mixture after 2 hours for the CDB RAFT agent. The polymerizations conducted with CDB (in Section 3.3.2) as RAFT agent showed that after the MAnh is completely consumed; one Sty monomer is added.

With regards to the structural differences of the monomers, it has previously been observed that the cumyl leaving group of CDB does preferentially add to the MAnh monomer due to the differences in electron densities of the cumyl group compared

to the MAnh.[2] Cross propagation of these two monomers has also been found to occur very swiftly.[34]

For the reaction done with BPT, approximately 80 % of the original Sty in the reaction mixture was consumed. As there were three Sty units relative to the RAFT agent, this showed that BPT is in fact capable of controlling the Sty polymerization beyond two Sty units, whereas with CDB, the retardation effect is tremendous as only approximately 30 % of the original amount of Sty is consumed after the same amount of time. McLeary *et al.* have investigated the RAFT polymerization kinetics and mechanisms regarding the initialization of Sty with CDB.[1] They concluded that the cumyl radical dominates the initialization phase which results in a noteworthy increase in the length of the initialization period, where the monomer consumption is significantly slower. They reported that a polymerization at 70 °C had an initialization period of 240 minutes and a polymerization at 84 °C had an initialization period of 50 minutes. The end of the initialization period is seen after the peak of the formation of the first adduct (C-Sty-DB) decreases. Figure 3.8 shows that after approximately 2 hours, the initial RAFT agent, when using CDB, has not been fully converted to the first adduct. This difference from the findings of McLeary *et al.* can be ascribed to the high RAFT to monomer ratio used in this study, as compared to the smaller ratio they used.

To monitor the formation of adducts and products in the reaction mixture, the relative concentration of all the relevant dithiobenzoate species were tracked. The integration of the methyl protons of the original RAFT group were monitored, as the original peak started to decrease as the macro-RAFT is formed. A constant dithiobenzoate count at any given point during the polymerization confirms that no side reactions occurred.

For CDB, at the end of the reaction, not all of the initial RAFT agent has been converted to the macro-RAFT that forms (in Appendix). The initial RAFT will be fully converted to the first monomer adduct, before the second monomer unit starts to grow the polymer chain. This confirms that one Sty monomer unit is being inserted into the RAFT agent at the end of the reaction.

It has been found that an increase in the RAFT concentration increases the time of the initialization period observed.[6] Due to the fact that an equimolar ratio of RAFT to MAnh is used, it is expected that the initialization period will be longer than for polymers with high targeted molecular weight.

CDB has been used to synthesize alternating copolymers of SMA.[2] These results show that a lower RAFT concentration decreases the initialization period. It also shows that Sty is consumed much faster as the ratio to MAnh increases when compared to a 2:1 ratio of Sty to MAnh. Due to the importance of controlling the sequence perfectly, equimolar amounts of RAFT to MAnh were used in this study.

3.4 Conclusion

The investigation of RAFT agents on the Sty monomer consumption provided detailed information to develop a system in order to synthesize a sequence-controlled polymer with a target sequence of (MAnh-Sty-Sty)$_n$. This is based on the fact that sequential addition of monomers will result in a copolymer where the sequence can be controlled, depending on the conversion of the monomers. Therefore, it is essential that the chosen RAFT agent should provide essentially complete consumption of the respective monomers.

It was found that only one unit of Sty is consumed when using cumyl dithiobenzoate (CDB). This did not persist with any of the other RAFT agents employed.

Therefore, a RAFT group with a cumyl R group and a phenyl group directly adjacent to the thiol group is not suitable for a system where RAFT, MAnh and Sty are present in a 1:1:2 molar ratio to synthesize a sequence-controlled polymer. Based on the work done by van den Dungen *et al.* it was expected that a RAFT group containing a cumyl leaving group would have faster polymerization rates, as the macro-RAFT is formed very quickly.[4] It should be noted that based on the work done, this is not the case for a 2:1 ratio of Sty to MAnh. Even though the MAnh is added to the RAFT agent rapidly when using CDB as RAFT, and even though the cross propagation of the first Sty monomer is also rapid (in fact the fastest of all the RAFT agents employed in this study), the addition of the second Sty is basically absent.

Both *S*-cumyl phenyldithioacetate (CPDA) and *S*-*n*-butyl *S'*-(2-phenylpropan-2-yl) trithiocarbonate (BPPT) proved to be worthy candidates, but with a longer reaction time to reach as high conversion as with BPT. It can be concluded that BPT is the most suitable RAFT agent for attempting to synthesize a sequence-controlled polymer, due to the high Sty conversion. It is not feasible to use any RAFT agent that does not allow complete consumption of any monomer.

Although BPPT and CPDA also provided promising results, BPT not only provided the highest Sty consumption, but the synthesis and the purification of the RAFT agent is rather effortless compared to the other RAFT agents. Therefore, it is proposed that BPT would be the most suitable RAFT agent to synthesize a sequence-controlled copolymer of Sty and MAnh with a target sequence of MAnh-Sty-Sty.

References

1. McLeary, J. B., Calitz, F. M., Mckenzie, J. M., Tonge, M. P., Sanderson, R. D. & Klumperman, B. *Macromolecules* 2005, *38*, 3151–3161
2. Klumperman, B., Mcleary, J. B., Van Den Dungen, E. T. A. & Pound. *Macromol. Symp.* 2007, *248*, 141–149
3. McLeary, J. B., Calitz, F. M., McKenzie, J. M., Tonge, M. P., Sanderson, R. D. & Klumperman, B. *Macromolecules* 2004, *37*, 2383–2394
4. Van Den Dungen, E. T. A., Matahwa, H., McLeary, J. B., Sanderson, R. D. & Klumperman, B. *J. Polym. Sci. Part A Polym. Chem.* 2008, *46*, 2500–2509
5. Drache, M. & Schmidt-Naake, G. *Macromol. Symp.* 2008, *271*, 129–136
6. Drache, M. & Schmidt-Naake, G. *Macromol. Symp.* 2007, *259*, 397–405
7. Barner-kowollik, C. *Handbook of RAFT Polymerization*, First edition, 2008, ISBN: 9783527319244
8. Moad, G., Rizzardo, E. & Thang, S. H. *Australian Journal of Chemistry* 2005, *58*, 379–410
9. Chong, B. Y. K., Krstina, J., Le, T. P. T., Moad, G., Postma, A., Rizzardo, E. & Thang, S. H. *Macromolecules* 2003, *36*, 2256–2272
10. Chiefari, J., Mayadunne, R. T. A., Moad, C. L., Moad, G., Rizzardo, E., Postma, A., Skidmore, M. A. & Thang, S. H. *Macromolecules* 2003, *36*, 2273–2283
11. Moad, G., Chong, Y. K., Postma, A., Rizzardo, E. & Thang, S. H. *Polymer* 2005, *46*, 8458–8468
12. Rizzardo, E., Chiefari, J., Chong, B. Y. K., Ercole, F., Krstina, J., Jeffery, J., Le, T. P. T., Mayadunne, R. T. a., Meijs, G. F., Moad, C. L., Moad, G. & Thang, S. H. *Macromol. Symp.* 1999, *143*, 291–307
13. Rizzardo, E., Chiefari, J., Mayadunne, R. T. A., Moad, G. & Thang, S. H. *In Controlled/Living Radical Polymerization*, First edition, 2000, ISBN: 9780841237070
14. Semsarilar, M. & Perrier, S. *Nat. Chem.* 2010, *2*, 811–820
15. Chong, B. Y. K., Le, T. P. T., Moad, G., Rizzardo, E. & Thang, S. H.

Macromolecules 1999, *32*, 2071–2074

16. Albertin, L. & Cameron, N. R. *Macromolecules* 2007, *40*, 6082–6093
17. Perrier, S., Takolpuckdee, P., Westwood, J. & Lewis, D. M. *Macromolecules* 2004, *37*, 2709–2717
18. Vosloo, J. J., Tonge, M. P., Fellows, C. M., D'Agosto, F., Sanderson, R. D. & Gilbert, R. G. *Macromolecules* 2006, *37*, 2371–2382
19. De Brouwer, H., Schellekens, M. A. J., Klumperman, B., Monteiro, M. J. & German, A. L. *J. Polym. Sci. Part A Polym. Chem.* 2000, *38*, 3596–3603
20. Quinn, J. F., Chaplin, R. P. & Davis, T. P. *J. Polym. Sci. Part A Polym. Chem.* 2002, *40*, 2956–2966
21. Moad, G., Rizzardo, E. & Thang, S. H. *Polymer* 2008, *49*, 1079–1131
22. Moad, G., Rizzardo, E. & Thang, S. H. *Aust. J. Chem.* 2006, *59*, 669
23. Bathfield, M., D'Agosto, F., Spitz, R., Ladavière, C., Charreyre, M. T. & Delair, T. *Macromol. Rapid Commun.* 2007, *28*, 856–862
24. Gao, Y., Lv, L., Zou, G. & Zhang, Q. *Macromol. Res.* 2017, *25*, 931–935
25. Vana, P., Davis, T. P. & Barner-Kowollik, C. *Macromol. Theory Simulations* 2002, *11*, 823–835
26. Lu, L., Zhang, H., Yang, N. & Cai, Y. *Macromolecules* 2006, *39*, 3770–3776
27. Perrier, S., Barner-Kowollik, C., Quinn, J. F., Vana, P. & Davis, T. P. *Macromolecules* 2002, *35*, 8300–8306
28. McLeary, J. B., McKenzie, J. M., Tonge, M. P., Sanderson, R. D. & Klumperman, B. *Chem. Commun.* 2004, *6*, 1950–1
29. Van Den Dungen, E. T. A. *Self-healing coatings based on thiol-ene chemistry* 2009, PhD, Stellenbosch University
30. Barner-Kowollik, C., Quinn, J. F., Nguyen, T. L. U., Heuts, J. P. A. & Davis, T. P. *Macromolecules* 2001, *34*, 7849–7857
31. Thang, S. H., Chong, B. Y. K., Mayadunne, R. T. A., Moad, G. & Rizzardo, E. *Tetrahedron Lett.* 1999, *40*, 2435–2438
32. Le, T. P. T., Moad, G., Rizzardo, E. & Thang, S. H. 1998, WO/1998/001478

33. DeVito, S. C. in *Kirk-Othmer Encyclopedia of Chemical Technology,* Fifth edition, 2007, ISBN: 9780471484967

34. Musa, O. M. *Handbook of Maleic Anhydride Based Materials: Syntheses, Properties and Applications,* First edition, 2016, ISBN: 9783319294544

Chapter 4

Synthesis of sequence-controlled SMA

A sequence-controlled copolymer of styrene (Sty) and maleic anhydride (MAnh) with a target sequence of MAnh-Sty-Sty (SSM) (refer to Figure 4.1) was synthesized via reversible addition-fragmentation chain transfer (RAFT) polymerization. Preliminary studies allowed an efficient system to be developed with regards to monomer conversion and reaction time. *S*-Butyl *S*'-(1-phenyl-ethyl) trithiocarbonate (BPT) was found to be the best RAFT agent for this system, as the use of this RAFT agent resulted in the highest Sty monomer conversion after each monomer addition. The effortless synthesis process of this RAFT agent also served as an advantage. The synthesized polymer was thoroughly characterized by size exclusion chromatography (SEC), mass spectrometry (MS), ^{1}H nuclear magnetic resonance (NMR) and ^{13}C distortionless enhancement by polarization transfer (DEPT) NMR spectroscopy. Klumperman and O'Driscoll found results in their study that confirmed the penultimate unit model (PUM) is followed during the synthesis of styrene-maleic anhydride (SMA) copolymers, in contradiction to the complex participation model (CPM)[1]. This is of essential importance as the

proposed idea to synthesize sequence-controlled copolymers relies on the addition of one monomer at a time in order to maintain a perfectly sequence controlled polymer.

The polymer of interest was, therefore, synthesized by employing RAFT polymerization with a tailored polymerization process where monomers were sequentially added throughout the polymerization, at specific time intervals.

4.1 Sequence-controlled copolymers

The control of the monomer sequence in synthetic polymers still remains a demanding topic in modern polymer chemistry.[2–4] Therefore, the key to modern day macromolecular chemistry is to design attainable approaches to synthesizing these polymers.

The term 'sequence-defined' was introduced by Lutz[2,5–8] and the control of sequences has been intensively investigated by Lutz and co-authors.[2,5–12] Zydziak *et al.* describe that sequence-controlled species contain low dispersities along with a small window of uncertainty regarding the placement of monomer units in the polymer chain. While, sequence-defined species contain no dispersion along with a perfectly placed monomer along the polymer chain.[4] Various examples of sequence-controlled polymers have been reported over the last couple of years[13–19], where only a few examples have been reported of sequence-defined polymers with the same precision level as nature.[20]

As mentioned in Chapter 2, the desired sequence of the monomer system originated from expected properties and the controlled sequence relies on the reactivity ratios of the monomers and their tendencies to homo – and crosspropagate. Although it was initially believed that cumyl dithiobenzoate (CDB) would be a suitable RAFT agent based on the work done by van den Dungen *et al.*[21–23] (on an alternating

monomer system), the work described in Chapter 3, served as proof that this RAFT agent would not be suitable. After several preliminary studies, the most optimal system was developed with regards to RAFT agent and reaction time.

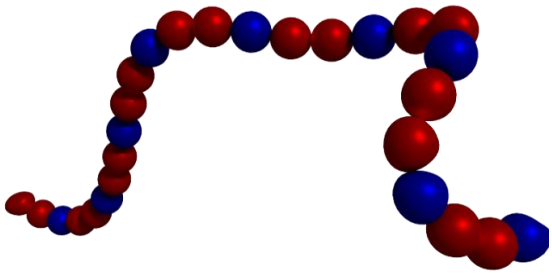

Figure 4.1: Predetermined sequence of MAnh (blue) followed by two Sty units (red). The model is courtesy of B. Klumperman.

4.1.1 Models describing the nature of SMA copolymers

There are different models describing the factors influencing the way monomer units are added to a growing polymer chain during a chain growth copolymerization. Various models has been used to describe the SMA copolymerization in the past.[1,24–27] Two of these models will be discussed briefly, namely the complex participation model (CPM) and the penultimate unit model (PUM.) The CPM has been used previously to describe copolymerization kinetics, monomer sequence distribution and copolymer composition. This specific model has been applied to explain the copolymerization of SMA frequently.

4.1.1.1 Complex participation model

It is generally known that electron acceptor and electron donor monomer pairs form charge-transfer complexes (CTCs), which is the case with Sty and MAnh.[26]

In this model, propagation reactions involve the addition of single monomers as well as CTCs, which is displayed as M_1M_2. The CPM mechanism is shown in Figure 4.2:

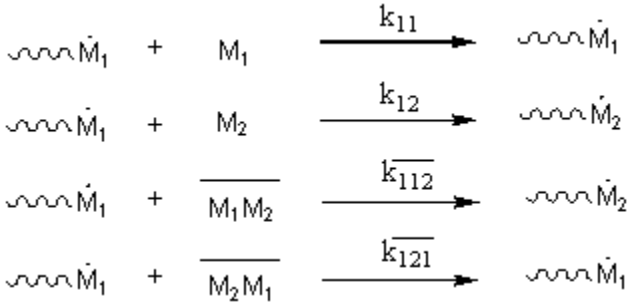

Figure 4.2: CPM for monomer 1.[26]

4.1.1.2 Penultimate unit model

In the penultimate unit model, the terminal monomer in a growing chain along with the penultimate unit, determine the rate constants of monomer addition for the two comonomers.[26] The PUM is shown in Figure 4.3:

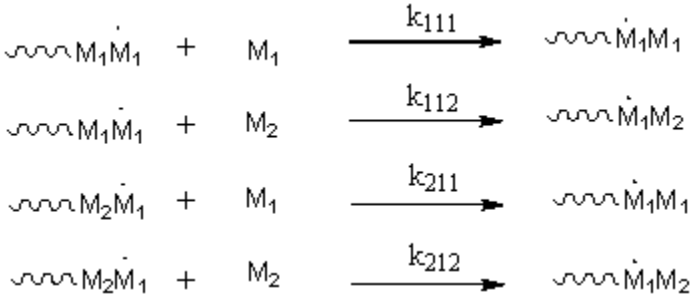

Figure 4.3: PUM for monomer 1.[26]

Klumperman reported that SMA copolymerization follows the PUM, where the monomer addition rate constants (for the respective comonomers) are determined by not only the terminal monomer within the growing polymer chain radical, but also by the penultimate unit.[26] This was confirmed by van den Dungen *et al.* as

they concluded that monomers are individually added to the growing chain.[22] These studies, along with the well-cited fact that the steric hindrance of MAnh causes the inability for homopolymerization of the monomer,[28] describes the alternating behaviour of SMA copolymers.

4.2 Experimental details

4.2.1 Characterization

^{13}C DEPT NMR spectra were recorded on approximately 10% w/v solutions in acetone-d6 using a Varian VXR-Unity (300 MHz) spectrometer.^{13}C $\pi/2$ pulse times were 22 and 15 μs respectively. Experiments were performed at 37 °C using a 2-s recycle time. This method is based on the work done by Barron *et al.*[29] The results were processed in MestReNova 11.0.1 and plotted in OriginPro 8.5.

MS was performed on a Waters Synapt G2 with Electron Spray Ionization (ESI) in the positive mode. A Waters UPLC C18, 2.1×100mm column was used.

Gel permeation chromatography (GPC) was performed in tetrahydrofuran (THF, HPLC-grade stabilized with BHT) on a setup consisting of a Waters 717 plus autosampler, Waters 600E system controller (run by Millennium^{32} V3.05 software), Waters 610 fluid unit connected to a Shimadzu LC-10AT pump. A Waters 2487 dual wavelength absorbance detector, operating at 320 nm and a Waters 410 differential refractometer were connected in series. A flow rate of 1 mL/min was maintained and the injection volume was 100 µL. The SEC system was calibrated using low dispersity polystyrene standards ranging from 800 to 2x10^6 g/mol.

All other characterization methods employed in this chapter are as described in Chapter 3.

4.2.2 Chemicals

SMA2000 was bought from Arkema (Elf Atochem) and used as received. The other chemicals used are as described in Chapter 3.

4.2.3 Preliminary studies of Sty monomer consumption with BPT as RAFT agent

Sty (0.416 g, 4.00 mmol), MAnh (0.195 g, 1.99 mmol), VAZO 88® (0.0489 g, 0.200 mmol) and BPT (0.301 g, 1.11 mmol) were accurately weighed off and transferred to a Schlenk flask containing a magnetic stirrer bar. 1,3,5-trioxane (0.737 g, 8.18 mmol) and 2 mL of dimethylformamide (DMF) were also added to the Schlenk flask, containing a magnetic stirrer bar. The trioxane served as an internal reference throughout the reaction. The reaction mixture was degassed in order to remove the oxygen present in the reaction mixture. An initial sample was taken before the flask was immersed in a pre-heated oil bath at 120 °C, where after several samples (with a sample size of 0.1 mL and at time intervals of 2 hours, 4 hours and 24 hours) were taken, using a gas-tight syringe, and ^{1}H NMR spectroscopy was performed on the samples.

4.2.4 RAFT-mediated polymerization of sequence-controlled SSM using BPT as RAFT agent

A tailored sequential addition (of monomers) polymerization were employed in order to synthesize the sequence-controlled copolymer. Sty (2.550 g, 24.490 mmol), MAnh (1.200 g, 12.224 mmol), VAZO 88® (0.607 g, 2.482 mmol) and BPT (3.349 g, 12.400 mmol) were accurately weighed off and transferred to a Schlenk flask containing a magnetic stirrer bar. 1,3,5-trioxane (0.456 g, 5.063 mmol) and 4 mL of DMF were also added to the Schlenk flask. An initial sample was taken in order to have a

reference to monitor the Sty monomer conversion during the experiment. The reaction mixture was degassed in order to remove the oxygen present. The flask was then immersed in a pre-heated oil bath at 120 °C. After three hours, a sample was taken, and analyzed. Sty (2.552 g, 24.503 mmol), MAnh (1.2083 g, 12.322 mmol), VAZO 88® (0.612 g, 2.505 mmol) and 1,3,5-trioxane (0.450 g, 4.998 mmol) were then accurately weighed off and transferred to a separate Schlenk flask, 4 mL of DMF was added and the solution was degassed. After removal of the oxygen in the solution, the solution was transferred to the original Schlenk flask using an air-tight syringe. After two hours, another sample was taken where after another addition was done. The method was repeated until a SSM sequence of $(SSM)_6$ (SSM2100) was obtained, therefore, a total of 6 monomer additions. Using the internal reference as a constant value, ^{1}H NMR spectroscopy was used to determine the Sty monomer conversion as a function of time. The polymer was isolated by precipitation in diethyl ether twice and dried at 40 °C in a vacuum oven, before performing SEC analysis on the samples.

A polymer containing $(SSM)_{13}$ (SMA4200) was also synthesized, to compare to the thermal properties of a copolymer synthesized via conventional radical polymerization (see Section 4.3.2.1) containing the same 30% MAnh content.

4.3 Results and discussion

4.3.1 Preliminary studies of Sty monomer consumption with BPT as RAFT agent

As mentioned in Chapter 3, BPT is the most suitable RAFT agent with regards to Sty monomer consumption and reaction time, to synthesize a sequence-controlled copolymer consisting of one MAnh unit followed by two Sty units.

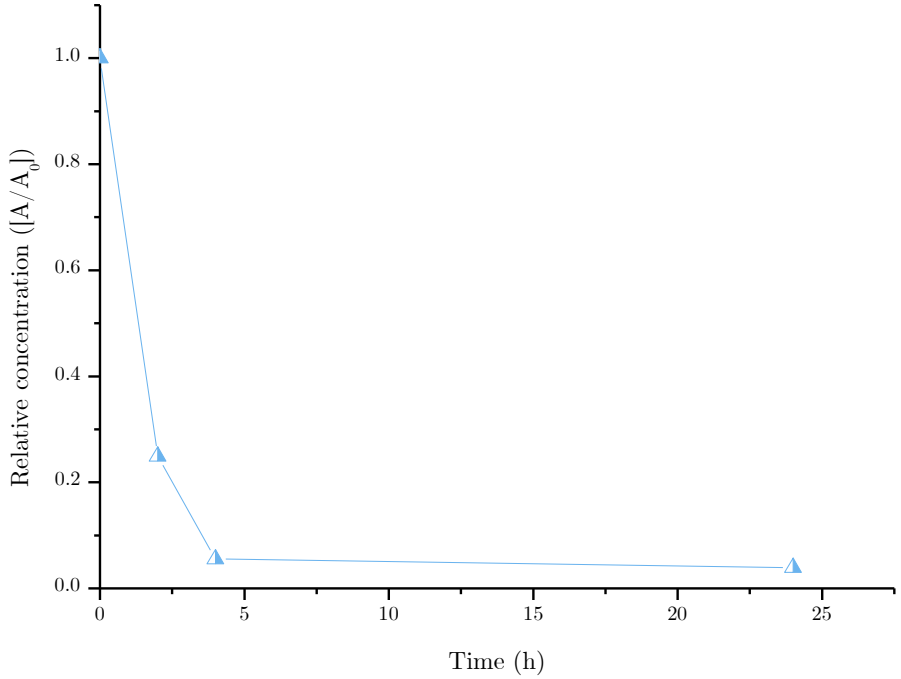

Figure 4.4: Sty monomer conversion plot for BPT as RAFT agent versus time. The reaction was done at 120 °C and samples were taken at 2 h, 4 h and 24 h. The ratio of Sty monomer to MAnh monomer is 2: 1.

From Figure 4.4, it is clear that 3 hours after the reaction commenced, the Sty monomer was essentially consumed. This is in good agreement with the *in-situ* results obtained in Chapter 3, Section 3.3.2.

4.3.2 Analysis and characterization of sequence-controlled SMA

As mentioned in Chapter 2, ^{13}C DEPT NMR spectroscopy is the only technique available to characterize the sequence of SMA copolymers in terms of the average value of Sty-centered triads in the methylene subspectrum.[29,30] This section explores ^{13}C DEPT NMR spectroscopy along with ^{1}H NMR spectroscopy as a tool for sequence determination of SMA copolymers, along with other methods to fully characterize the polymer synthesized.

Sequential addition of monomers, proves to be a worthy technique for the synthesis of sequence-controlled SMA. From ^{1}H NMR spectroscopy, the amount of residual monomer left after every addition, as well as the conversion could be determined from the crude samples. The first Sty addition (P-MAnh-Sty-BT) takes longer than any other addition to the growing polymer chain. The experiment was optimized by establishing sufficient times to add more monomers, which was done by tracking the remaining monomer concentrations by ^{1}H NMR spectroscopy. After three hours step one (the addition of one MAnh unit and two Sty units) was completed. For step two, after two hours, essentially a complete addition of another "round" of monomers were added (another MAnh followed by two Sty units).

In Figure 4.5 the Sty monomer consumption as a function of time is plotted, while several additions are made. The relative consumed Sty concentration before the following addition proceeded is also displayed as a percentage.

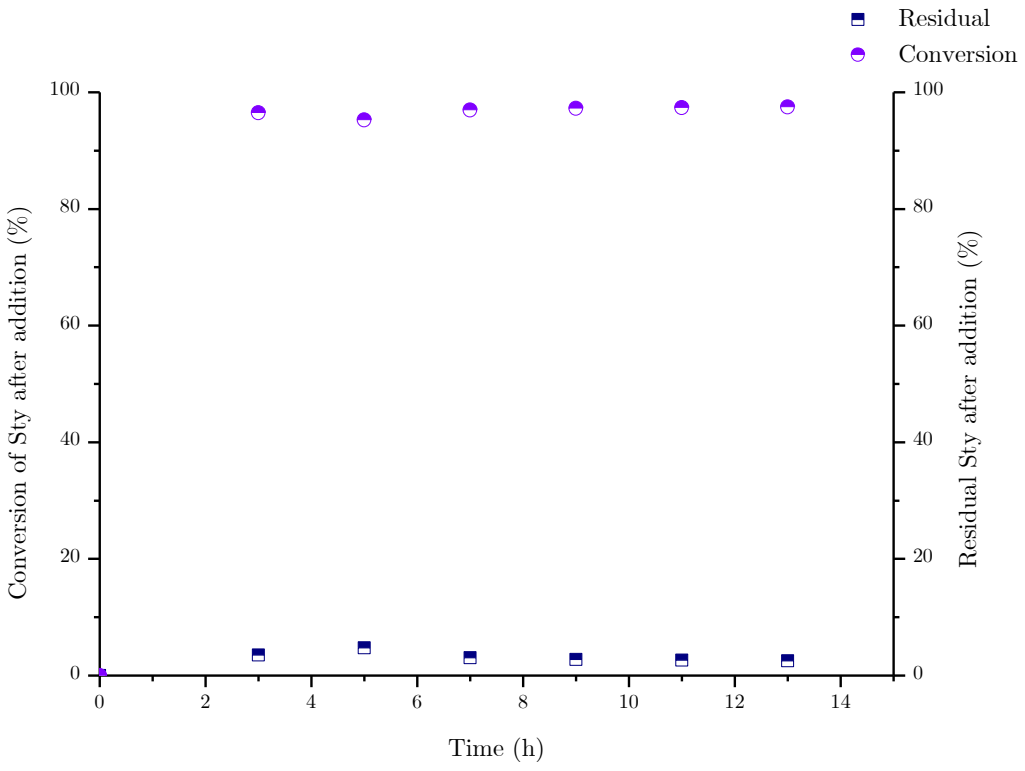

Figure 4.5: Sty monomer consumption as a function of time while several additions are made is displayed (left y-axis). The residual Sty left before the following addition is displayed as a percentage (right y-axis).

The growth of the polymer chain as a function of time was monitored by performing ^{1}H NMR spectroscopy on the isolated samples, and can be seen in Figure 4.6.

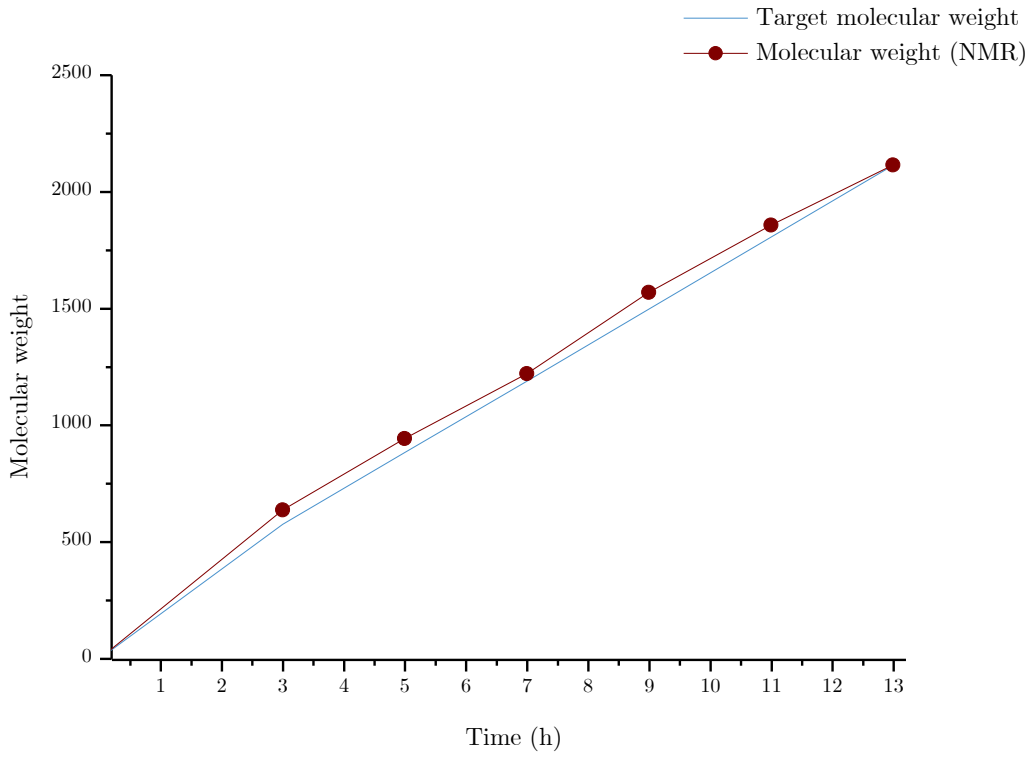

Figure 4.6: Number average molecular weight (M_n) as determined by ^{1}H NMR spectroscopy against reaction time. The targeted molecular weight is also plotted as calculated using the molar masses of the monomers and BPT. The reaction was done for 13 hours in total at 120 °C.

MS was employed in order to look at the molecular ions, and if these ions corresponded to the expected (MAnh-Sty-Sty) sequence. This was done to confirm the results obtained from ^{13}C DEPT NMR spectroscopy. By bombarding the sample with electrons (in order to ionise the sample) the sample is broken up into charged

fragments. Therefore, the molecular ion pattern can be investigated in order to determine the sequence of the copolymer, as seen in the segment of the MS spectrum in Figure 4.7.

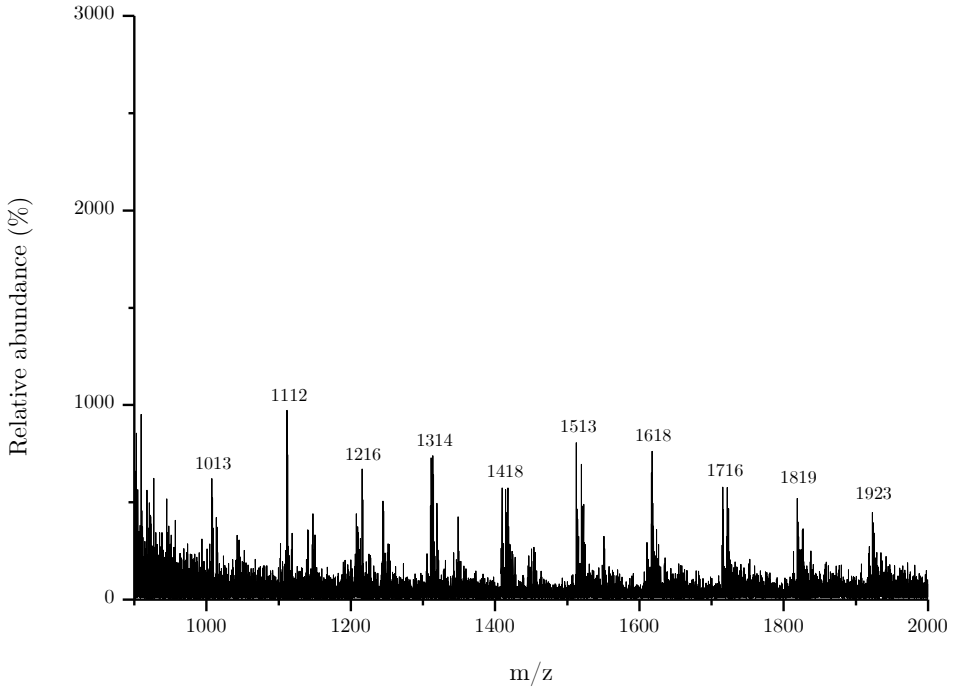

Figure 4.7: Segment of MS spectrum in the high molar mass region of SSM copolymer after five monomer additions.

The loss in mass to charge ratio from 1923 to 1819 corresponds to the loss of one Sty unit, the loss from 1819 to 1716 corresponds to another Sty unit and the loss from 1716 to 1618 corresponds to the loss of one MAnh unit. The sequence follows as described.

Ideally, every polymer chain has RAFT end groups.[21] Calculating the molecular weight from ^{1}H NMR spectroscopy is a frequently used technique for polymer characterization.[31,32] A typical equation can be derived in order to determine the amount of MAnh and Sty repeat units in the polymer chain. The ratio of repeat

units of the two monomers give the copolymer composition of the polymer and in accordance with ^{13}C DEPT NMR spectroscopy, the sequence can be confirmed.

$$a_1 = n_1 m_1 \qquad \text{Eq. (4.1)}$$

Where $a_1$is equal to the intensity or area of the peak of monomer 1 in the ^{1}H NMR spectrum; n_1 is the number of repeat units of monomer 1 and m_1 is the number of protons corresponding to monomer 1. The same is true for another monomer in the system.

$$a_2 = n_2 m_2 \qquad \text{Eq. (4.2)}$$

In order to get the ratio of the two monomers in the polymer, the ratio of the calculated repeat units (a) can be determined.

$$\frac{n_1}{n_2} = \frac{\frac{a_1}{m_1}}{\frac{a_2}{m_2}} \qquad \text{Eq. (4.3)}$$

In Figure 4.8, the ^{1}H NMR spectroscopy spectrum displays the various peaks used to determine the ratio of the monomers present in the polymer. The peaks a, b and c represent the Sty in the polymer, the MAnh in the polymer and the RAFT end groups respectively. The ratio of these integration values can be used to determine the monomer ratio in the polymer (by subtracting the overlapping RAFT amounts).

The integral of peak c was set to 3, as this is the number of protons represented by the RAFT group for this peak. Values of 5 and 3 were subtracted from the integrals of peaks a and b respectively in order to get the integral related to the number of repeat units for only the monomers in the polymer chain. Dividing both integral values (the integral corresponding to the MAnh and Sty) by the smallest value,

which corresponds to the MAnh monomer, a ratio of 2.115 was obtained. This is in good agreement with the results obtained from ^{13}C DEPT NMR spectroscopy (refer to Section 4.3.2.1).

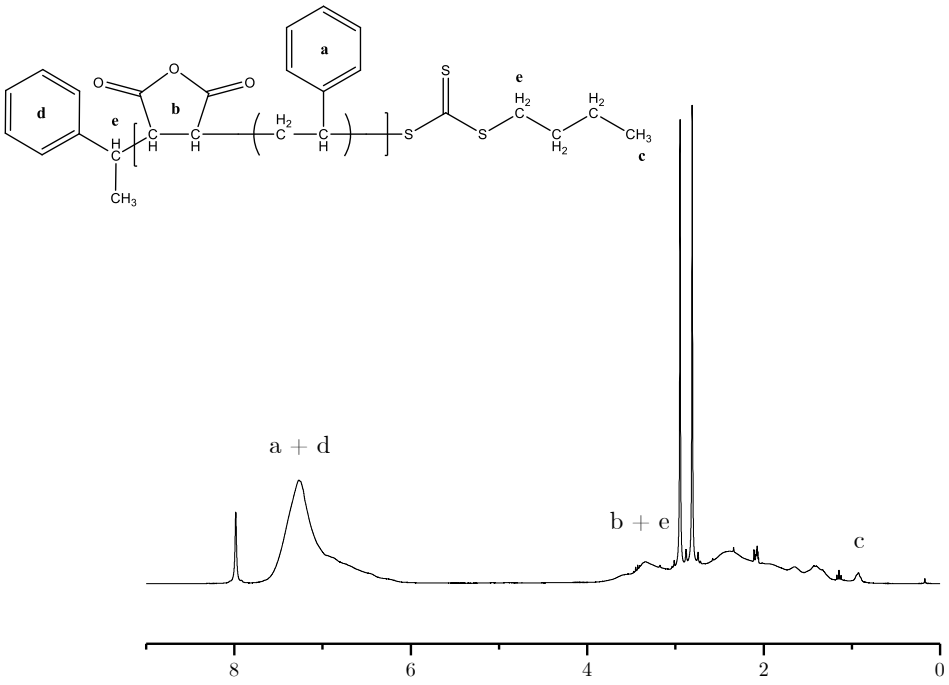

Figure 4.8: Proton NMR spectrum of SSM2100 with peaks a, b and c. A represents 5 protons from the Sty monomer in the polymer and 5 protons from the RAFT agent, where b represents 2 protons from the MAnh monomer present in the polymer and 2 protons from the RAFT agent and c represents 3 protons from the RAFT agent.

4.3.2.1 ^{13}C DEPT NMR spectroscopy

SMA2000 is a commercially available, low molecular weight polymer with a high $Đ$ consisting of circa 2:1 mole ratio of Sty to MAnh, as shown in Figure 4.9 (where n=2). The copolymer is synthesized via conventional free radical polymerization.

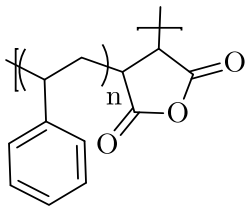

Figure 4.9: SMA2000 where n is equal to two in average.

A reference ^{13}C DEPT NMR spectroscopy spectrum of SMA2000 was acquired and is shown in Figure 4.10. Integrating over the entire triad region (which is from the methylene sub-spectrum as discussed in Section 2.1.5), makes up the total sequence distribution of SMA copolymers (refer to Section 2.1.5 for the peak assignments for each Sty-centered sequence). By integrating over the respective SSS, SSM plus MSS, and MSM triad, the sequence of the copolymer can be expressed as a fraction or percentage of the total sequence distribution of the polymer.

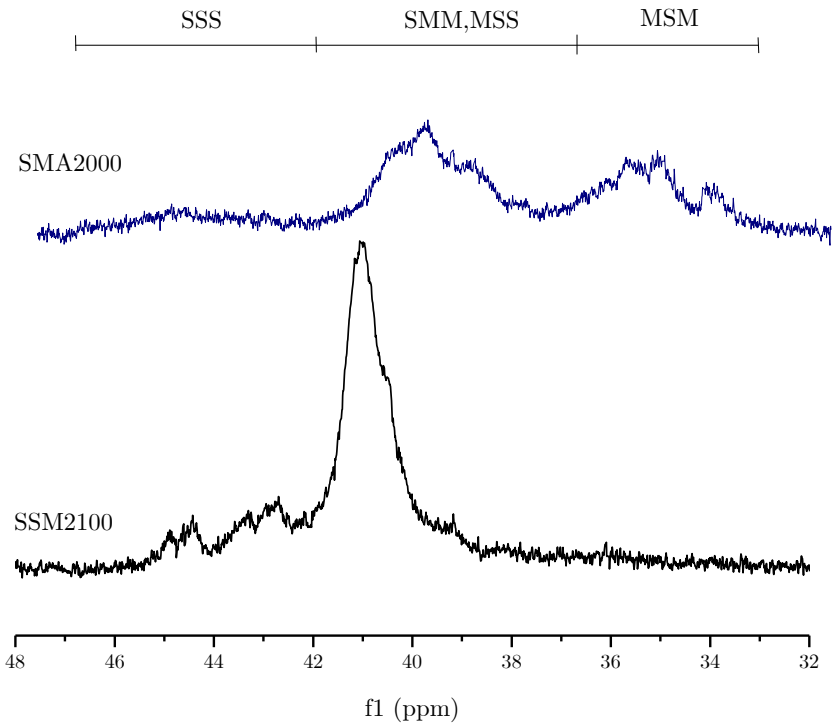

Figure 4.10: ^{13}C DEPT NMR spectroscopy spectrum of SMA2000 and SSM2100. The top spectrum represents the SMA2000 in blue and the bottom spectrum the SSM2100. The triad regions are as follow: 33-37 ppm for the MSM triad, 37-42 ppm for both the SSM and MSS triads and 42-47 for the SSS triad.

The MSM triad is present as a significant fraction in the DEPT spectrum of SMA2000 and this spectrum serves as a reference spectrum when compared to the

SSM copolymer. By increasing the Sty content in a FR polymerization, the SSS triad in the methylene sub spectrum is increased.[29,30] The MSM triad confirms the alternating sequence is still present during the synthesis of SMA2000.

The ^{13}C DEPT NMR spectroscopy provides information regarding the copolymer composition of a sequence-controlled SSM copolymer synthesized via RAFT polymerization.

It can be seen that the alternating sequence is significantly suppressed, confirmed by virtually no detection of the MSM triad. The presence of the SSS triad can be explained on the basis of residual styrene before each new addition as shown in Figure 4.5, as slightly more than 100 % of Sty is consumed after the third addition.

The results from the ^{13}C NMR analysis SMA2000 and SSM2100 are tabulated in Table 4.1. The summarized sequence distribution and molar masses from SEC and NMR spectroscopy are shown.

Table 4.1: Tabulated values of the targeted molecular weight, the molecular weight and dispersity determined by size exclusion chromatography, molecular weight determined by NMR spectroscopy and the respective triad contents of the methylene sub-spectrum for SMA2000 and SSM2100.

	M_n^{Target}	M_n^{SEC}	Đ	M_n^{NMR}	SSS	MSS, MSS	MSM
SSM2100[a]	2100	2067	1.35	2058	7	93	-
SMA2000[b]	-	3000	2.5	-	13	50	37

[a]polymer was synthesized via RAFT polymerization using BPT as RAFT agent at 120 °C.
[b]commercial polymer synthesized via conventional radical polymerization with a 2:1 ratio of styrene to maleic anhydride.

4.3.3 Thermal properties of SSM

The thermal stability of polymers depend predominantly on the molecular structure of the polymer.[33] Bhuyan *et al.* reported that the incorporation of MAnh into

polystyrene (PS) decreases the thermal stability of the latter.[34] This has also been reported by Baruah *et al.*[35] They synthesized various copolymers containing varying compositions of Sty to MAnh and found that the copolymers containing a higher MAnh ratio, exhibit a lower degradation temperature.

The thermal stability of sequence-controlled SMA was compared to SMA2000, synthesized by conventional radical polymerization containing relatively the same content of Sty (2:1 compared to the MAnh) in the polymer chain. The thermal stability was determined using TGA.

The SSM4200 exhibits a decrease in weight percentage starting at a temperature of 100 °C which corresponds to the loss of the RAFT end groups (the RAFT contributes roughly 13% to the molar mass of the polymer, which corresponds to the percentage weight lost at this point). The two polymers exhibit very similar thermal stability behaviour, although the SMA2000 starts to experience a weight loss at a higher temperature (around 300 °C) than SSM4200 (200 °C). Therefore, it can be concluded that the controlled sequence does result in a lower thermal stability of the polymer, as the polymer starts to slightly degrade at a lower temperature than SMA2000. It should be noted that the presence of the RAFT end groups could possibly accelerate the decomposition of the polymer chain.

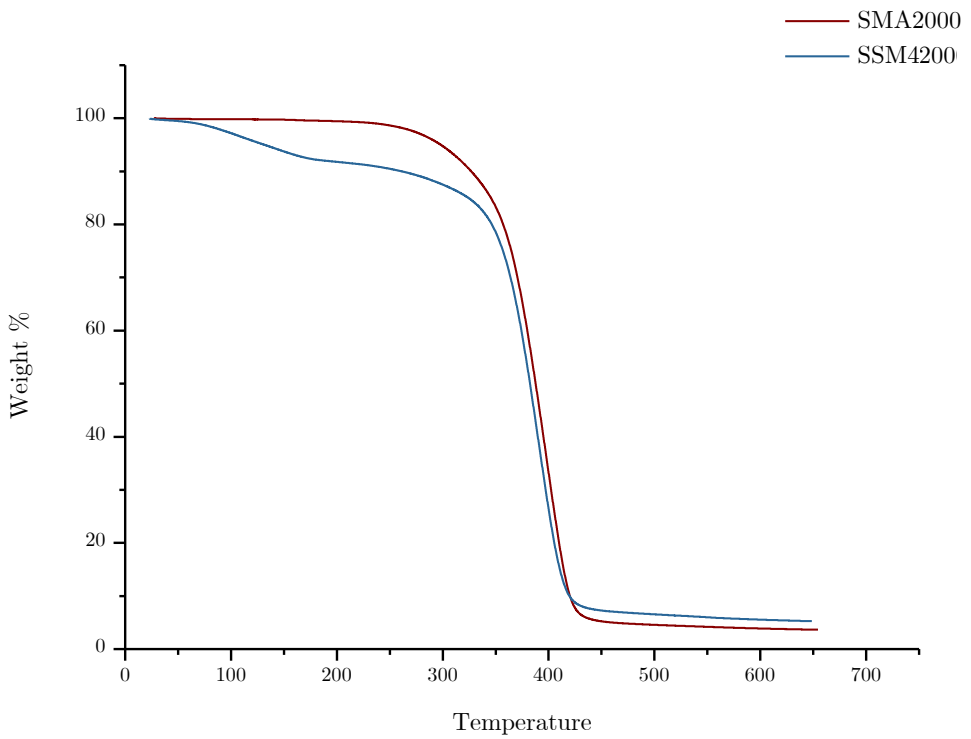

Figure 4.11: TGA results of SMA2000 synthesized via conventional free radical polymerization and SSM4200 synthesized by sequential addition of monomers using RAFT-mediated polymerization.

4.4 Conclusion on the synthesis of sequence-controlled SSM

Using BPT as RAFT agent, a SSM and MSS sequence of 93 % was successfully obtained for a polymer consisting of a molar mass around 2100 Da., as confirmed by ^{13}C DEPT NMR spectroscopy. This is also confirmed by the ratio of Sty to MAnh from ^{1}H NMR spectroscopy. The use of sequential monomer addition, and the optimization of the system w.r.t Sty monomer consumption, suppressed the formation of alternating SMA. ^{1}H NMR spectroscopy can be used in conjunction with ^{13}C DEPT NMR spectroscopy for sequence determination of SSM2100. The use of ^{1}H NMR spectroscopy by itself for precise sequence determination is not sufficient, as it only provides information regarding the overall polymer composition. The copolymer was also characterized using MS and SEC. The thermal stability of

the sequence-controlled SSM was compared to SMA2000 by applying TGA to the samples. The general curve of thermal stability of a copolymer synthesized via RAFT-mediated polymerization compared to a copolymer synthesized via conventional free radical polymerization seem identical, where only the SSM4200 experiences a weight loss that contributes to the RAFT agent end groups .

References

1. Klumperman, B. & O'Driscoll, K. F. *Polymer* 1993, *34*, 1032–1037
2. Lutz, J.-F., Ouchi, M., Liu, D, R. & Sawamoto, M. *Science* 2013, *341*, 1238149-1-1238149–8
3. Solleder, S. C., Wetzel, K. S. & Meier, M. A. *Polym. Chem.* 2015, *6*, 3201–3204
4. Zydziak, N., Konrad, W., Feist, F., Afonin, S., Weidner, S. & Barner-Kowollik, C. *Nat. Commun.* 2016, *7*, 13672
5. Chan-Seng, D., Zamfir, M. & Lutz, J. F. *Angew. Chemie - Int. Ed.* 2012, *51*, 12254–12257
6. Lutz, J.-F. *Polym. Chem.* 2010, *1*, 55
7. Pfeifer, S. & Lutz, J.-F. F. *J. Am. Chem. Soc.* 2007, *129*, 9542–9543
8. Lutz, J.-F., Meyer, T.Y., Ouchi, M. & Sawamoto, M. *ACS Symposium Series*; 1170, 2014, ISBN: 9780841230019
9. Lutz, J.-F., Pakula, T. &Matyjaszewski, K. *ACS Symposium Series*; 854, 2003, ISBN: 9780841238541
10. Baradel, N., Gok, O., Zamfir, M., Sanyal, A. & Lutz, J. *Chem. Commun.* 2013, *49*, 7280
11. Zamfir, M. & Lutz, J.-F. *Nat. Commun.* 2012, *3*, 1138
12. Ouahabi, A. Al, Kotera, M., Charles, L. & Lutz, J. F. *ACS Macro Lett.* 2015, *4*, 1077–1080
13. Alsubaie, F., Anastasaki, A., Wilson, P. & Haddleton, D. M. *Polym. Chem.* 2015, *6*, 406–417
14. Chuang, Y. M., Ethirajan, A. & Junkers, T. *ACS Macro Lett.* 2014, *3*, 732–737
15. Anastasaki, A., Nikolaou, V., Pappas, G. S., Zhang, Q., Wan, C., Wilson, P., Davis, T. P., Whittaker, M. R. & Haddleton, D. M. *Chem. Sci.* 2014, *5*, 3536–3542
16. Martin, L., Gody, G. & Perrier, S. *Polym. Chem.* 2015, *6*, 4875–4886
17. Xu, J., Shanmugam, S., Fu, C., Aguey-Zinsou, K. F. & Boyer, C. *J. Am.*

Chem. Soc. 2016, *138*, 3094–3106

18. Moriceau, G., Gody, G., Hartlieb, M., Winn, J., Kim, H., Mastrangelo, A., Smith, T. & Perrier, S. *Polym. Chem.* 2017, *8*, 4152-4161
19. Zamfir, M. & Lutz, J.-F. *Nat. Commun.* 2012, *3*, 1138
20. Gody, G., Zetterlund, P. B., Perrier, S. & Harrisson, S. *Nat. Commun.* 2016, *7*, 10514
21. Van Den Dungen, E. T. A. *Self-healing coatings based on thiol-ene chemistry* 2009, PhD, Stellenbosch University
22. Van Den Dungen, E. T. A., Matahwa, H., McLeary, J. B., Sanderson, R. D. & Klumperman, B. *J. Polym. Sci. Part A Polym. Chem.* 2008, *46*, 2500–2509
23. Klumperman, B., McLeary, J. B., Van Den Dungen, E.T.A. & Pound, G.E.N. *Macromol. Symp.* 2007, *248*, 141–149
24. Hill, D. J. T., O'Donnell, J. H. O. & O'Sullivan, P. W. O. *Macromolecules* 1985, *17*, 9–17
25. Brown, P.G. & Fujimori, K. *Polym. Chem.* 1994, *32*, 2971–2978
26. Klumperman, B. *Polym. Chem.* 2010, *1*, 558–562
27. Hagiopol, C. Copolymerization: *Toward a Systematic Approach*, First edition, 2012, ISBN: 9781461541837
28. Odian, G. *Principles of Polymerization,* Fourth edition, 2004, ISBN: 0471274003
29. Barron, P. F., Hil1, D. J. T., O'donnell, J. H. & O'sullivan, P. W. *Macromolecules* 1984, *17*, 1967–1972
30. Lessard, B. & Marić, M. *Macromolecules* 2010, *43*, 879–885
31. Brar, A. S., Arunan, E. & Kapur, G. S. *Polym. J.* 1989, *21*, 689–695
32. Randall, J. C. *Polymer Sequence Determination: Carbon-13 NMR Method*, First edition, 1977, ISBN: 0125780508
33. Madorsky, S. L. & Straus, S. *J. Res. Natl. Bur. Stand. Sect. A Phys. Chem.* 1959, *63A*, 261–268
34. Bhuyan, K. & Dass, N. N. *J. Therm. Anal.* 1989, *35*, 2529–2533

35. Baruah, S. D. & Laskar, N. C. *J. Appl. Polym. Sci.* 1996, *60*, 649–656

Chapter 5

Zwitterionic styrene-maleic anhydride copolymer derivatives

In this chapter, the dissociation behaviour of styrene-maleic anhydride (SMA) copolymer derivatives, containing both a carboxylic acid (COOH) and tertiary amine (NR_3) functionality, was investigated by relating to and conducting a model study with a small molecule analogue. The study was further extended to the polymeric system, with the goal to establish conditions where an isoelectric point (pI) can be located in order to form zwitterionic SMA based copolymers. This study was followed by the investigation of the influence of the microstructure, by comparing the classical alternating AB type structure to a sequence-controlled ABB sequence. Further applications of SMA derivatives were also explored in this chapter, such as the use of the incorporation of a tertiary amine for cell membrane disruptions of malignant cells. The use of nanoparticles that contain the same functional, ionizable groups, allowed cytotoxicity studies to be completed. The use of nanoparticles allowed for cellular uptake to occur, due to their size when compared to polymers. Therefore, with the use of nanoparticles and cytotoxicity

studies, the feasibility of the functional groups in the biological field could be explored.

5.1 Introduction

SMA copolymers are used for various applications. The significance of copolymers consisting of styrene (Sty) and maleic anhydride (MAnh) is ascribed to their utilization in a variety of areas for numerous purposes.[1] Over the last number of decades, SMA copolymers have shown to be able to undergo chemical modifications to impart useful characteristics. The SMA copolymer is classified as a functional polymer due to the MAnh present in the polymer backbone. This is highly reactive towards nucleophilic reagents such as amines.[2] Upon the introduction of nucleophilic compounds, new materials can be obtained.[3]

The incorporation of a compound, such as 3-(*N*,*N*-dimethylamino)propyl-1-amine (DMAPA), on a SMA copolymer, results in one site that can be positively charged (the tertiary amine) and one site that can be negatively charged (carboxylic acid of MAnh). Should this occur at the same moment, it will exist as a zwitterion with a net charge of zero. The pH where this happens is known as the isoelectric point (pI). In order for zwitterion detection and an in depth understanding, a few important concepts need to be discussed.

The acid dissociation constant (K_a) is a value used to describe the tendency of acids to dissociate. Therefore, it can be expressed in terms of the general proton-transfer reaction[4],

$$HA \rightleftharpoons H^+ + A^- \qquad \text{Eq. (5.1)}$$

Eq. (5.2)

$$K_a = \frac{[H^+][A^-]}{[HA]}$$

Where K_a is the equilibrium constant and $[A^-]$, $[H^+]$ and [HA] are the concentrations of the deprotonated species, the protons and the protonated species, respectively. The pH of the solution is defined as the negative logarithm of the proton concentration in solution ($pH = -\log [H^+]$).

The corresponding concept of the acid dissociation constant (pK_a) is a frequently used parameter in chemistry[5] and known as follows,

$$pK_a = -\log K_a \qquad \text{Eq. (5.3)}$$

The Henderson-Hasselbalch equation can be used to calculate the pK_a if the pH and concentrations of the acid and conjugate base are known,

$$pH = pK_a + \log_{10} \frac{[A^-]}{[HA]} \qquad \text{Eq. (5.4)}$$

Titration curves are readily used for the determination of the $pK_a$of compounds.[4,6] When the amount of titrant neutralizes the analyte solution, the equivalence point is reached and half of the equivalence volume, is known as the half-equivalence point. The same amount of acid ([HA]) and conjugate base ($[A^-]$) are present in solution at this point. This results in the second term of Equation 5.4 becoming zero and thus the pH is equal to the pK_a at this point.

The pH corresponding to this volume value is equal to the pK_a of the reaction at that point,

$$pH_{half\ titration} = pK_a \qquad \text{Eq. (5.5)}$$

An illustration of this point is shown in Figure 5.1, along with the equivalence point.

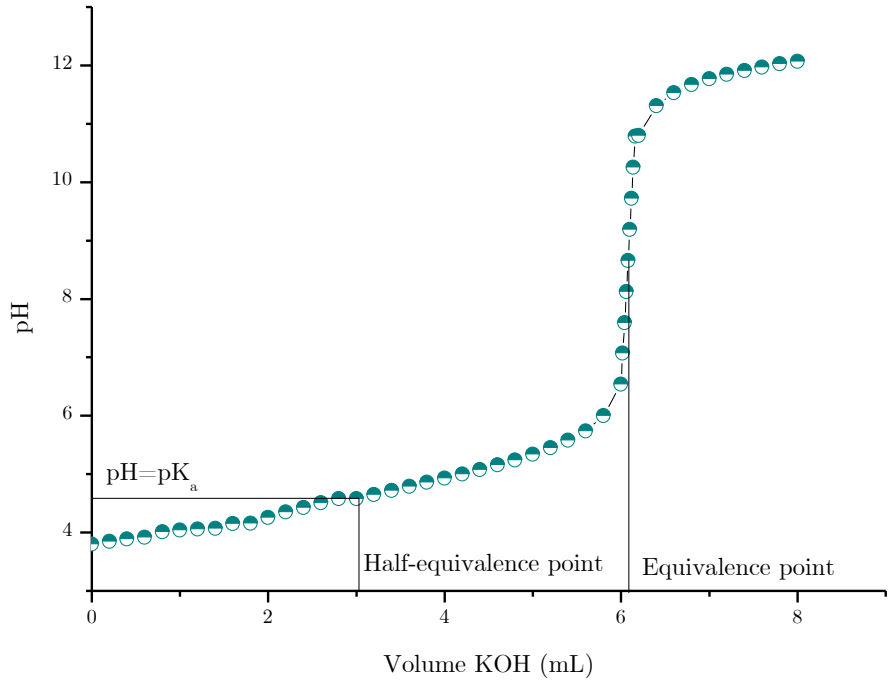

Figure 5.1: Representation of endpoint and half titration values used for pK_a calculation. The endpoint occurs at the middle of the inflection point. Half of this volume corresponds to the volume where the pH is equal to the pK_a.

However, reading the equivalence point off of the titration curve is merely an estimation. Alternatively, by plotting the first derivative of the titration curve versus the volume, a maximum that corresponds to the equivalence point, can be obtained. Furthermore, linear regression methods can also be used[7–11] and Johansson has reported that by using a linear regression method results in the calculation of the equivalence point with increased precision.[11]

5.1.1 Model compounds

The modification of SMA with DMAPA (ring-opened) results in two functional groups of interest being present as side groups of the polymer – a carboxylic acid and a tertiary amine, connected to an amide by a hydrocarbon chain. Two compounds with similar structures to the anhydride and amine in the polymer backbone were chosen, as these compounds would exhibit similar pK_a values compared to the functional groups in the polymer. Butyric acid (BA) and *N*-((3-dimethylamino)propyl)propionamide (*N*-DMAPPA) were found to be suitable candidates for this model study. The reported pK_a values of butyric acid are 4.8[12] or 4.82.[13] There is no reported pK_a value for *N*-DMAPPA in literature.

Figure 5.2: Structures of butyric acid and *N*-(3-dimethylamino)propyl)propionamide employed in the model study.

Although SMA copolymers can be readily modified (to incorporate ionizable functionalities), in order for the polymers to be applicable in the biological and medical field, the size plays a crucial role as

In order for a cell to take up polymeric materials via endocytosis into the endosome, the particle/micelle size has to be of a relatively small size, similarly to those of nanoparticles.[18–20] Therefore, SDBM nanoparticles were modified and exposed to cells. Other than the size of the nanoparticles, the use of SDBM nanoparticles allow the tracking of the particles, as they auto-fluoresce.[21]

5.2 Experimental details

5.2.1 Characterization

The pH was measured using a Eutech pH 700 meter. The pH meter was calibrated using calibration pH buffers at pH 4.0, 7.0, and 12.0 (Sigma Aldrich).

Fourier transform infrared (FTIR) spectra were recorded on a Nexus FTIR spectrometer, while equipped with a Smart Golden Gate attenuated total reflectance (ATR) diamond purchased from Thermo Nicolet with ZnSe lenses. The samples were analysed by 64 scans with 4.0 cm^{-1} resolution. The data analysis was performed on Omnic 7.2.

The cytotoxicity of styrene-divinylbenzene-maleic anhydride (SDBM) nanoparticles was determined using the XTT assay. The nanoparticles were sonicated in order to eliminate particle aggregation, centrifuged and dispersed into fresh Roswell Park Memorial Institute (RPMI) 1640 culture media. Cells were seeded at $6x10^3$ cells/well. Cells were then treated with RPMI containing the nanoparticles at concentrations of 10 µg/mL and 1 mg/mL for 1h, 2h, 4h and 24h before viability assessment by XTT assay. The cell studies were performed by Johan Visser, under supervision of Professor Carine Smith at the Department of Physiological Sciences of Stellenbosch University.

All other characterization methods employed have been described in earlier chapters.

5.2.2 Chemicals

BA, propionic acid, potassium hydroxide (KOH) pellets and 32 % hydrochloric acid (HCl) were bought from Merck and used as received. Toluene and DMAPA were bought from Sigma-Aldrich and used as received.

Styrene-divinylbenzene-maleic anhydride (SDBM) nanoparticles were supplied by a fellow group member. The particle size diameter was 169 nm.

Ethical clearance exemption for isolation of human primary monocytes from intentionally donated blood was obtained from the Subcommittee C Human Research Ethics Committee (HREC) of Stellenbosch University (Reference # X15/05/013). Monocytes were secured from buffy coat blood, supplied by the Western Province Blood Transfusion (WPBTS), via double gradient centrifugation as specified by Menck, K 2014. Monocytes were cultured for up to 6 days in advanced RPMI media (bought from Life Technologies) containing 10% human serum (bought from Sigma-Aldrich) and 1% penicillin/streptomycin (bought from Sigma-Aldrich) in the presence of 50 ng/mL granulocyte monocyte colony-stimulating factor (GM-CSF) (bought from Sigma-Aldrich), before 24 h polarization to M1 type macrophages with 50 ng/mL lipopolysaccharide from *E. coli* (LPS) (bought from Sigma-Aldrich) and 20 ng/mL interferon gamma (bought from Sigma-Aldrich).

The other chemicals used have been described in earlier chapters.

5.2.3 Synthesis of *N*-((3-dimethylamino)propyl)propionamide

N-DMAPPA was synthesized according to a similar procedure available in literature by Ghumare *et al.*[14]

DMAPA (7.526 g, 0.0737 mol) was slowly added to propionic acid (5.271 g, 0.0712 mol) in dry toluene (40 mL) under a constant stream of argon gas, in the dark, at room temperature. The reaction was allowed to proceed for 24 hours. The progress of the reaction was followed by TLC. The product was purified by fractional distillation. ^{1}H NMR (300 MHz, $CDCl_3$) δ: 8.71 (s, 1H, -NH), 2.82 (t, J = 7.4 Hz,

2H, -CH2-NH), 2.32 (t, J = 7.9 Hz, 2H, -CH_2-R_3N), 2.16 (s, 6H, -$(CH3)_2$-R_3N), 2.08 (q, J = 7.6, 2H, -CH_2-C=O), 1.75 (p, 2H, -CH_2-CH_2-R_3N), 1.00 (t, J = 7.7 Hz, 3H, -CH3). ^{13}C NMR (300 MHz, $CDCl_3$) δ: 180.79, 57.10, 44.43, 38.75, 30.00, 24.23, 10.24. The product was obtained with a yield and purity of 75 % and of 95 % respectively.

Scheme 5.1: Synthesis of *N*-((3-dimethylamino)propyl)propionamide.

5.2.4 Synthesis and modification of polymers

Alternating and sequence-controlled copolymers of Sty and MAnh (Chapter 4) were synthesized.

5.2.4.1 Synthesis and modification of SSM

For a typical functionalization of the polymers with DMAPA, the SSM polymer synthesized in Chapter 4 was dissolved in a minimum amount of DMF. DMAPA (1.5 eq. to the MAnh in the polymer backbone) was added drop wise to the polymer solution. A-SSM was retrieved by precipitation in diethyl ether twice. The polymer was dried in a vacuum oven at room temperature for 24 hours.

5.2.4.2 Synthesis and modification of SMA

Alternating SMA with various molecular weights were synthesized. For a typical reaction, Sty (2.001 g, 0.019 mol), MAnh (1.883 g, 0.019 mol), CDB (0.224 g, 0.821 mmol) and 2,2'-azobis(isobutyronitrile) (AIBN) (0.027 g, 0.164 mmol) were accurately weighed off and transferred to a Schlenk flask along with methyl ethyl

ketone (MEK) (5 mL) and a magnetic stirrer bar. The solution was thoroughly degassed with argon gas for one hour prior to the start of the reaction. The flask was immersed in a preheated oil bath at 70 °C for 24 hours and the polymer was isolated by precipitation from diethyl ether, and dried under vacuum, at room temperature, for 24 hours with a yield of 58 %.

The functionalization was completed as follows: SMA (1.002 g, 0.162 mmol) was dissolved in 5 mL THF. DMAPA (0.780 g, 7.634 mmol) was added to the solution in a dropwise manner, while the solution was stirred. The A-SMA was retrieved by precipitation in diethyl ether. The polymer was dried in a vacuum oven at room temperature for 24 hours.

Full characterization of these polymers were obtained via SEC, ^{1}H NMR spectroscopy and ATR-FTIR spectroscopy as described in Chapter 3 and Chapter 4.

5.2.4.3 Synthesis and modification of SSM

The synthesis and modification of SSM is as described in Chapter 4. The characterization methods are also as described in Chapter 4. The general surface modification reaction is shown in Scheme 5.2

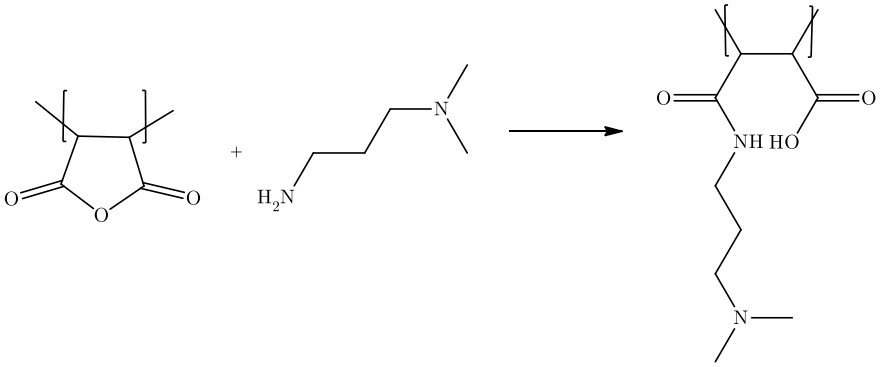

Scheme 5.2: Surface modification on the MAnh unit with DMAPA.

5.2.5 Titrations of model compounds

BA and *N*-DMAPPA were titrated with 0.1 M solutions of KOH and HCl respectively. The obtained pH values were plotted versus the added volume of titrant and their pK_a values were calculated using the method described.

5.2.5.1 Titration of BA

BA (0.102 g, 1.116 mmol) was dissolved in 25 mL of distilled water and transferred to a titration cell, containing a magnetic stirrer bar, thermostated at 25 °C. The solution was titrated with 0.1 M KOH. After every addition (0.2 mL), the pH was taken after stabilization of the pH electrode. The measurements were converted into pH versus volume plots.

5.2.5.2 Titration of *N*-DMAPPA

N-DMAPPA (0.191 g, 1.201 mmol) was dissolved in distilled water (25 mL). The solution was transferred to a titration cell, while a constant temperature of 25 °C was maintained, containing a magnetic stirrer bar. The solution was titrated with 0.1 M HCl. Upon stabilization of the pH electrode after every addition (0.2 mL), the pH reading was recorded. The measurements were converted into pH versus volume plots.

5.2.5.3 Titration of polymers

For a simple titration, 0.2 mL of 0.1 M KOH was added to the titration cell, containing the polymer solution (0.1008 g, 0.016 mmol), using a burette. After the pH stabilized, the pH was taken and the titration proceeded until the solution reached a pH around 12.

5.2.5.4 Modification of nanoparticles

A small amount of tetrahydrofuran (THF) (2 mL) was added to the nanoparticles (1.081 g) while stirring at room temperature. A 1.5 equivalence to the MAnh of DMAPA (0.456 g, 4.467 mmol) was used to functionalize the nanoparticles to incorporate the tertiary amine functionality. Successful modification was confirmed by ATR-FTIR spectroscopy. The same procedure for the functionalization was followed as in Section 5.2.4.2.

After modification, the amine-functionalized particles were dialysed for 48 hours in water, to remove the excess DMAPA and THF. The particles were then freeze dried.

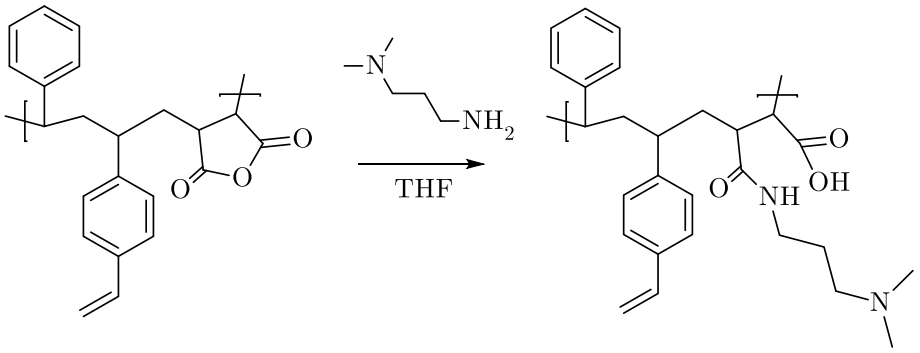

Scheme 5.3: Surface modification of SDBM nanoparticles with DMAPA on the MAnh unit.

5.3 Results and discussion

5.3.1 Model study

The equivalence point in a titration experiment can be determined by locating the maximum in the first derivative of the titration curve. Johansson stated that the equivalence point can be determined with increased precision by using a linear regression method.[11] He stated that the most straightforward and accurate method is to transform the titration curve into a straight line, by the QUOTEQ method as

discussed in the work done by Johansson.[9] For the general proton-transfer reaction, $[H^+]$ is equal to 10^{-pH} and $[A^-]$ is proportional to the volume of the titrant added, V. If, $10^{-pH} \cdot V$ is therefore plotted against V, a straight line that intersect the x-axis at the equivalence point is obtained. This calculation method was first reported by Sørensen[15] and Gran[8] investigated the method in further detail. Therefore, before the equivalence point, y_1 can be calculated using Equation 5.6 and y_2 can be calculated using Equation 5.7 and these values can be plotted against the measured pH values serving as the x values for weak acids.

$$y_1 = (V_0 + V) x \frac{10^{pH}}{C_B} \qquad \text{Eq. (5.6)}$$

$$y_2 = (V_0 + V)\ x \frac{K_w}{(C_B\ x\ 10^{pH})} \qquad \text{Eq. (5.7)}$$

Where C_B is the concentration of the titrant and K_w is the waterautoprotolysis constant of waterautoionization constant and equal to 1 x 10^{-14}.[16]

5.3.1.1 Synthesis of *N*-((3-dimethylamino)propyl)propionamide

^{1}H NMR spectroscopy was conducted to confirm successful synthesis of the product. The most indicative peaks of formation are the disappearance of both the proton peaks of the primary amine and the proton peak from the OH group of the carboxylic acid. The appearance of the peak at 8.71 ppm also confirms that the desired product has been formed. The respective NMR spectra of the starting reagents can be seen in Figure 5.3 and the product can be seen in Figure 5.4.

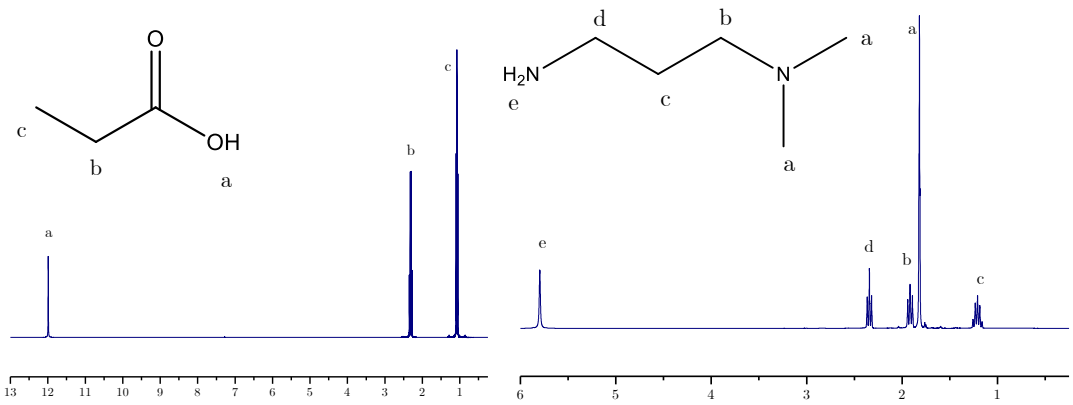

Figure 5.3: ^{1}H NMR spectroscopy spectra of propionic acid (left) and DMAPA (right) used as starting reagents for this synthesis of *N*-((3-dimethylamino)propyl)propionamide.

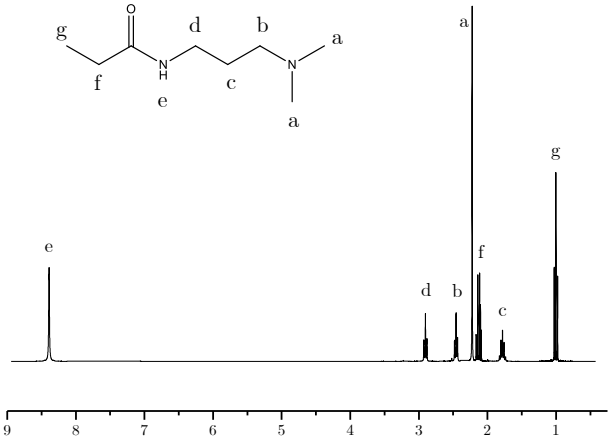

Figure 5.4: ^{1}H NMR spectroscopy spectrum of *N*-((3-dimethylamino)propyl)propionamide.

5.3.1.2 Titration of butyric acid

A plateau, known as the buffer region, is observed before the equivalence point. Since butyric acid is a weak acid and is titrated by a strong base, the Henderson-Hasselbalch equation can be used to calculate the pK_a.

For the titration of BA with 0.1 M KOH, the equivalence point can be seen where the inflection point occurs. After this point, the acid becomes deprotonated as there now exists an excess of base concentration ([OH^-]) in the solution. From the titration curve, the equivalence point can be calculated by using the pH at half the equivalence point volume. The maximum of the first derivative occurs at 5.804 mL. The half-equivalence volume is therefore 2.902 mL and the pH corresponding to this value is 4.61.

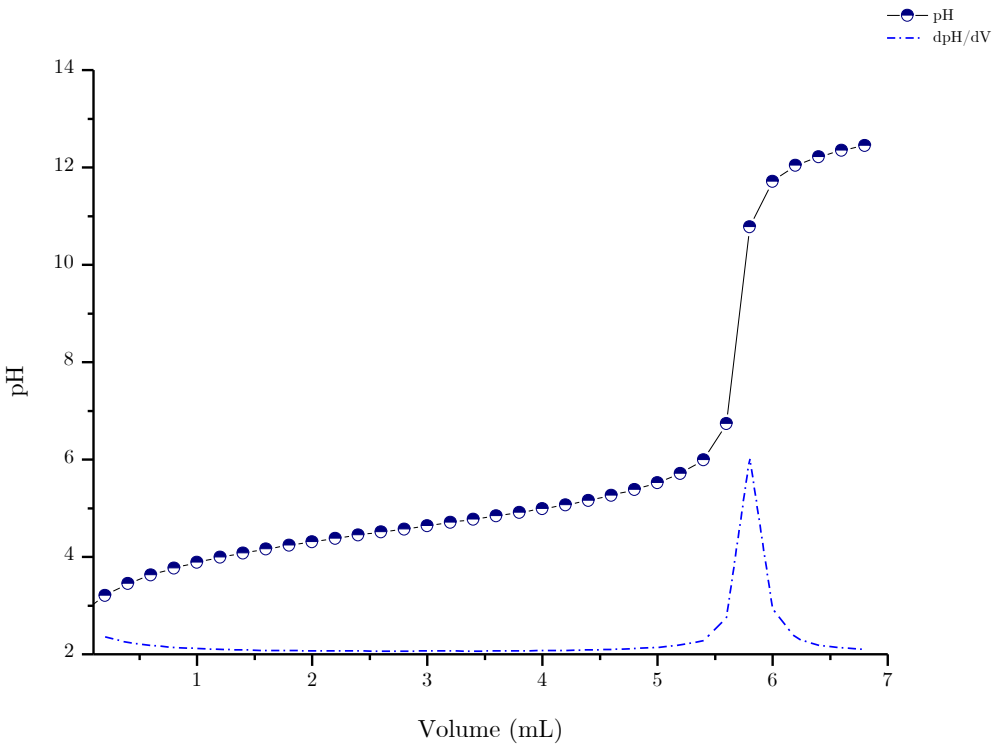

Figure 5.5: pH versus volume plot of BA for constant addition of 0.1 M KOH. This is plotted along with the first derivative of this curve. The maximum in the first derivative indicates the equivalence point.

The equivalence point was then calculated using the linear regression method reported by Johansson and can be seen in Figure 5.6.[11]

The x-intercept was found by fitting a linear trend line to the y_1 and y_2 values and extrapolating to the x-axis. The equivalence point was calculated to occur after the

addition of 5.746 mL of titrant. This calculated value is well in agreement with the inflection point observed in Figure 5.5. The pH, and therefore the pK_a, corresponding to the half-equivalence volume is 4.56.

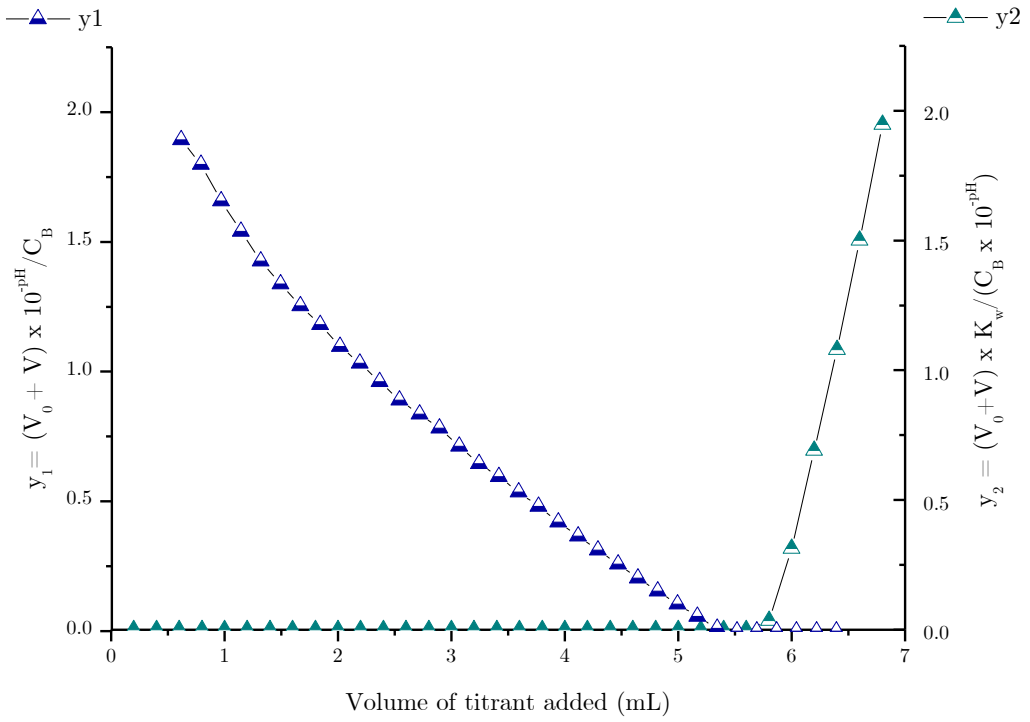

Figure 5.6: Equivalence point calculation of BA using the method described by Johansson.[11]

Table 5.1 summarizes the respective values calculated and obtained.

Table 5.1: Summary of equivalence volumes and pK_a values for BA with the method of maxima for the first derivative of the titration curve, along with the linear regression method reported by Johansson.[11]

Method	Equivalence volume	Half-equivalence volume	pK_a
First derivative	5.804	2.902	4.61
Linear regression[11]	5.746	2.873	4.56

5.3.1.3 Titration of *N*-DMAPPA

From

Figure 5.7, it is evident that *N*-DMAPPA has two pK_b values – one corresponding to the amino group of interest and the other to the amide group.

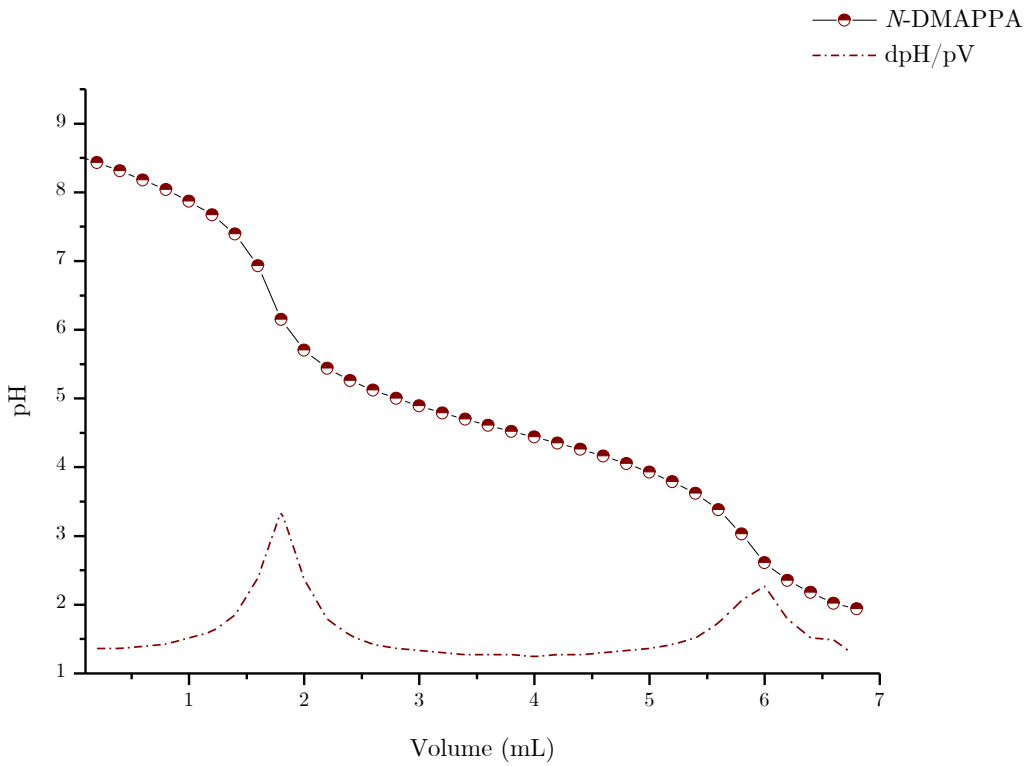

Figure 5.7: pH versus volume plot of *N*-DMAPPA for constant addition of 0.1 M HCl. This is plotted along with the first derivative of this curve. The maxima in the first derivative indicate the equivalence points.

The same equivalence point calculations are applied to *N*-DMAPPA. As both nitrogen groups can be protonated, there exist two equivalence points. The delocalization of the lone pair electrons on the amide nitrogen can be used to determine which group will be protonated first. The lone pair on the amino group is localized on the nitrogen atom, whilst the lone pair of the amide nitrogen is

delocalized between the oxygen and nitrogen through resonance.[2] This results in the amide being much less basic when compared to the amino group.

From the first derivative, the equivalence points occur at a volume of 1.80 mL and 5.97 mL. The equivalence points were then calculated using the linear regression method reported by Johansson.[11]

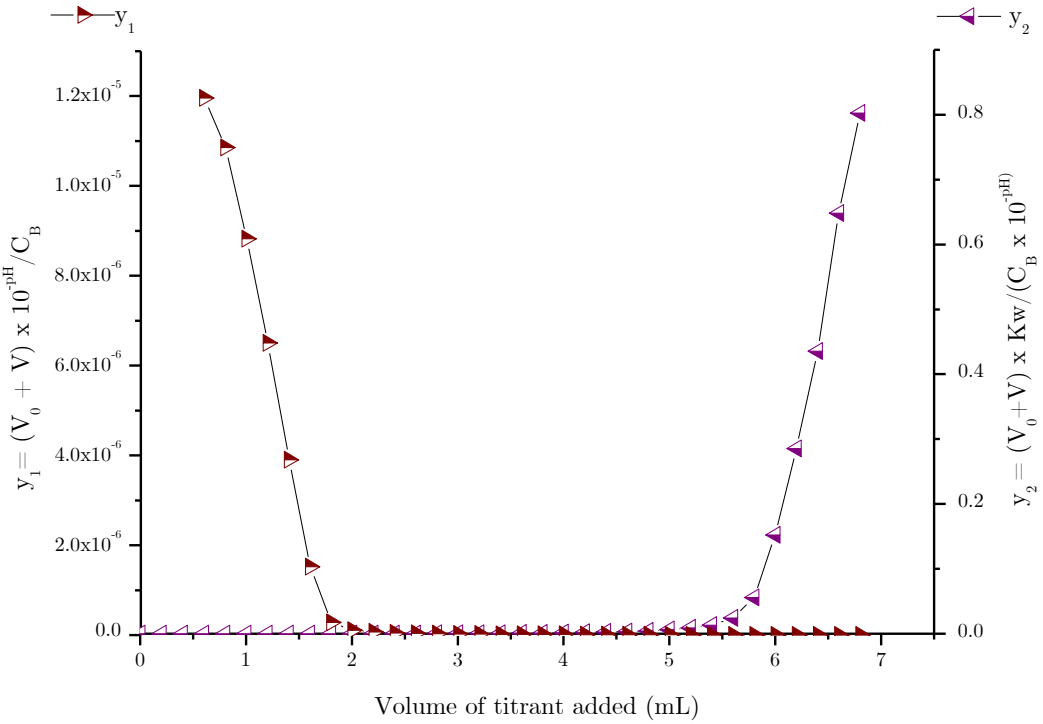

Figure 5.8: Equivalence point calculation of *N*-DMAPPA using the method reported by Johansson.[11]

For the linear regression method, the calculated values (1.798 mL and 5.694 mL) are well in agreement with the inflection points observed in

Figure 5.7. Therefore, the half-equivalence volumes are 0.899 mL and 2.847 mL respectively. The pK_{a1} (amino group) value is 7.87 and pK_{a2} (amide group) is 4.84. Table 5.2 summarizes the respective values calculated and obtained.

Table 5.2: Summary of equivalence volumes and pK_a values for *N*-DMAPPA with the method of maxima for the first derivative of the titration curve, along with the linear regression method reported by Johansson.[11]

Method	Eq volume 1	Eq volume 2	pK_{a1}	pK_{a2}
First derivative	1.798	5.972	7.98	4.89
Linear regression[11]	1.798	5.694	7.97	4.96

The calculated pK_a values for the titration of *N*-DMAPPA using the first derivative and the linear regression method are in very close agreement with each other.

5.3.1.4 Protonation probabilities of BA and *N*-DMAPPA

Scheidelaar *et al.* reported that the protonation state of one mono-mol unit can be used to distinguish between the degree of protonation (or ionization) of a substance.[17] The mono-mol unit is defined as the smallest possible component of the substance that depicts the overall composition of the substance. The two substances BA and *N*-DMAPPA, can carry charges of negative one and positive two, respectively. The acid-base titration curves can be converted into protonation states versus pH curves.

Ullmann reported that the protonation probability $\langle x \rangle$ of monoprotic groups that can be protonated is expressed by Equation 5.4.[4] This equation is algebraically equal to the Henderson-Hasselbalch equation with $\lambda = 10^{-pH}$

$$\langle x \rangle = \frac{10^{pK_a - pH}}{1 + 10^{pK_a - pH}} \qquad \text{Eq. (5.4)}$$

For diprotic compounds, the following equation is used,

$$\langle x \rangle = \frac{10^{pK_1 - pH} + 2(10^{pK_1 + pK_2 - 2pH})}{1 + 10^{pK_1 - pH} + 10^{pK_1 + pK_2 - pH}} \qquad \text{Eq. (5.5)}$$

The values calculated for every measured pH, are plotted against the measured pH to yield Figure 5.9.

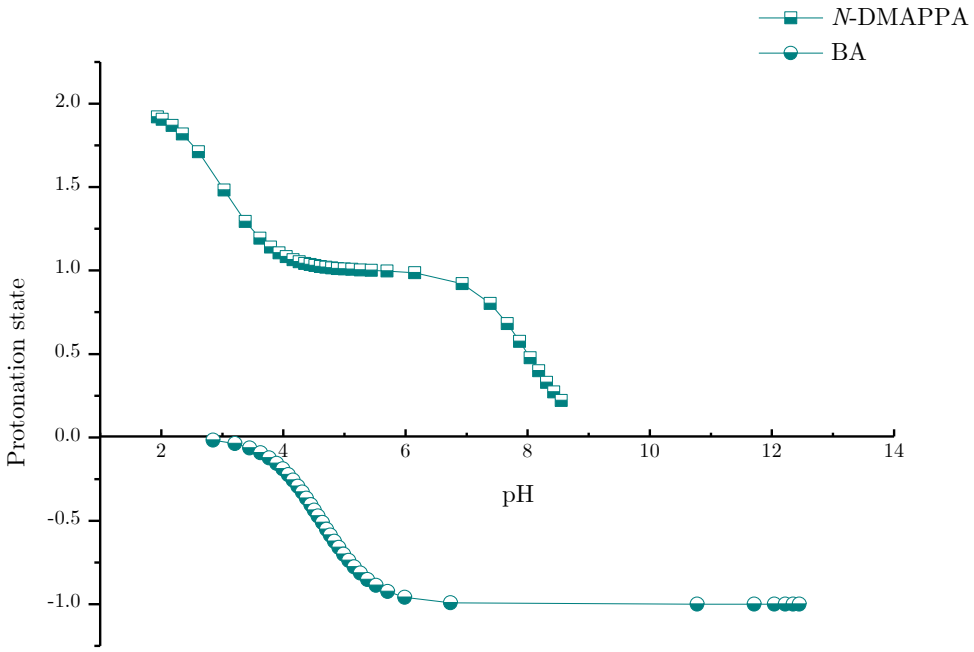

Figure 5.9: Protonation probability of BA and *N*-DMAPPA versus pH.

Figure 5.9 displays the protonation states of BA and *N*-DMAPPA. As mentioned in Section 5.3.1.3, the amide group will also be deprotonated first. As discussed in Chapter 2, the pI is the average of the two pK_a values of the carboxylic acid and the amine. The average of the two pK values of the carboxylic acid and the amino group is 6.29. There thus exists a window where the BA carries a negative charge and the amino group still carries a positive charge.

5.3.1.5 Outcome of model study

Using the calculation method described[8,11,15] and the first derivative of the titration curve, the pK_a values of BA and *N*-DMAPPA were successfully determined. Johansson reported that the equivalence point calculated by the linear regression method presents a more accurate value[11], than estimating the value from the graph. It will be investigated if the same calculation methods can be used to accurately determine the pK_a values for the different (ionic) functional groups in modified SMA copolymers.

Based on the calculation from Ullman, the window observed in Figure 5.9 serves as a good indication that a zwitterionic compound containing the same functional groups should exhibit an isoelectric point (pI) – where the carboxylic acid group is deprotonated at the same time where the amine group is protonated. Although the first derivative method provided values closer to the value reported in literature of BA, it had to be investigated if the same method could be applied to the polymeric system.

5.3.2 Synthesis of SMA

Table 5.3 shows the targeted molecular weight, along with the dispersities obtained with size exclusion chromatography (SEC), the molecular weight obtained via SEC and the molecular weight from ^{1}H NMR spectroscopy.

Table 5.3: Molecular weights of various alternating SMA copolymers synthesized by RAFT polymerization with the targeted molecular weight, the molecular weight obtained by SEC, along with the dispersity and the molecular weight from NMR.

	$M_{n,\,target}$[a]	$M_{n,\,SEC}$[b]	$Đ$[c]	$M_{n,\,NMR}$[d]
SMA 5000	5000	5800	1.29	6100
SMA 8000	8000	9000	1.19	9200
SMA 11000	11000	12600	1.13	12800

[a]Targeted molecular weight calculated by the following equation,

$$M_{n,th} = \frac{[M]_0 x}{[RAFT]_0 + (1+d) f [I]_0 (1-exp[-k_d t])} \cdot MW_M + MW_{RAFT}$$

[b] Number average molecular weight, in g/mol, determined by aqueous SEC relative to polystyrene standards.

[c] $Đ = \frac{M_w}{M_n}$

[d] Number average molecular weight, in g/mol, determined by ^{1}H NMR spectroscopy. The same method of calculation was used as the calculation described in Chapter 4 for the molar mass determination of SSM2100

5.3.3 Modification of SSM

The sequence defined SMA copolymer was modified with DMAPA. The acquired FTIR spectra are displayed in overlay in Figure 5.10. The most distinctive peaks of the A-SSM are the appearance of the acid O-H stretch at 3400 cm^{-1} and the disappearance of the carbonyl anhydride peaks at 1855 and 1775 cm^{-1} and the C-O-C stretching bands at 917 and 1220 cm^{-1}which correspond to the cyclic anhydride.

The complete disappearance of the carbonyl anhydride peaks, along with the appearance of the acid O-H stretch indicates that the SSM has been fully converted to the ring opened A-SSM. The ring opened MAnh unit, along with the tertiary amine from the DMAPA allows these specific functional groups to be ionized. With the one group being able to carry a positive charge (tertiary amine) and the other a negative charge (carboxylic group from ring opened MAnh) allows for the polymers to experience an isoelectric point.

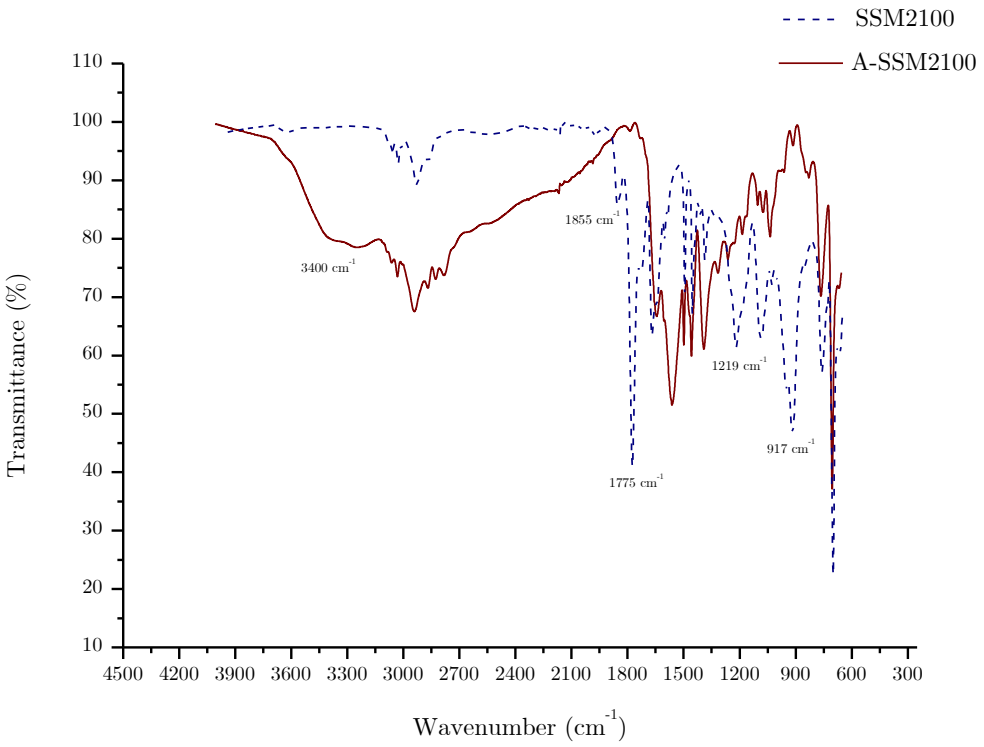

Figure 5.10: ATR-FTIR spectroscopy of SSM (dotted blue line) and A-SSM (red line).

5.3.4 Modification of SMA copolymers

Successful addition of DMAPA was confirmed using ATR-FTIR spectroscopy and can be seen in Figure 5.11. It also confirmed that the MAnh unit remained ring opened after the addition of the amine. The most distinctive peaks of the A-SMA are the appearance of the acid O-H stretch at 3400 cm^{-1} and the complete disappearance of the asymmetric and symmetric C=O vibrations at 1886 cm^{-1} and 1773 cm^{-1} and the C-O-C stretching bands at 919 and 1220 cm^{-1}which correspond to the cyclic anhydride. All the modification methods were identical and the IR spectrum of SMA11000 is shown. The modification of SMA5000, SMA8000 and SMA2000 are similar.

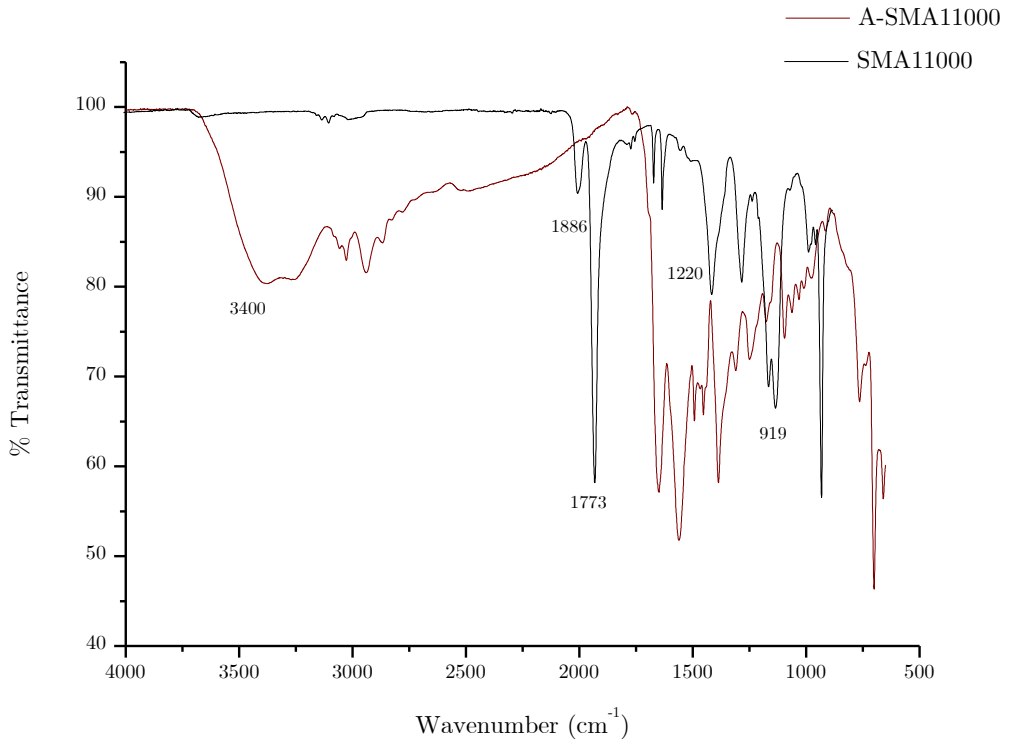

Figure 5.11: ATR-FTIR of SMA11000 before and after modification with DMAPA. The unmodified SMA11000 is represented by the black line, while the A-SMA11000 is represented by the maroon line. The most relevant peaks are labelled on the figure.

5.3.5 Determination of zwitterionic nature by titration of A-SMA copolymers

The various molecular weight A-SMA copolymers were all titrated with 0.1 M KOH. The polymer was dissolved in 25 mL degassed, distilled water, before the titration was performed. Upon dissolution, the polymers presented a basic pH, therefore HCl was added and the titration proceeded from low to high pH.

In Figure 5.12, two equivalence points can be observed for SMA5000. The first equivalence point is reached after a titrant volume of about 8 mL and a second at 12 mL. The half equivalence volumes can be used to estimate the respective pK_a values. These values can then be used to calculate the pI. The same method was applied as with the model study.

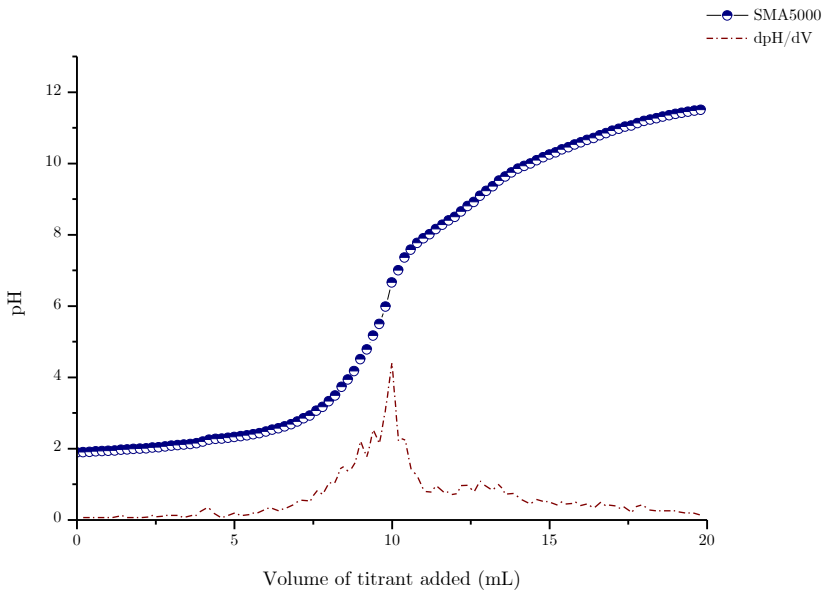

Figure 5.12: Titration of A-SMA5000 with 0.1 M KOH along with the first derivative of the titration curve.

Figure 5.13 and Figure 5.14 shows the titration curves for SSM2100 and SMA2000 respectively.

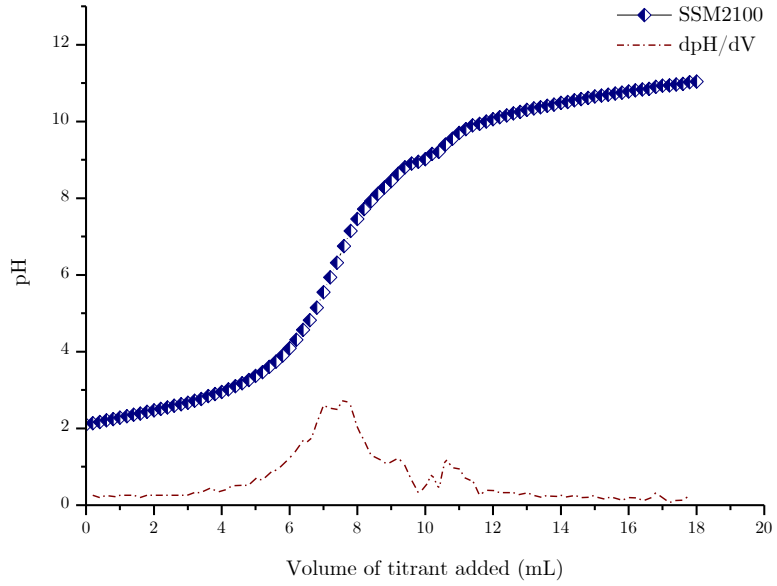

Figure 5.13: Titration of A-SSM (synthesized via RAFT-mediated polymerization with a predetermined sequence of one MAnh unit followed by two Sty units and a molecular weight of 2100 Da.) with 0.1 M KOH as well as with the first derivative of the titration curve.

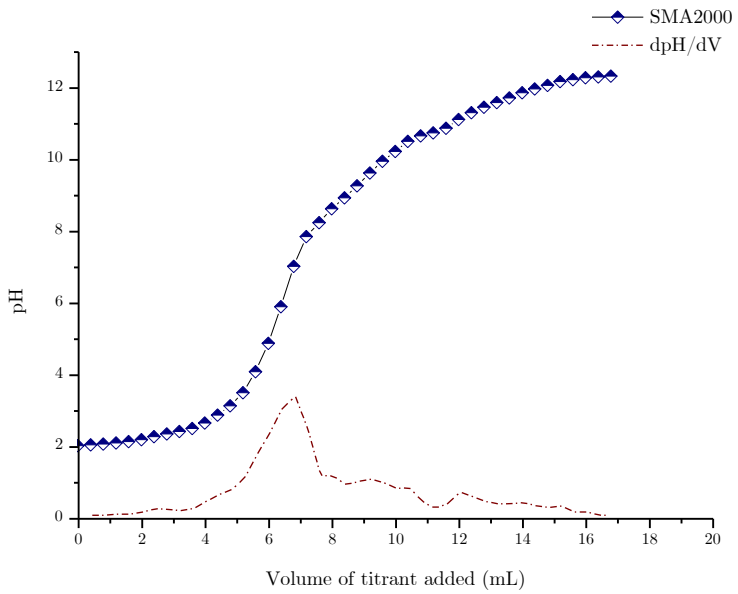

Figure 5.14: Titration of SMA2000 with 0.1 M KOH as well as with the first derivative of the titration curve.

The respective pK values, along with the pI could not be calculated using the equivalence point calculation method using the first derivative, as it was very difficult to locate the second maximum in the first derivative graphs for some of the polymers. The peaks were also ill-defined and broad in some cases. Therefore, it was decided to apply the linear regression method by Johansson.[11] The linear regression method for SMA5000 can be seen in Figure 5.15.

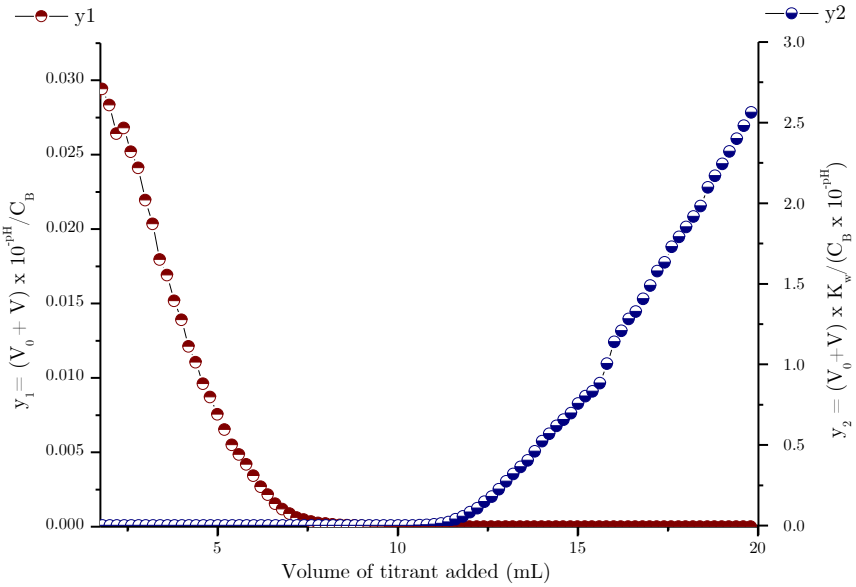

Figure 5.15: Equivalence point calculation of BA using the method described by Johansson[11] for A-SMA5000.

The analysis was done on all the copolymers and the results are summarized in Table 5.4. Table 5.4 summarizes the calculated pKa_1, pKa_2 and the pI values of the polymers of interest in this study.

Table 5.4: Calculated pK and pI values of SMA5000, SMA8000, SMA11000, SSM2100 and SMA2000 using the linear regression method.

Sample	pK_{a1}	pK_{a2}	pI
SMA2000[a]	2.7	11.1	6.90
SMA5000[b]	2.5	8.7	5.60
SMA8000[b]	2.5	8.8	5.65
SMA11000[b]	2.5	8.4	5.45
SSM2100[c]	3.1	9.8	6.45

[a] Polymer was bought from Arkema and synthesized via conventional radical polymerization.
[b] Polymer was synthesized via RAFT polymerization, following by the molecular weight.
[c] Sequence controlled copolymer consisting of one MAnh unit followed by two Sty units synthesized using RAFT polymerization.

From Table 5.4 it is evident that there is no trend observed for the differences in molar mass of the respective copolymers synthesized. The calculated pI's for the alternating SMA copolymers are similar. The decrease in polarity of the sequence-controlled SSM results in an increase of the pK_a values and therefore also in the pI. Interestingly the observed pI value for SMA2000 appeared to be the highest. This is attributed to the uncontrolled, hydrophobic segments of Sty in the polymer chain.

The protonation probabilities were calculated using the diprotic equation reported by Ullman (see Equation 5.9). For a zwitteronic compound to exist, there needs to be both a positive and negative site, while the overall charge remains zero.

These probabilities are plotted against the pH in Figure 5.16. The protonation state versus pH plot is quite different from the one obtained in the model study, as the functional groups are now combined, and are located on the same polymer. In Figure 5.16, it can be seen that at a high pH (where the titration was started with 0.1 M HCl) the polymer contains a charge of minus one. This corresponds to the BA being deprotonated at this pH as the pH is increased, the minus charge increases towards a neutral charge. At the expected pI of the SMA derivatives, the polymers have a neutral charge, as this corresponds to the zwitterionic region. This is quite a large region, as it seems to extend over two pH units. The calculated pK_a values of the polymers compared to the model compounds are in close proximity, although the values for the carboxylic acid are slightly lower for the polymers and the values for the tertiary amines are slightly higher for the polymers.

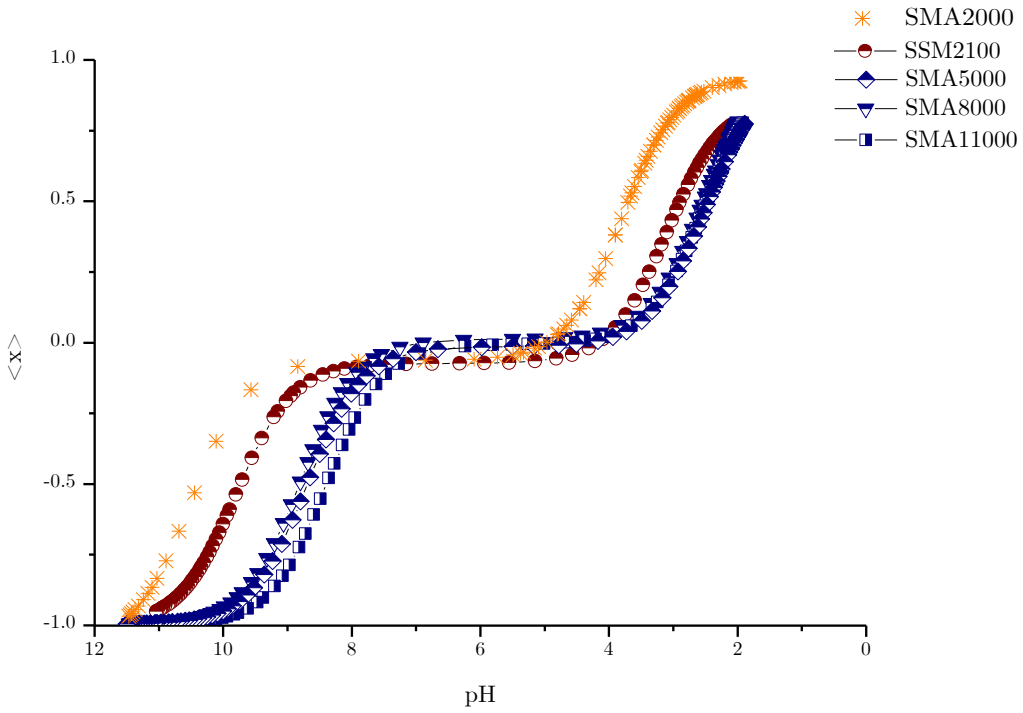

Figure 5.16: Protonation probability of various molecular weight alternating A-SMA copolymers, along with A-SSM2100 and A-SMA2000.

5.3.6 Nanoparticles for cellular uptake

To extend the applications of SMA copolymers to the biological/medical field, cytotoxicity studies regarding the specific functional groups can be employed. For this to be done, cellular uptake of the material in cells needs to be ensured. As mentioned in Section 5.1, for cellular uptake to occur via endocytosis, the particle/micelle size has be of a relatively small size, similarly to those of nanoparticles.[18–20] Nanoparticles have been extensively studied, as exposure to cells results efficient cellular uptake, contrary to polymers.[30] SDBM nanoparticles were modified using DMAPA in the following section. The divinyl benzene serves as a crosslinker to form the nanoparticles. Although the structure of the divinyl benzene differs to that of Sty, the ratio of hydrophobic (Sty and divinylbenzene) units to

the MAnh remains the same (see Scheme 5.3 for the structure of SDBM nanoparticles before and after surface modification). Therefore, the use of nanoparticles which contain the same ionizable groups than modified SMA copolymers, possibly allows for applications in the biological and medical field. Due to the polymerization method of the nanoparticles, the sequence of the nanoparticles cannot be controlled (the insoluble character of the nanoparticles also prohibits characterization methods such as NMR spectroscopy and SEC and basic titrations reactions), however, it is expected that a copolymer consisting of 30% MAnh relative to the hydrophobic groups (Sty and divinyl benzene in the case of the nanoparticles) should experience a zwitterionic region around a pH of 6.5.

5.3.6.1 Modification of nanoparticles

The successful modification of the nanoparticles is illustrated by distinctive peaks observed by ATR-FTIR spectroscopy. The tertiary amine does not produce a signal and the distinctive modification peaks are identical to those of A-SMA.

The most distinctive peaks of the nanoparticles are the appearance of the acid O-H stretch at 3401 cm^{-1} and the amide C=O stretch at 1691 cm^{-1} and are seen in Figure 5.17.

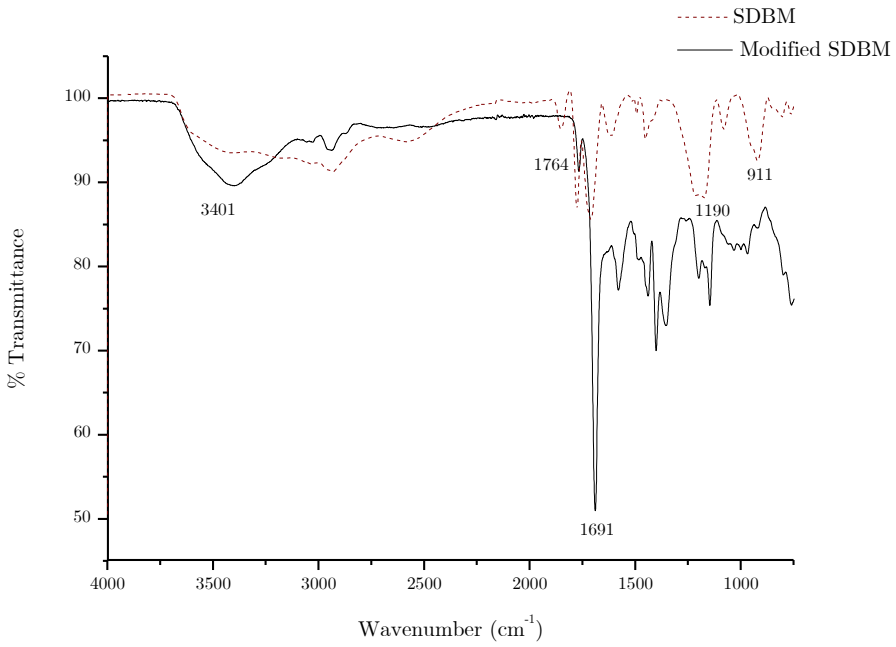

Figure 5.17: ATR-FTIR of SDBM before and after modification with DMAPA. The unmodified SDBM is represented by the dashed maroon line, while the modified SDBM nanoparticles are represented by the black line. The most important peaks are labelled in the figure.

5.3.6.2 Cytotoxicity studies on nanoparticles

Cytotoxicity studies were conducted in order to determine if the modified nanoparticles are harmful to cells, in order to expand the applications of SMA copolymers (more specific SMA containing ionizable groups) to the biological field. A colorimetric assay, known as XTT (which is a second-generation tetrazolium dye with a structure shown in Figure 5.18), was used to evaluate cell viability as a function of cell number[22,23], which is based on metabolic activity. The detection of this assay is done using standard microplate absorbance readers.

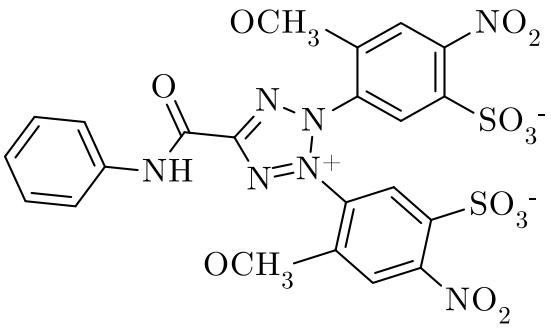

Figure 5.18: Chemical structure of XTT which is a second generation tetrazolium dye known as 5,5'-(5-(phenylcarbamoyl)-2*H*-tetrazole-3-ium-2,3-diyl)bis(4-methoxy-2-nitrobenzenesulfonate).

The assay was conducted to determine the effectiveness of cells to preserve or recuperate viability[24], essentially evaluating the cytotoxicity against cell cultures. The relative cell viability (%), which is comparative to control wells that contain cell culture medium without SDBM nanoparticles, is expressed as follows,

$$\textit{Relative cell viability (\%)} = \frac{\textit{Test169nm(cells/particles)} - \textit{Control169nm(no cells/particles)}}{\textit{Control169nm(no cells/particles)} - \textit{Control169nm(no cells/particles)}} \quad \text{Eq. (5.6)}$$

The graph obtained, represents the relative mitochondrial reductive capacity of primary isolated human macrophages (type M1) and the treatment with 10 µg/mL is displayed in Figure 5.19.

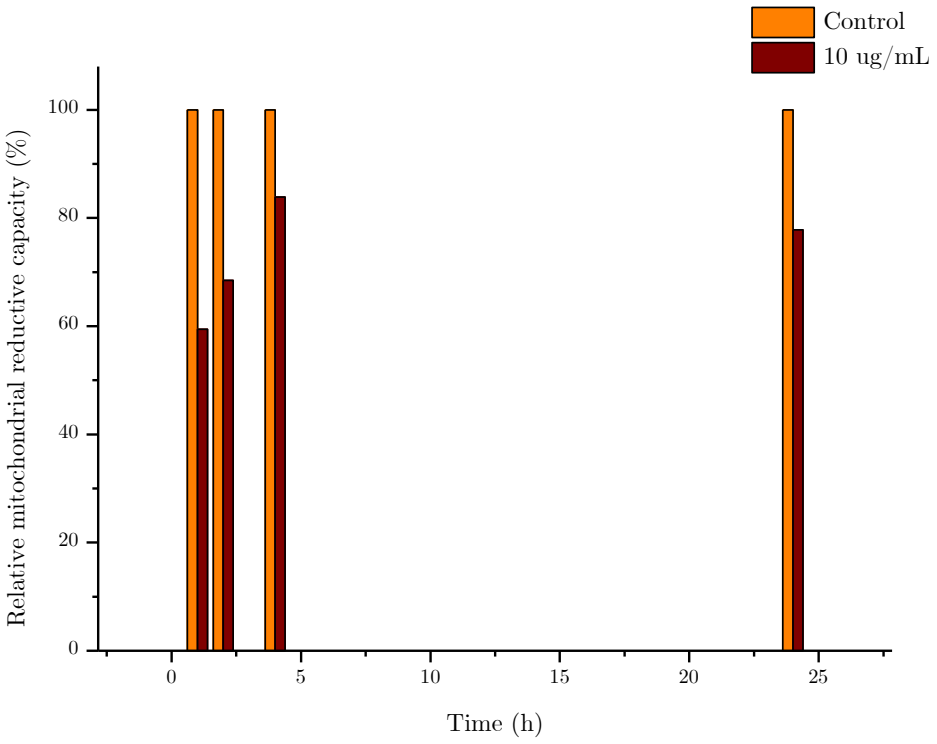

Figure 5.19: XTT assay of modified SDBM particles showing the relative mitochondrial reductive capacity of primary isolated human macrophages with a treatment of 10 µg/mL.

From these results, it would seem that the introduction of modified SDBM particles at low concentration (10 µg/mL) resulted in reduced mitochondrial activity over a short time period (1 h). Whereas mitochondrial activity was restored during extended treatment with SDBM particles at the same concentration, compared to 1 h.

For the treatment at a higher nanoparticle concentration (1 mg/mL), the mitochondrial activity is significantly upregulated during short treatment periods when compared to the control, as seen in Figure 5.20. After the upregulation after 4 h, the mitochondrial activity is reduced to ~ 95 % after 24 hours.

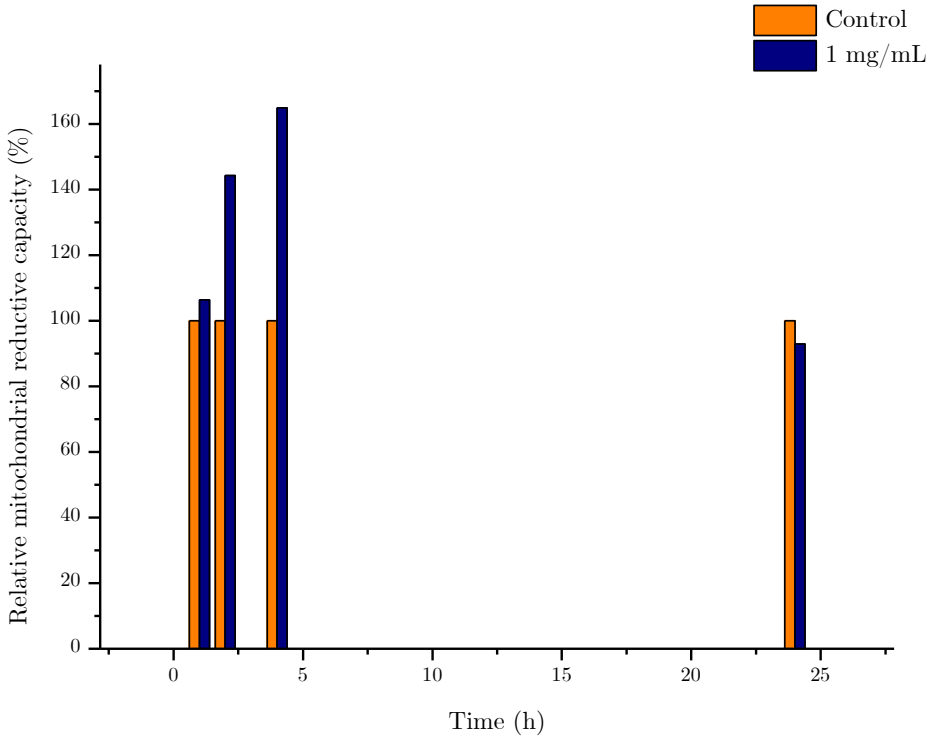

Figure 5.20: XTT assay of modified SDBM particles showing the relative mitochondrial reductive capacity of primary isolated human macrophages with a treatment of 1 mg/mL.

5.4 Conclusion

Successful surface modification of SMA and SSM was also successfully done and confirmed by ATR-FTIR spectroscopy. Thus was done to incorporate ionic groups, which allowed the possibility of a zwitterionic compound. For a zwitterion to exist, there needs to be both a positively and negatively charged site, while the overall charge of the compound remains zero.

The equivalence point calculation method introduced by Johansson[11] can be applied to amine-modified polymers of Sty and MAnh to accurately calculate the respective pK_a values. The protonation probabilities could also be calculated using the equation reported by Ullman.[4] This plot could be used to confirm that the overall protonation

state is neutral at the pI. From the model study, it is clear that a polymer with the same functional groups as BA and *N*-DMAPPA, will experience a zwitterionic region. Therefore, the work done in this chapter proved that copolymers of SMA modified with DMAPA do experience a zwitterionic window, where the proton from the carboxylic acid is taken up by the tertiary amine. This allows copolymers of SMA to be used for applications where ionic properties are a requirement, such as zwitterions for cell membrane disruption of tumor/acidic tissues (although zwitterions are very benign to cells, the acidic nature of tumor cells should result in a loss of the negative charge and the cationic species will be membrane disruptive), and this can be achieved by modifying the polymer with the desired ionic group (such as a tertiary amine).

The effect of the Sty-Sty sequence on the ionic properties were also investigated. It is clear that the increased Sty content results in increased pK values, and in turn a higher pI. This is attributed to fewer MAnh groups (along with DMAPA) being present with an increase of Sty content. For the titration of SMA2000, which consists of the same composition of SSM2100 but with a different sequence, the pI is even higher. This shows that the uncontrolled sequence also has an increasing effect on the pK values. This allows the manipulation of the pK values of SMA copolymers.

The XTT results proved that exposure of modified SDBM nanoparticles to primary isolated human macrophages did not result in an extreme reduction of the relative mitochondrial capacity, even after 24 hours. Upon a reduction in the relative mitochondrial capacity, the relative mitochondrial capacity was rescued up to around 80 % with a treatment of 10 µg/mL. For the treatment with increased concentration, the relative mitochondrial capacity seemed to increase after short exposure, where after 24 hours, it almost consists of a relative mitochondrial

capacity similar to the initial reading. Therefore, it can be concluded that the modified SDBM nanoparticles are not cytotoxic to primary isolated human macrophages.

As mentioned in Chapter 2, the pH of cancer cells is known to be lower than the pH of healthy cells.[25] The variation in pH of healthy cells and cancer cells can be exploited for SMA derivatives, functionalized with a tertiary amine, to exist as zwitterionic polymers in malignant cells. While being in an acidic environment (for all the polymers investigated at pH<5 the polymer will start to carry a positive charge – see Figure 5.16) the polymers will be positively charged, and cationic compounds are known to disrupt cell membranes.[26–29] Therefore, nanoparticles consisting of 30% MAnh can possible be used in the cationic cell disruptions of acidic, tumor cells, and in turn potentially expand the applications of surface modified SMA copolymers to the biological/medical field.

References

1. Mpitso, K. *Synthesis and characterization of styrene - maleic anhydride copolymer derivatives* 2009, MSc, Stellenbosch University
2. Clayden, J., Greeves, N. & Warren, S.*Organic Chemistry*, Second edition, 2012, ISBN: 9780199270293
3. Saad, G. R., Morsi, R. E., Mohammady, S. Z. & Elsabee, M. Z. *J. Polym. Res.* 2008, *15*, 115–123
4. Ullmann, G. M. *J. Phys. Chem. B* 2003, *107*, 1263–1271
5. Bashford, D. & Karplus, M. *Biochem.* 1990, *29*, 10219–10225
6. Reijenga, J., van Hoof, A., van Loon, A. & Teunissen, B. *Anal. Chem. Insights* 2013, *8*, 53–71
7. Still, E. *Anal. Chim. Acta* 1979, *107*, 377–381
8. Gran, G. *Acta Chem. Scand.* 1950, *4*, 559–577
9. Gran, G. *Anal. Chim. Acta* 1988, *206*, 111–123
10. Granholm, K., Sokalski, T., Lewenstam, A. & Ivaska, A. *Anal. Chim. Acta* 2015, *888*, 36–43
11. Johansson, A. *Analyst* 1970, *95*, 535–540
12. Small, D. M., Cabral, D. J., Cistola, D. P., Parks, J. S. & Hamilton, J. A. *Hepatology* 1984, *4*, 77s–79s
13. Martin, J. R., Petitdemange, H., Ballongue, J. & Gay, R. *Biotechnol. Lett.* 1983, *5*, 89–94
14. Ghumare, A. K., Pawar, B. V & Bhagwat, S. S. *J. Surfactants Deterg.* 2012, *16*, 85–93
15. Sørensen, P. *Kern. Maanedsbl. Nord. Handel. Kern. Ind* 1951, *32*, 73
16. Skoog, D. A., West, D. M., Holler, F. J. & Crouch, S. R. *Fundamentals of Analytical Chemistry*, Eight edition, 2004, ISBN: 100030355230
17. Scheidelaar, S., Koorengevel, M. C., van Walree, C. A., Dominguez, J. J., Dörr, J. M. & Killian, J. A. *Biophys. J.* 2016, *111*, 1974–1986
18. Zhang, S., Li, J., Lykotrafitis, G., Bao, G. & Suresh, S. *Adv. Mater.* 2009, *21,* 419-424

19. Reece, J. C., Vardaxis, N. J., Marshall, J. A., Crowe, S. M. & Cameron, P. U. *Immunol. Cell Biol.* 2001, *79,* 255-263

20. Rejman, J., Oberle, V., Zuhorn, I. S. & Hoekstra, D. *Biochem. J.* 2004, *377,* 159-169

21. Harmzen-Pretorius, E. *Synthesis of polymer nanoparticles and various applications* 2017, PhD, Stellenbosch University

22. Scudiero, D. a, Shoemaker, R. H., Paull, K. D., Scudiere, D. a, Paul, K. D., Monks, A., Tierney, S., Nofziger, T. H., Currens, M. J., Seniff, D. & Boyd, M. R. 1988, 4827–4833

23. Altman, F. P. *Histochem. J.* 1976, *8*, 501–506

24. *XTT Cell Proliferation Assay Kit by Cellular Enzymes I,* Instruction manual. 1988, 2-6.

25. Tannock, I. F. & Rotin, D. *Cancer Res.* 1989, *49*, 4373–4384

26. Mason, A. J., Gasnier, C., Kichler, A., Pre, G. & Aunis, D. *Antimicrob. Agents Chemother.* 2006, *50*, 3305–3311

27. Fröhlich, E. *Int. J. Nanomedicine* 2012, *7*, 5577–5591

28. Palermo, E. F., Lee, D., Ramamoorthy, A. & Kuroda, K. *J. Phys. Chem* 2011, *115*, 366–375

29. Chen, J., Hessler, J. A., Putchakayala, K., Khan, D. P., Hong, S., Mullen, D. G., Dimaggio, S. C., Som, A., Tew, G. N., Lopatin, A. N., Baker, O. J. R., Holl, M. M. B. & Orr, B. G. *J. Phys. Chem* 2009, *113*, 11179–11185

30. Capaco, D. G.& Chen, Y., *Nanomaterial: Impacts on Cell Biology and Medicine*, First edition, 2014, ISBN: 9789401787383

Chapter 6

Epilogue

6.1 General conclusions

During this study, several conclusions could be drawn. Firstly, the formation of alternating SMA could be suppressed, using sequential monomer addition. This was achieved using a RAFT agent that provided high monomer conversions of both monomers. This RAFT agent is known as *S*-butyl-*S*'-(1-phenyl ethyl) trithiocarbonate (BPT) was found to be the most suitable RAFT agent with regards to styrene (Sty) monomer conversion and reaction times. Two other RAFT agents namely *S*-cumyl phenyldithioacetate (CPDA) and *S*-*n*-butyl *S'*-(2-phenylpropan-2-yl) trithiocarbonate (BPPT) provided promising results, and the occurrence upon employment of the polymerization with *S*-cumyl dithiobenzoate (CDB) seemed to only convert half of the original Sty content to Sty in the polymer chain. To the best of our knowledge, the synthesis of $(SSM)_n$, and in turn the control over the microstructure, have not yet been reported. The desired polymer, consisting of one maleic anhydride (MAnh) unit followed by two styrene (Sty) units, was synthesized with a MSS, SSM triad content (from the methylene sub spectrum) from ^{13}C DEPT NMR spectroscopy of 93 %, indicating the amount of control of the polymerization.

The thermal properties of this sequence-controlled polymer was investigated using thermal gravimetric analysis (TGA). Bhuyan *et al.* and Baruah *et al.* reported that the incorporation of MAnh into a polystyrene (PS) chain results in a decrease in the thermal stability of the copolymer.[1,2] The TGA results showed that the SSM copolymer exhibits a weight loss corresponding to the RAFT end groups, where after it adapt to the same overall curve to that of SMA2000 displayed, which is a polymer with the same Sty content synthesized by conventional radical polymerization. Therefore, the controlled sequence does not seem to affect the thermal stability of the copolymer.

Secondly, the polymer synthesized containing the desired sequence was successfully modified using 3-(*N*,*N*-dimethylamino)propyl-1-amine (DMAPA), along with the modification of several different molar mass SMA alternating copolymers. The model study employed, proved that a polymer consisting of similar functional groups than those of butyric acid (BA) and *N*-((3-dimethylamino)propyl)propionamide (*N*-DMAPPA) should experience a zwitterionic region around a pH of 5.5. The equivalence point method reported by Johansson was used to calculate the equivalence points[3] along with using the first derivative maxima of the titration curve. These two values seem in close agreement with one another, while the method using the maxima of the first derivative corresponded more closely to the reported literature value of BA. The same methods were applied to the polymeric system. The method using the first derivative yielded one maxima, although the second maxima was difficult to locate, along with broad peaks observed for the sequence-controlled system. The respective isoelectric points (pIs) of these polymers were calculated using the linear regression method. The work done in this section concluded that the length of the polymer chain of alternating SMA leads to negligible differences in the calculated pIs. However, an increase in the Sty content

resulted in an increase in the pI of the polymer, as the polymer containing higher fractions of Sty leads to the polymer being less polar. This is due to fewer functional ionic groups being present in the polymer chain.

Nanoparticles containing Sty, MAnh and a crosslinker (divinyl benzene) were modified with DMAPA. This was done in order to establish if a functionalized system of these comonomers are cytotoxic to cells, by applying a cell viability study. It was concluded that the nanoparticles are not cytotoxic.

6.2 Future recommendations

Chapter 3 focuses on finding a suitable RAFT agent to synthesize the sequence-controlled copolymer. The observation in the CDB mediated copolymerization requires additional investigation. It is quite remarkable that only one Sty equivalent is consumed when a [Sty] : [MAnh] : [RAFT] mixture of 2 : 1 : 1 is reacted. The inability of certain RAFT agents to yield high Sty conversions could also be explored, as interesting phenomena such as initialization[4–8] during the early stages of a RAFT-mediated polymerization, have come to light over the last decade.

The length of the styrene (Sty) sequence could possibly be further explored, followed by the thermal properties of these polymers. Other monomer systems can also be explored, relying on the electron-rich, electron-poor polymerization principle.

Styrene-divinylbenzene-maleic anhydride (A-SDBM) nanoparticles have shown to be non-toxic to primary monocytes, and although the mechanism of cellular uptake for these nanoparticles are not yet known, phagocytosis has been ruled out.[9] Therefore, it can be expected that the particles will be taken up by cancer cells via the same mechanism, due to the fact that cancer cells do not undergo phagocytosis. Therefore, the cell interaction studies can be expanded to other cell types (including

tumor cells) in the future. The acidic nature of tumor cells could possibly result in the loss of the negative charge on the zwitterionic particles, resulting in a positive substance that can undergo cell membrane disruptions.

References

1. Bhuyan, K. & Dass, N. N. *J. Therm. Anal.* 1989, *35*, 2529–2533
2. Baruah, S. D. & Laskar, N. C. *J. Appl. Polym. Sci.* 1996, *60*, 649–656
3. Johansson, A. *Analyst* 1970, *95*, 535–540
4. Drache, M. & Schmidt-Naake, G. *Macromol. Symp.* 2008, *271*, 129–136
5. Drache, M. & Schmidt-Naake, G. *Macromol. Symp.* 2007, *259*, 397–405
6. McLeary, J. B., Calitz, F. M., Mckenzie, J. M., Tonge, M. P., Sanderson, R. D. & Klumperman, B. *Macromolecules* 2005, *38*, 3151–3161
7. McLeary, J. B., Calitz, F. M., McKenzie, J. M., Tonge, M. P., Sanderson, R. D. & Klumperman, B. *Macromolecules* 2004, *37*, 2383–2394
8. Lu, L., Zhang, H., Yang, N. & Cai, Y. *Macromolecules* 2006, *39*, 3770–3776
9. Harmzen-Pretorius, E. *Synthesis of polymer nanoparticles and various applications* 2017 PhD, Stellenbosch University

Appendix

1 A RAFT agent consumption using BPT as RAFT at 80 °C

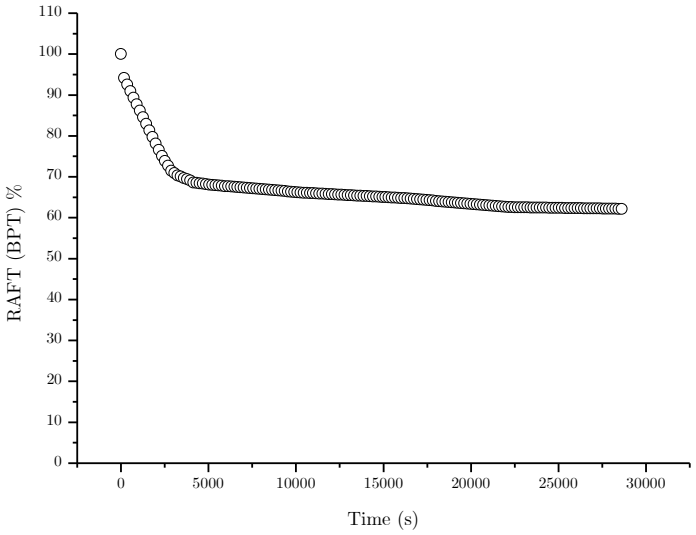

The above figure shows the percentage methyl protons of the BPT RAFT agent. After approximately 30%, the rate of consumption decreases.

2 A Total percentage of RAFT species for homopolymerization of Sty with CDB

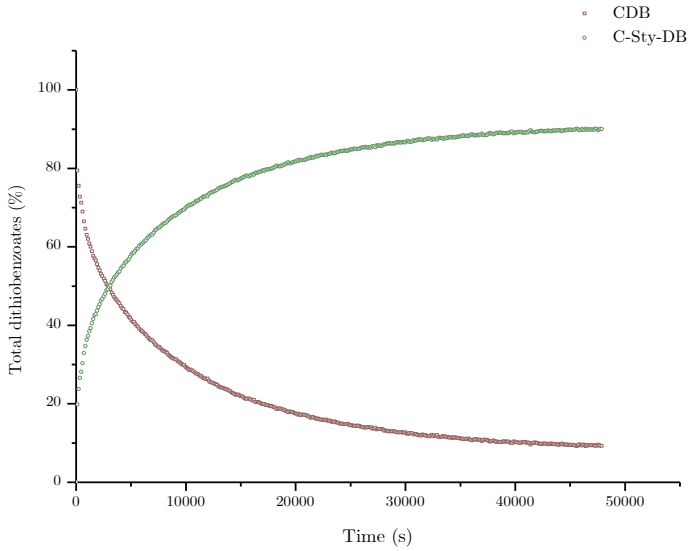

Total RAFT species of RAFT-mediated reaction with CDB as RAFT agent.

3 A Modification of polymers

a. Modification of SMA5000

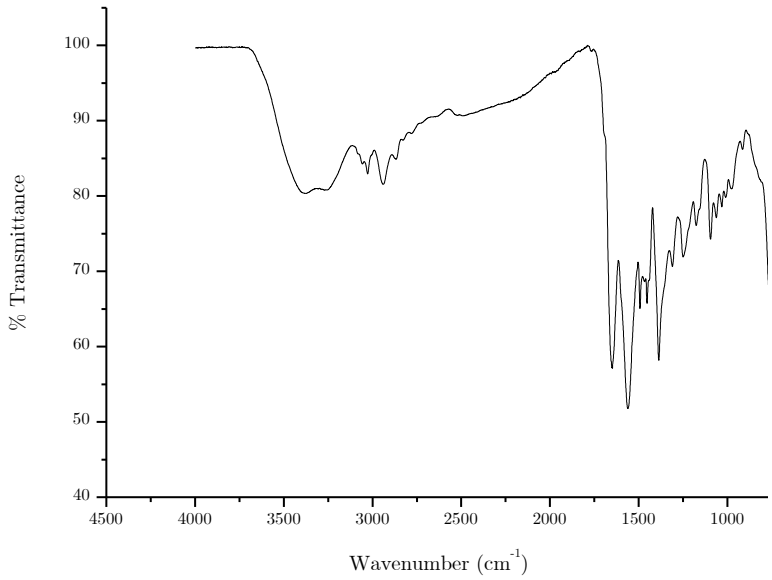

Modification of SMA5000 with DMAPA.

b. Modification of SMA8000

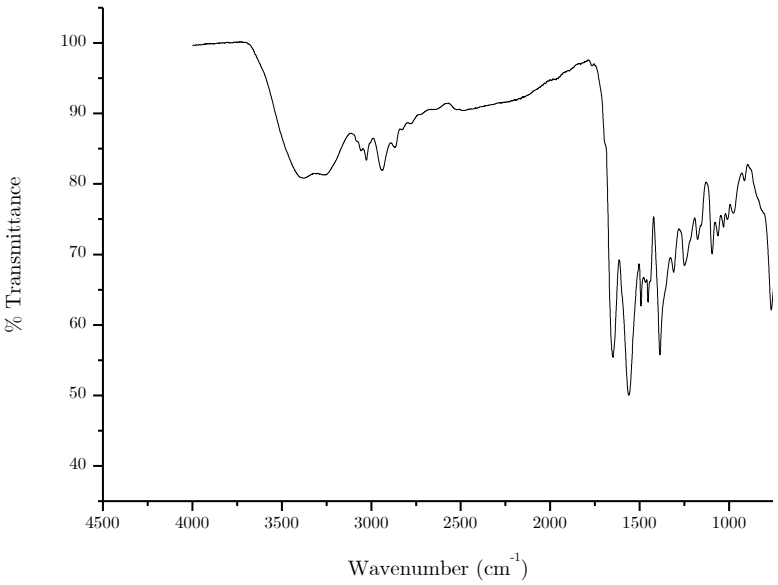

Modification of SMA8000 with DMAPA.

c. Modification of SMA2000

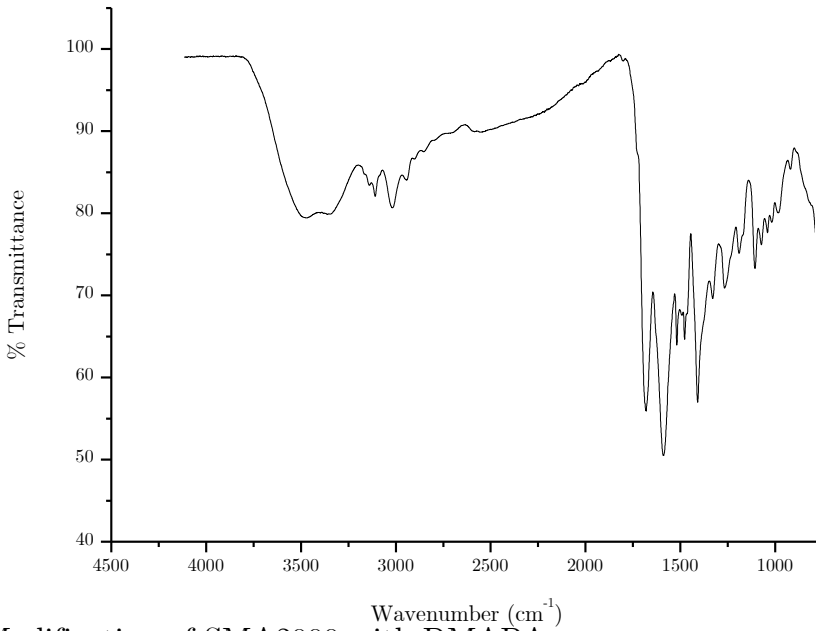

Modification of SMA2000 with DMAPA.